2008

A WHOLE CELL BASED BIOSENSOR FOR MONITORING PHYSIOLOGICAL TOXINS AND EARLY SCREENING OF CANCER

Gargi Ghosh
University of Kentucky, gghos0@engr.uky.edu

ABSTRACT OF DISSERTATION

Gargi Ghosh

The Graduate School

University of Kentucky

2007

A WHOLE CELL BASED BIOSENSOR FOR MONITORING PHYSIOLOGICAL TOXINS AND EARLY SCREENING OF CANCER

ABSTRACT OF DISSERTATION

A dissertation submitted in partial fulfillment of the
requirements for the degree of Doctor of Philosophy in the
College of Engineering
at the University of Kentucky

By
Gargi Ghosh

Lexington, Kentucky

Director: Dr. Kimberly W. Anderson, Professor of Chemical Engineering

Lexington, Kentucky

2007

ABSTRACT OF DISSERTATION

A WHOLE CELL BASED BIOSENSOR FOR MONITORING PHYSIOLOGICAL TOXINS AND EARLY SCREENING OF CANCER

Recently a whole cell based biosensor has been developed in our laboratory that consists of a monolayer of human umbilical vein endothelial cells (HUVECs) on the asymmetric cellulose triacetate (CTA) membrane of an ion selective electrode (ISE). When a confluent cell monolayer is formed across the membrane, response from the sensor is inhibited due to inhibited ion transport across the membrane. When the cell based biosensor is exposed to permeability modifying agents, the permeability across the cell monolayer is altered facilitating more ion transport and as a result the response from the sensor increases. This sensor response can be related to the concentration of these agents. One objective of this research was to investigate the ability of the sensor to detect a physiological toxin, alpha toxin from *Staphylococcus aureus*. Studies demonstrated that the biosensor can detect 0.1ng/ml alpha toxin. Considering the fact that the concentration of this toxin is 100-250 ng/ml in whole blood in humans, this biosensor has the ability to act as the diagnostic tool for staphylococcal diseases. Another part of this research was to investigate the ability of the biosensor to measure angiogenesis by measuring the changes in permeability induced by cytokines such as vascular endothelial growth factor (VEGF), basic fibroblast growth factor (bFGF), hepatocyte growth factor (HGF) and tumor necrosis factor –α (TNF- α) individually and in combination. The sensor response was then compared with the common *in vitro* assays for angiogenesis. The study demonstrated that at the concentrations studied the sensor response in the presence of cytokines was much higher than that observed for other angiogenesis assays, thereby bolstering the potential of the biosensor to act as a quick screening tool for angiogenesis. Furthermore, epithelial cell based sensor responses to the same cytokines were compared with the responses from endothelial cell based sensor and the mechanisms behind the increased sensor response were elucidated. Finally, to investigate the ability of the sensor to screen cancer, the biosensor was exposed to the serum from healthy individuals and cancer patients. The results showed that the sensor can distinguish between healthy individuals and cancer patients and the results correlate with the stages of cancer.

KEYWORDS: Biosensors, Mammalian cells, Staphylococcal alpha toxin, Angiogenesis, Screening cancer

Gargi Ghosh

12/17/07

A WHOLE CELL BASED BIOSENSOR FOR MONITORING PHYSIOLOGICAL TOXINS AND EARLY SCREENING OF CANCER

By

Gargi Ghosh

Dr. Kimberly Anderson

Director of Dissertation

Dr Barbara Knutson

Director of Graduate Studies

12/17/07

Date

RULES FOR THE USE OF DISSERTATIONS

Unpublished dissertations submitted for the Doctor's degree and deposited in the University of Kentucky Library are as a rule open for inspection, but are to be used only with due regard to the rights of the authors. Bibliographical references may be noted, but quotations or summaries of parts may be published only with the permission of the author, and with the usual scholarly acknowledgements.

Extensive copying or publication of the dissertation in whole or in part also requires the consent of the Dean of the Graduate School of the University of Kentucky.

A library that borrows this dissertation for use by its patrons is expected to secure the signature of each user.

Name	Date

DISSERTATION

Gargi Ghosh

The Graduate School

University of Kentucky

2007

A WHOLE CELL BASED BIOSENSOR FOR MONITORING PHYSIOLOGICAL TOXINS AND EARLY SCREENING OF CANCER

DISSERTATION

A dissertation submitted in partial fulfillment of the
requirements for the degree of Doctor of Philosophy in the
College of Engineering
at the University of Kentucky

By
Gargi Ghosh

Lexington, Kentucky

Director: Dr. Kimerly W. Anderson, Professor of Chemical Engineering

Lexington, Kentucky

2007

ACKNOWLEDGEMENTS

I would like to thank and acknowledge Dr. Kimberly W. Anderson for her valuable guidance during my Ph.D research. Her ingenious ideas and constant encouragement have helped me immensely in completing the research work. I am and shall be ever grateful to her for all the kindness and affection she had bestowed on me. I would also like to thank my committee member Drs. Kalika, Hilt and Bachas for all their support.

I would like to thank Mary Gail for the assistance with the TEM analysis and Dr. Kimberly May for training me in culturing cells. Special thanks to Morgan, Samantha and Matt for maintaining such a nice working atmosphere in the lab. I would like to thank William Hawthorne, Abagail Cornette, Ishan Metha, Chris Brown and Jenna Shapiro for their undergraduate research assistance.

Thanks to all my friends who have made my stay at Lexington memorable.

A special thanks to my husband and best friend Saurav for his constant encouragement and for extending the helping hand whenever I was in need. I would also like to express my gratitude to my family members and in laws for their constant support. Finally and most importantly, I would like to express my heartfelt gratitude to my parents for their constant motivation, encouragement and for all the sacrifices they made for me. I could have never reached this juncture without them.

I would like to acknowledge KY NASA/EPSCoR and Kentucky Science and Engineering Foundation (KSEF) for funding the research.

Table of Contents

List of Tables

List of Figures

List of Files

Gargi_Dissertation.pdf……. 2 MB

Chapter 1 : Introduction

A sensor consists of a recognizing element which responds to the analytes being measured and a transducer which converts the observed change into a measurable signal. In the case of a biosensor, the recognition system is a biological element, living organisms or components of living organisms. Thus, a blood-oxygen sensor is not a biosensor even though it is measuring a biologically important parameter; but is a chemical sensor that has biomedical applications (Harsanyi 2001). On the other hand, a microorganism based sensor, detecting heavy metals in industrial effluent, is a biosensor simply because the recognizing unit is a biological element. In the last two decades, tremendous growth in research related to biosensors has been observed with the applications extending to the food and agriculture industry, medical, environmental as well as in military fields.

Currently, there exits a need for simple, reliable yet less expensive devices which can act as physiological detection tools. Recently a whole cell based biosensor, had been developed in our laboratory, which takes advantage of cell-barrier dysfunction to detect the presence of small quantities of permeability modifying agents. The biosensor incorporates a monolayer of human umbilical vein endothelial cells (HUVECs) on the asymmetric cellulose triacetate (CTA) membrane of an ion-selective electrode (ISE). The presence of a confluent monolayer of cells inhibits the transport of ions to the membrane surface resulting in an inhibited response from the sensor. When the permeability across the cell monolayer is altered by exposing the cell based sensor to these permeability modifying agents, the response from the sensor increases. The response thus obtained can then be related to the concentration of these agents. Earlier studies have shown that the endothelial cell based sensor can detect the presence of histamine and VEGF (May et al. 2005; May et al. 2004a)

The overall goal of this research was to investigate the use of the whole cell based biosensor for detecting physiological toxins as well as for early screening of cancer. Specifically, the biosensor has been used to detect the presence of staphylococcal alpha toxin. *Staphylococcus aureus* is one of the most common pathogens in a nosocomial setting. Alpha toxin, a protein exotoxin produced by the majority (85-90%) of *S. aureus*

strains (Mollby 1983), plays a critical factor in *S. aureus* induced pathogenicity. The biosensor was also used to measure permeability changes induced by different cytokines such as vascular endothelial growth factor (VEGF), basic fibroblast growth factor (bFGF), hepatocyte growth factor (HGF) and tumor necrosis factor – α (TNF-α), as an alternate assay for measuring angiogenesis. Angiogenesis, sprouting of new blood vessels from existing vasculature, is observed in several diseases such as cancer, arthritis and diabetes. In cancer, angiogenesis occurs during the early phase of cancer, leading to the release of elevated concentrations of different cytokines in the blood of cancer patients as compared to healthy individuals (Dirix et al. 1997; Sezer et al. 2001). Based on the hypothesis that any device that can measure angiogenesis can act as a quick screening tool for cancer, the responses of the biosensor to the serum samples from healthy individuals and cancer patients (different origin and stages) were measured to determine the ability of the sensor to screen cancer. Since permeability across an epithelial cell monolayer is altered by different cytokines, LLC-PK1, porcine kidney epithelial cells were also seeded on ISE membranes surface, and the response of the sensor to the presence of the cytokines was measured. Moreover, studies were also conducted to elucidate the mechanism behind the increased permeability induced by different cytokines across HUVEC and LLC-PK1 monolayers.

Specific objectives of the research include:

- To investigate the use of the HUVEC based biosensor for detecting staphylococcal alpha toxin, a toxin involved in various infections including septicemia, endocardytis, septic arthritis, etc.
- To investigate the use of the HUVEC based biosensor for assaying angiogenesis and to compare the responses of the sensor to the responses obtained from common in-vitro angiogenesis assays.
- To investigate the ability of a porcine epithelial cell, LLC-PK1, based sensor to detect the presence of cytokines.
- To study the mechanisms involved in altering permeability of HUVEC and LLC-PK1 monolayers.
- To investigate the ability of the HUVEC based sensor to act as a screening tool for cancer.

In Chapter 2, a general background on biosensors and ISEs is given. The general materials and methods employed for culturing HUVECs and LLC-PK1s as well as for fabricating the asymmetric membranes for the biosensor and evaluating the responses are discussed in Chapter 3. Chapter 4 discusses the study involving the effect of staphylococcal alpha toxin on sensor response as well as on HUVEC morphology. Moreover, the detection limit of the biosensor is determined and the correlation obtained between the sensor response and intercellular gap formation evaluated. To study the ability of the biosensor to measure angiogenesis, the effect of different cytokines, vascular endothelial growth factor (VEGF), basic fibroblast growth factor (bFGF), hepatocyte growth factor (HGF) and tumor necrosis factor – α (TNF- α), individually and in combination, on the biosensor response is evaluated in Chapter 5. The responses thus obtained are compared with the responses obtained from common in-vitro angiogenesis assays. Since cytokines also alter the permeability of epithelial cells, the effect of VEGF, HGF, bFGF and TNF- α on a LLC-PK1 cell-based biosensor response is discussed in Chapter 6. Moreover, the mechanisms involved behind the altered permeability across HUVEC and LLC-PK1 monolayer have also been elucidated. Furthermore, the effect of these cytokines on the cell-matrix adhesion has also been discussed. Chapter 7 discusses the responses obtained from the biosensor upon exposing it to the serum samples from healthy individuals as well as cancer patients. The responses have been studied as a function of cancer types as well as stages of cancer. Chapter 8 summarizes the results of the current studies. The aspects of future studies have been discussed in Chapter 9.

Chapter 2 : Background

2.1 Biosensors

Biosensors consist of a biological sensing/recognition system connected to a transducer. The biological element, which consists of living organisms or components of living organisms, interacts with the substrates/analytes and then the transducer converts the observed change into a measurable signal. The magnitude of this signal is related to the concentration of the analytes. A schematic diagram of a biosensor is shown in Figure 2.1. Over the past two decades biosensors have been increasingly used in environmental, toxicological, medical as well as in defense applications (Alocilja and Radke 2003; Bousse 1996; Paddle 1996; Rodriguez-Mozaz et al. 2004). Such a rapid development in the field of biosensors can be attributed to the fact that biosensors have immense potential to act as low – cost yet rapid and sensitive measuring tools.

The classification of a biosensor is broadly based on the following:

a) the recognition element,
b) immobilization techniques,
c) the principle of detection and
d) applications

Recognition Element

A biosensor can be divided into three categories based on the recognition element, namely molecular sensors, cellular sensors and tissue based sensors. In molecular sensors, biomolecules such as enzymes, cell receptors, antibodies, nucleic acids etc act as the sensing elements whereas in cell or tissue based sensors microorganisms, mammalian cells or slices of tissue constitute the recognition unit.

Enzymes, the biocatalysts, are the most common biological elements in biosensors. Enzymes catalyze numerous reactions when they come in contact with the substrate. The most common enzyme biosensor is the sensor for detecting glucose, where the *glucose oxidase* (GOX) enzyme oxidizes glucose to gluconic acid and hydrogen peroxide (Eq. 2.1). The decrease in concentration of oxygen is measured using an oxygen electrode.

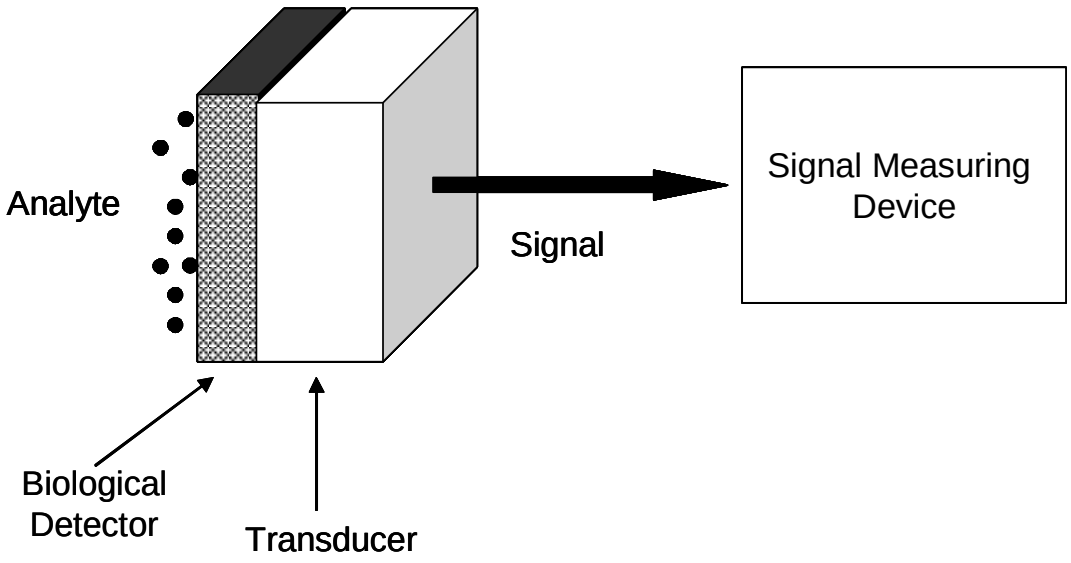

Figure 2.1 Schematic showing the components of biosensor, modified from Eggins 1996. The signal arising out of the interaction between the biological detector and analyte is converted into electrical signal by the transducer. The signal is then processed by signal processor.

$$\text{glucose} + O_2 \xrightarrow{\text{GOX}} \text{gluconic acid} + H_2O_2 \qquad 2.1$$

Another common example of an enzyme based biosensor is when *urease* is used to measure urea by breaking down urea to ammonia and carbon dioxide.

The above two scenarios are examples of enzyme based biosensors where purified enzymes have been immobilized on the surface of a transducer. However, instead of using purified enzymes, in many cases cells or slices of tissue are used as the sources of enzymes for catalyzing reactions. The most well known tissue based biosensor is the "bananatrode". The fact that banana tissue contains polyphenolases which in turn can oxide molecules containing catechol groups was used to develop a biosensor for dopamine (Sidewell and Rechnitz 1985). Another example involves the breakdown of arginine by bovine liver to urea and orthinine (Rechnitz 1978). Microorganism based biosensors involving bacteria, yeast or fungi find applications such as in waste water treatments, brewing industries and detection of pesticides (Lei et al. 2005; Rodriguez-Mozaz et al. 2004).

Other known biological components of biosensors include antibodies, nucleic acids and receptors. Antibody based biosensors involve the highly specific interactions between the antibodies and the antigenic regions of the substrates. Interactions between the antibodies and antigens have been utilized in many optical and piezoelectric biosensors for detection of cocaine, trinitrotoluene, toxins like *Clostridium botulinum* and ricin as well as contaminants of food like mycotoxins (Devine et al. 1995; Narang et al. 1997; Ogert et al. 1992; Suleiman and Guilbault 1994; Thompson and Moragos 1996; Whelan et al. 1993). Hybridization of known DNA probes with the complimentary strands in the test sample acts as the backbone of the nucleic acid based biosensors. Specificity of nucleic acid based sensors are higher than antibody based sensors as antibodies at times can react with antigens other than the analyte of interest (Pancrazio et al. 1999). However, extensive sample preparation, hybridization and amplification limit the application of the nucleic acid based sensors.

Immobilization Techniques

Biosensors can also be classified on the basis of the mode of biomolecule immobilization on the transducer surface. Immobilization of biomolecules plays a critical role in biosensor stability and performance. Figure 2.2 represents a schematic of some of the common techniques for biomolecule immobilization. The methods include adsorption of the biomolecule on the surface, covalent binding between the biological component and the transducer surface, cross-linking between molecules, entrapment of the biological component within a gel matrix or polymer and microencapsulation of the biological element within membranes (Collings and Caruso 1997; Eggins 1996). The adsorption of biomolecules on the sensor surface can either be based on weak forces like van der Waals forces, hydrogen bonding or electrostatic interactions (physisorption) or much stronger chemical bonds in the case of chemisorption. Even though physisorption involves the simplest approach of biomolecule incorporation, the strong dependence of the binding forces on pH, temperature and ionic strength, however reduces biosensor stability (Ahuja et al. 2007). Incorporation of crosslinking agents such as glutaraldehyde, hexamethyl diisocyanate and 1,5–dinitro-2,4 difluorobenzene between the biomolecule and transducer can eliminate some of the problems associated with the physisorption method. For example co-immobilization of acetylcholine (AChE) with choline oxidase (ChO) on a Pt surface in the presence of glutaraldehyde resulted in increased enzyme attachment on the transducer surface (Amine et al. 2006). Glutaraldehyde was once again the crosslinker during the immobilization of AChE in a nylon net on a gold electrode (Gulla et al. 2002). However, denaturation of the enzyme due to crosslinking, diffusion limitations as well as the poor stability of the biosensors due to exposure of the enzyme to the bulk solution are some of the limitations of this immobilization technique (Amine et al. 2006). Microencapsulation, one of the oldest immobilization techniques, involves the use of a membrane for trapping the biomaterial (Eggins 1996). For example, clinically important biosensors were constructed by physically trapping various oxidoreductase enzymes in poly (2-hydroxylethyl methacrylate) hydrogels (Brahim et al. 2002). Layer by layer deposition of polyallylamine hydrochloride /polystyrene sulphonate on GOX microparticles resulted in enhanced loading of the enzyme (Trau and Renneberg 2003). The matrix entrapment of the biomolecule is also used where the biomolecule is mixed

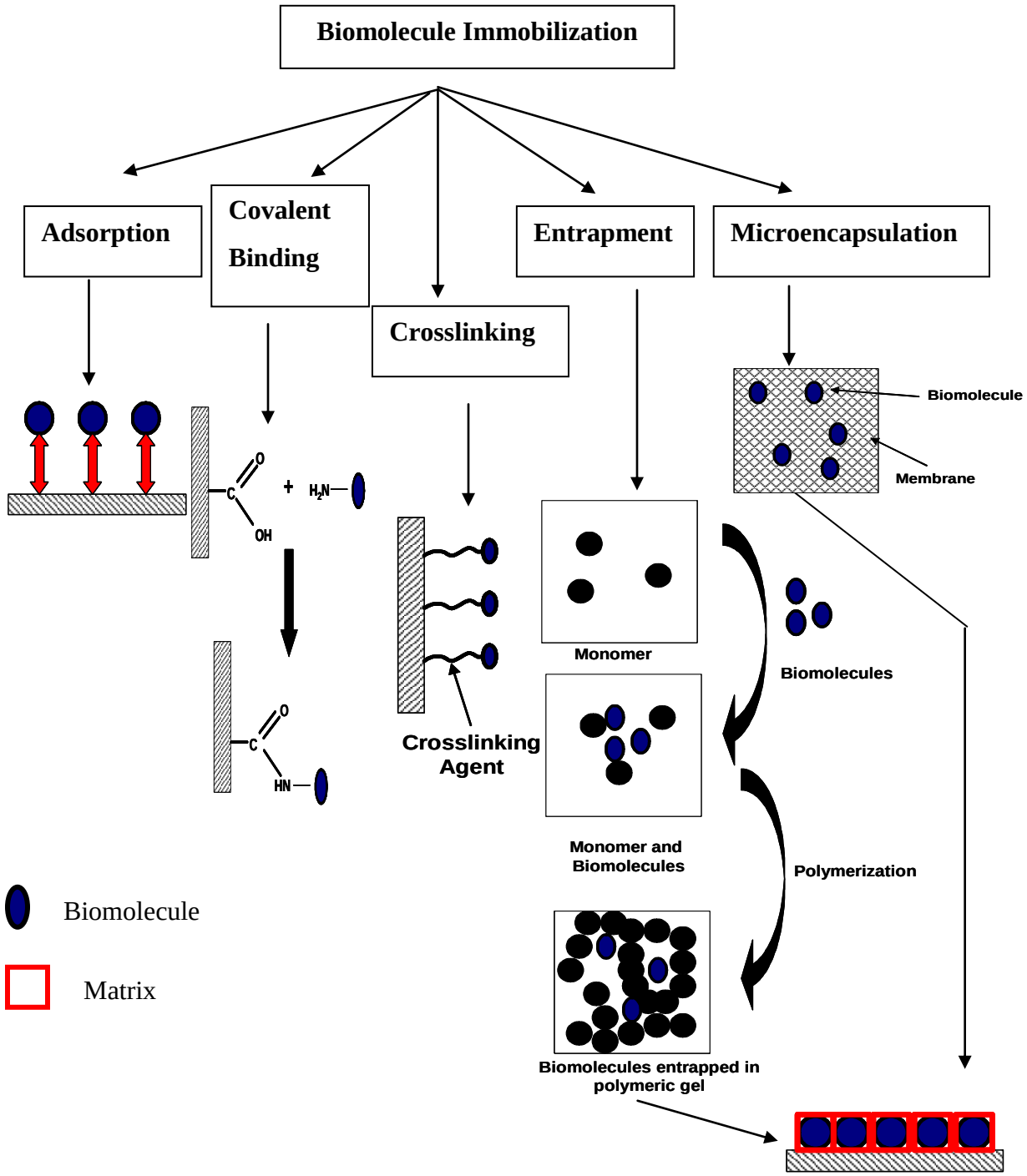

Figure 2.2 Schematic showing the different techniques of biomolecule immobilization

with the monomer and polymerized to form a gel entrapping the biomolecule (Eggins 1996). Entrapment of GOX during the growth of an osmium complex modified polypyrrole has been demonstrated (Reiter et al. 2001). Careful tailoring of covalent bonds between the sensor surface and the biomolecule by utilizing the functional groups of the biomolecule which are not essential for its activity is another method of biomolecule immobilization. The advantages of this method include low mass transfer resistance and reduced leaching of the biomolecule. Some examples of covalent immobilization of biomolecules include the binding of GOX to poly(*o*-amino benzoic acid) for glucose sensing, pyruvate oxidase binding to nanoparticle containing poly(terthiophene carboxylic acid) for phosphate ion detection and tyrosinase binding to an electrochemically prepared copolymer poly(N-3-aminopropyl pyrrole-co-pyrrole) film for detection of phenol (Rahman et al. 2006; Rajesh et al. 2004; Ramanathan et al. 2000). Recent research efforts have been directed towards entrapping biomolecules within electrochemically synthesized polymers. Presence of conjugated π electron backbones in the electroactive polymers has induced in them electrochemical properties such as high conductivity and electron affinity. Some of these common conducting polymers are polyacetylene, polyaniline, polypyrrole and polythiopene (Ahuja et al. 2007). Studies have demonstrated improved stabilization of enzymes such as GOX, *urease* and *glutamate dehydrogenase* when incorporated into conducting polymers (Gambhir et al. 2001; Reiter et al. 2001).

Principle of Detection

Biosensors can also be classified based on the type of transducer.The most common type of transducer is the electrochemical transducer. The indifference of the electrochemical transducers to the turbidity or color of the sample solution, simple equipment set up and relatively easy calibration in aqueous solution have enabled these sensors, based on potentiometry, amperometry or conductivity measurements, to become popular in the fields of analytical and clinical chemistry. The most common potentiometric transducer is the ion selective electrode (ISE), which measures cell potential at zero current. ISEs are mostly used as enzyme biosensors, whereby changes in the concentration of ions due to the enzymatic catalysis of the reaction lead to a change in potential (Racek 1995).

Optical transducers measure a change in photometric properties. Interaction between a receptor and an analyte can lead to the formation of a product with different photometric properties. Biosensors based on optical transducers can then detect the analytes by utilizing common techniques like ultraviolet-visible as well as fluorescence spectroscopy, bioluminescence, chemiluminescence and internal reflection spectroscopy. The following is an example of a biosensor involved in the detection of creatine kinase, by utilizing bioluminescence by luciferin. Creatine kinase converts creatine phosphate to creatine along with the production of ATP. This ATP can then act as a cofactor in oxidizing luciferin to oxyluciferin, thereby emitting luminescence (Eggins 1996).

$$\text{AMP + creatine phosphate} \xrightarrow{\text{Creatine kinase}} \text{ATP + Creatine} \qquad 2.2$$

$$\text{ATP + luciferin + } O_2 \xrightarrow{\text{luciferase}} \text{AMP + pyrophosphate + } CO_2 + \text{oxyluciferin + } h\nu \qquad 2.3$$

Biosensors based on the principle of surface plasmon resonance (SPR) have been increasingly used in food industries for detecting food borne pathogens such as *Listeria monocytogenes* and *E. coli* O157:H7 (Leonard et al. 2005; Waswa et al. 2007). SPR biosensors are also used for detecting various pesticides, proteins, veterinary drug residues in milk products such as chloramphenicol, penicillin and streptomycin (Baxter et al. 2001; Gaudin et al. 2001; Gaudin and P.Maris 2001; Gustavsson et al. 2004; Mauriz et al. 2007). SPR biosensors are optical biosensors which measure the change in refractive indices on the sensor surfaces due to the interactions between the sensing elements and the analytes. SPR biosensors are advantageous over spectroscopy based biosensors due to the fact that they employ a label free mode of operation for detecting analytes (Eggins 1996).

Piezoelectric biosensors find their applications in pesticides as well as in health care (Abad et al. 1998; Suleiman and Guilbault 1994; Zhou et al. 2002). A piezoelectric biosensor consists of a piezo crystal with a characteristic resonant frequency. The resonant frequency depends on the mass of the crystal as well as that of the coating. Adsorption and desorption of analytes from the crystal surface leads to a change in the

resonant frequency (Δf). The change in frequency can then be related to the change in mass according to equation 2.4.

$$\Delta f = Kf^2 \Delta m / A \qquad 2.4$$

where A is the sensor area, f is frequency and K is equilibrium constant (Eggins 1996). Quartz crystal microbalance (QCM) is the most commonly known piezoelectric biosensor. The QCM based biosensors have been used in many applications ranging from detection of HIV – 1 tat protein to *Salmonella sp.* in milk samples (Park et al. 2000; Tombelli et al. 2005).

Biochemical reactions generate or adsorb heat. Thermal based biosensors measure the change in heat and relate it to the extent of the reaction. This technique involves the use of highly sensitive thermometers having the ability to track changes in temperature as low as 0.001 ^{0}C. Thermal biosensors have been used mostly for detecting pesticides (YiHua et al. 2005a; YiHua et al. 2005b).

Applications

Biosensors are increasingly used in the food and agricultural industry, environmental, toxicological as well as in defense applications and most importantly in medical applications.

Conventional methods for analyzing the body fluids involving chemical analysis of samples of blood, urine, etc require several days. This becomes critical for patients in intensive care or in emergency situations. This problem resulted in the patronization of sensors in the field of health care. Biosensors provide fast on the spot analyses of body fluids. Biosensors can analyze body fluids to determine the levels of glucose, sodium, potassium, calcium, creatine kinase, ammonia, etc in a very short time. The first biosensor that was successful commercially was the glucose sensor launched by Exatech in 1987.

The detection of contaminants in food, monitoring the quality of food and product freshness are some of the areas where biosensors can be potentially utilized in the food industry. Another requirement in the food industry is the identification of different components of food like vitamins, essential amino acids, flavoring agents, preservatives, allergens etc on the food labels. Researchers have also demonstrated the ability of a

biosensor array to detect food allergens as well as common proteins and amino acids (Sarkar and Turner 2004; Shriver-Lake et al. 2004). Researchers have shown that biosensors have the ability to detect various drug residues in milk products such as chloramphenicol, penicillin and streptomycin (Baxter et al. 2001; Gaudin et al. 2001; Gaudin and P.Maris 2001; Gustavsson et al. 2004). Opportunities exist for applications of biosensors in the beer industries to control and improve their products. Researchers have shown that enzyme based biosensors are capable of detecting diacetyl in beer (Vann and Sheppard 2005). The fact that biosensors are inexpensive yet highly selective is increasing their chances of success in modern food production technology.

With the high demands for treatment of industrial and urban wastewater effluent, recent years have seen a tremendous boost in the development of biosensors for water treatment. Increased use of pesticides has resulted in their widespread presence in water and soil. Recent efforts have been directed in the detection of organophosphorous and carbamate pesticides by using biosensors (Abad et al. 1998). Conventional techniques used for detecting heavy metals like Cu^{2+}, Cd^{2+}, Zn^{2+}, Hg^{2+}, etc. are facing tough competition from biosensors. In general, while cell based biosensors have been used for determining the toxicity of heavy metals (Campanella et al. 1996; Liu et al. 2007), enzyme based biosensors are generally used for monitoring levels of metals.

Over recent years, the defense and security industries have witnessed a rapid growth in the development of biosensors. The terrorist attacks and the wave of anthrax letters have revealed the endangered conditions of the civil populations, thereby providing the required momentum for research involving biosensors. Detection of hazardous materials or germs, chemical warfares, illicit drugs, explosives etc are some of the avenues where biosensors can find potential applications. Researchers have already demonstrated the ability of biosensors to detect explosives and nerve agents (Lei et al. 2005; Whelan et al. 1993).

2.2 Tissue and Cell-Based Biosensors

Even though research on cells has been carried out for a very long time, the concept of using cells as the recognition element to detect different analytes is comparatively new

(Bousse 1996). The potential applications of whole cell based biosensors are in the field of drug discovery, clinical diagnostics and for monitoring toxins, chemicals, heavy metals, pesticides or herbicides (Bousse 1996; Campanella et al. 1996; Liu et al. 2007; Pancrazio et al. 1998; Pancrazio et al. 1999; Ziegler 2000). There are several advantages of using cell based biosensors over the commonly used enzyme or antibody based biosensors. Purification and isolation of enzymes are difficult, and many enzymes lose their activity during these stages. These stages can be readily omitted if cellular and tissue biosensors are used. In addition, cells are more tolerant over a range of temperature and pH than the purified enzymes or other proteins (Eggins 1996; Racek 1995). Moreover, the enzymes being within the cell, their natural environment, are more stable as they are less susceptible to denaturation. As a result, the lifetime of cell based biosensors is much longer than the enzyme based sensors. For example, while the glutaminase based biosensor for detecting glutamine is useable only for one day, the bacterial cell *Sarcina flava* based sensor can be used over a period of twenty days, and the tissue based biosensor containing a slice of porcine kidney is stable for a month. Whole cells are the smallest self sustaining biological entities; thus, if cells can be used for the sensor, the sensors become inexpensive (Eggins 1996; Racek 1995). On the other hand, since the substrate now has to diffuse through the cell membranes before coming in contact with the enzyme, the response time of these sensors can be greater. Secondly, since cells/tissue host multiple enzymes within them, the selectivity associated with purified enzyme based sensors is reduced. For example, banana tissue, containing polyphenolases, can be used to determine dopamine, a catecholamine as well as catechol itself and flavanols (Eggins 1996; Sidewell and Rechnitz 1985).

These sensors can be further categorized based on cell type depending on whether microorganisms, mammalian cells or animal or plant tissue have been immobilized (Racek 1995; Ziegler 2000). Cell based biosensors can also be categorized on the basis of their measurement principle (Ziegler 2000). Some examples where the whole cell based sensor technology has been used include: (i) measurement of the metabolic products / energy metabolism and (ii) measurement of the mechanical contact between cells and between cell and substrates (Pancrazio et al. 1999; Ziegler 2000). Metabolic activity in cells can be measured by the rate of acidification of the extracellular environment of the

cells (Owicki and Parce 1992) or by the change in the oxygen, glucose or lactose content (Ziegler 2000). For measuring the cell-cell contact, the cells are either cultured on an array of planar electrodes or on the top of a water porous filter membrane.

2.2.1 Tissue Based biosensors

Biosensors based on tissue slices are easy to prepare. A slice of tissue can be cut with a razor blade and directly placed on the transducer surface or can be immobilized within a semipermeable membrane such as a nylon mesh (Racek 1995). Because the integrity of the tissue is high, chances of single cell detaching from the surfaces are low. Moreover, slices of tissue from plants like spinach leaf, ground beet root or banana pulp can be mixed with graphite powder and mineral oil to form a carbon electrode paste (Racek 1995). Similarly, tissue slices from animals have also been used as the recognition unit. For example, tissue from white pig liver has been used for detecting uric acid (Wu et al. 2005b). The presence of urate oxidase in the tissue has been utilized to oxidize uric acid to produce hydrogen peroxide. H_2O_2 thus produced, reacts with luminol in the presence of potassium hexacyanoferrate (III) generating chemiluminescence signal (Wu et al. 2005b). Similarly, tissue slices from heart and kidney from pork have been used for detecting pyruvic and lactic acid respectively (Wu et al. 2006; Wu et al. 2005a). Tissue based biosensor can be stored for long time without affecting its applicability. For example, ascorbate oxidase activity in a tissue slice from yellow squash was retained for one year (Macholan and Chmelikova 1986). Table 2.1 lists some tissue based biosensors.

2.2.2 Microbial Cell-Based Biosensors

Microorganisms such as yeast, bacteria and algae, play critical roles in biotechnology processes such as fermentation, waste water treatment etc. Over the years, the applications of microbial cells as biosensors have ranged from detection of chemicals and pesticides to monitoring water quality. Sensors incorporating cells from bacteria and yeast coupled with oxygen electrodes have been used to detect many chemicals including formaldehyde (Korpan et al. 1993) and cholanic acid (Campanella et al. 1996). The alteration in the reduction of the iron complex ($[Fe(CN)_6]^{3-/4-}$) due to the change in the photosynthetic activity of cyanobacteria in the presence of herbicides has been utilized to

Table 2.1 Tissue Based Biosensors. (Modified from Eggins 1996, Racek 1995)

Substrate	**Tissue**	**Device/Probe**
Glutamate	Yellow squash	CO_2
Dopamine	Banana pulp	O_2
Tyrosine	Sugar beet	O_2
Cysteine	Cucumber leaf	NH_3
Ascorbic acid	Yellow squash	O_2
Catecholamines	Spinach leaf	O_2
Asparagine	Petal of magnolia	NH_3
Glutamine	Porcine kidney	NH_3
Hydrogen peroxide	Bovine liver	O_2
Oxalate	Banana skin	H_2O_2
AMP	Rabbit Muscle	NH_3
Guanine	Rabbit Liver	NH_3
Glutamine	Porcine kidney mitochondria	NH_3
Adiuretine	Toad Bladder	Na^+

detect the presence of herbicides (Rawson et al. 1989). Another approach using microbial cells is to immobilize genetically engineered cells on a sensor surface. Sensors containing bacterial cells with bioluminescent reporter genes have been utilized in the detection of benzene, toluene and mercury (Applegate et al. 1998; Burlage et al. 1994; Selifonova et al. 1993). Another example is the utilization of the genetically engineered *E. coli*, expressing organophosphate hydrolase enzyme, to detect insecticides or nerve agents such as sarin gas (Campanella et al. 1996; Pancrazio et al. 1999). The presence of toxic compounds has been determined by using light producing genes as the reporter genes. In these toxicity assays, genetically engineered bacterial cells, expressing *lux* gene, are used. Decrease in the production of the light can then be related to the presence of the toxic elements in the sample (Hansen and Sorensen 2001). Table 2.2 lists some common microorganism based biosensors.

Freeze drying of bacterial and yeast cells have been utilized to store the microbial cells over a substantial period of time. Moreover, these sensors can also be stored at + 4 ^{0}C by immersing the electrode tip in the working buffer containing required nutrients (Racek 1995).

2.2.3 Mammalian Cells-Based Biosensors

Recent years have witnessed tremendous interests in studies related to the structure, function and characteristic of mammalian cells. The fact that these cells house many proteins, enzymes and receptors enables them to respond to many biological analytes. As a result, the applications of the mammalian cell based sensors range from screening drugs to determining toxins and monitoring the environment. The increased applications of cell based biosensors are also expected to reduce the use of live animals for drug testing purposes.

Rapid developments in organic chemistry and genomics have led to the discovery of molecules having the ability to act as drugs. Sensitive screening tests of these potential drugs are necessary to identify the most promising candidates. Cell-based biosensors have been increasingly used for this screening purpose. For example evaluation of the chemosensitivity of tumor cells has been used to predict the effect of anticancer drugs on

Table 2.2 Microbial Cell Based Biosensors (Modified from Eggins 1996 and Racek 1995)

Substrate	Microorganism	Device/Probe
Glucose	*Pseudomonas fluorescence*	O_2
Acetic Acid	*Trichosporon brassicae*	O_2
Ethanol	*Trichosporon brassicae*	O_2
Glutamic acid	*Escherichia coli*	CO_2
BOD	*Trichosporon cutaneum*	O_2
Ammonia	Nitrifying bacteria	O_2
Ascorbic acid	*Enterobacter agglomerans*	O_2
Asparagine	*Serratia marcescens*	NH_3
Aspartame	*Bacillus subtilis*	O_2
Arginine	*Streptococcus lactis*	NH_3
Cholesterol	*Nocardia erythrocytes*	O_2
Cysteine	*Proteus morgani*	H_2S
Lactate	*Escherichia coli*	O_2
Methane	*Methylomonas flagellate*	O_2

patients (Metzger et al. 2001; Torisawa et al. 2003; Torisawa et al. 2004; Torisawa et al. 2005). For this purpose, the effect anticancer drugs such as 5-fluorouracil, adriamycin, ocetaxel, cisplatin and paclitaxel on different human cancer cell lines such as MCF-7, BT474, PC12, A549, HL-60 and K562 were determined (Metzger et al. 2001; Torisawa et al. 2003; Torisawa et al. 2004; Torisawa et al. 2005).

Heavy metals being toxic pose great threat to human health even when present in trace amounts. It is not the total concentration of these metals, but rather the bioavailable concentration that correlates with toxicity. This initiated the development of mammalian cell-based sensors for toxicity determination. Researchers have shown that cardiac cell based biosensors can detect different heavy metal ions such as Hg^{2+}, Pb^{2+}, Cd^{2+}, Zn^{2+}, Cu^{2+} and Fe^{3+} at concentrations of 10 μM within 15 min (Liu et al. 2007). Exposure of the cardiac cells, cultured on light addressable potentiometric sensor, to these heavy metals resulted in change in frequency, duration and amplitude of sensor signals. Another approach for monitoring environmental conditions has been in the development of the olfactory cell based sensor. Recent research has demonstrated the ability of an olfactory cell based biosensor to act as potential bioelectronic nose (Liu et al. 2006).

Another type of mammalian cell-based sensor was developed to measure metabolic rate. The rate of metabolism can be obtained from the rate of acidification of the extracellular environment of the cell or from the change in concentration of oxygen, glucose etc (Owicki and Parce 1992; Ziegler 2000). Research has demonstrated that exposure of primary neurons to γ - aminobutyric acid, an inhibitory neurotransmitter, and kainic acid, an excitatory neurotransmitter, led to an increase in cell metabolism and eventually to the increased rate of acidification of the extracellular environment (Pancrazio et al. 1999).

Another approach of mammalian cell-based biosensor relies on the mechanical contact between the cells. For this purpose, the cells are either cultivated directly on the top of electrodes or on top of water porous filter membranes. Impedance, measured as a function of time and changed environment, can be related to the change in the cell adhesion, spreading and motility (Giaever and Keese 1986, 1991, 1993; Mitra et al. 1991). The fact that intact living cells are good insulators at low frequencies has been utilized in

the development of sensors based on electric cell-substrate impedance sensing (ECIS). In the absence of cells on the electrode surface, there is but little impedance. As the cells grow and migrate to form confluent monolayer across the electrode surface, effective impedance increases. This technique has been utilized in detecting motion of cells at nanometer levels (Giaever and Keese 1991, 1993; Noiri et al. 1997). Impedance measurements have also been used to detect the effect of different inflammatory agents on the permeability of cell monolayers (Abdelghani et al. 2002; Hillebrandt et al. 2001). Impedance measurements of cell-cell contact has also been applied to investigate fundamental morphological science of cells such as studying healing of wounds induced in endothelial cell layers, blood-brain barrier properties or apoptosis (Arndt et al. 2004; Ziegler 2000). Table 2.3 lists some common mammalian cell based biosensors.

2.3 Ion Selective Electrodes

The present study utilizes mammalian cell permeability dysfunction to detect the presence of small quantities of permeability modifying agents. For the purpose, cells were seeded across the asymmetric cellulose triacetate (CTA) membrane of an ion selective electrode (ISE). Since ISEs play an integral part in the present study, background information on ISEs is provided in this section.

Ion selective electrodes are electrochemical sensors which can determine the activity of specific ions in a sample, as a function of electromotive force (emf). Typically the primary components of a membrane based ISE are: (A) the indicator electrode or working electrode and (B) the reference electrode (Bakker et al. 1997). Figure 2.3 shows a schematic of an ISE. The indicator electrode consists of an inner reference electrode (Ag/AgCl), the inner filling solution and an ion selective membrane. The indicator electrode generates a potential corresponding to the activity of the ion of interest in the sample solution. The reference electrode maintains a constant potential against which the potential of the indicator electrode is measured (Morf 1981). The ion selective membrane acts as the barrier between the sample solution and the inner filling solution. In polymer membrane ISEs, the membrane consists of i) a plasticized polymeric phase, most commonly with poly (vinyl chloride) and cellulose triacetate as the polymer matrix, ii) an

Table 2.3 Mammalian Cell -Based Biosensors

Substrate	**Cell type**
Hydrogen Peroxide	Human erythrocytes
Glutamine	Pork kidney cells
Anti tumor drugs	Mouse leukemia cells
Anti tumor drugs	Human cancer cells
Heavy metal ions	Mouse cardiac cells
Histamine	Human umbilical veins endothelial cells

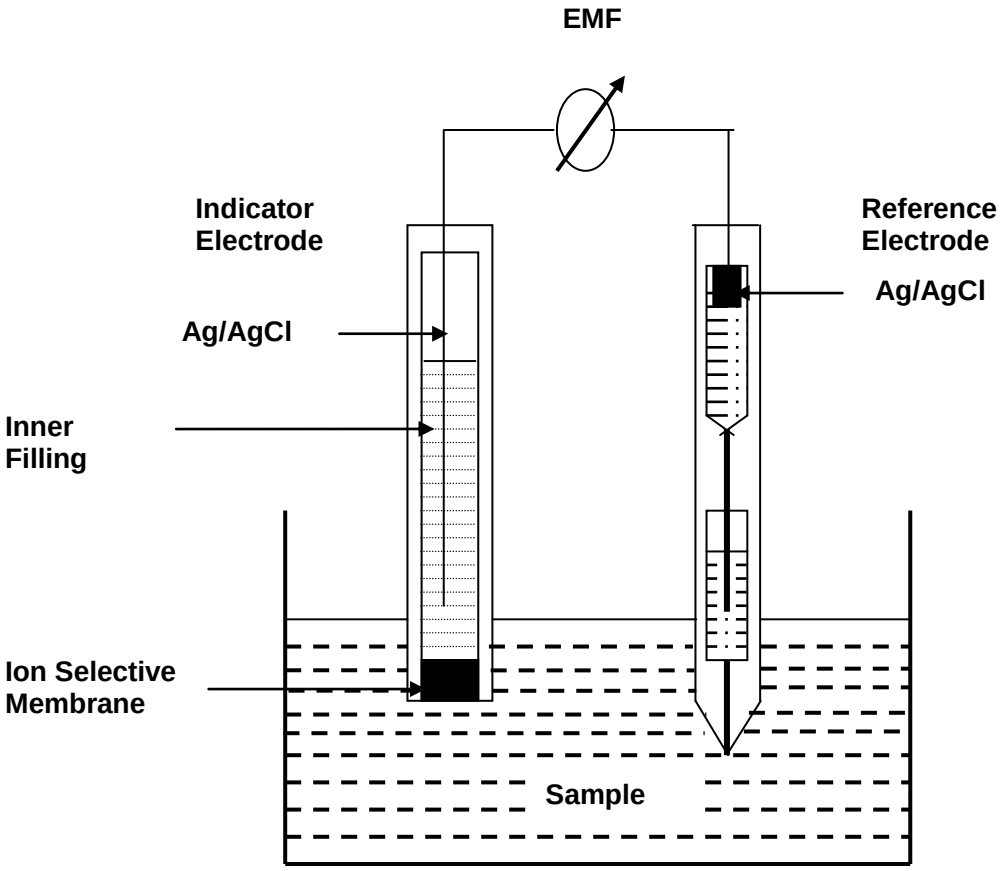

Figure 2.3 Schematic diagram of a membrane-based ISE. (Modified from Bakker et al. 1997)

ionophore that provides selectivity to the membrane by binding specifically to the ion of interest, iii) a lipophilic salt that helps in maintaining the elctroneutrality within the membrane and iv) plasticizer that helps in dissolving of the ionophore within the membrane. Table 2.4 shows the typical composition of the membrane of an ion selective electrode.

With ISEs, the changes in electromotive forces (emf) are measured, as a function of the activity of the ion of interest, under zero current conditions. The response of the ISE can be described by the phase boundary model. The potential developed at the interface of the aqueous and the organic phase (the polymeric membranes are assumed to behave as the organic liquid) is measured by using the thermodynamic equilibria and electroneutrality conditions within each phase. This model assumes that the ion transport processes are considerably fast between the phases (Bakker et al. 1999). The other theories which describe the response mechanism of ISE are the kinetic or ion transport model and the membrane surface or space charge model (Morf 1981). However, the ion transport model, which considers that the selectivities are related to the ionic mobilities, reduces to the phase boundary model when the assumption of equal mobilities is made (Bakker et al. 1999). The space charge model assumes that the membrane surface processes are only relevant for the generated potential (Bakker et al. 1999). Since, this model also assumes the existence of equilibrium at the membrane surface, the obtained predictions about emf responses from this model are the same as the given by the phase boundary model (Bakker et al. 1999). Even though the latter two models explain the response mechanism in more detail, they also incorporate more assumptions and parameters (Bakker et al. 1999). It has been documented that the simpler phase boundary potential model has the ability to explain the experimental results satisfactorily (Bakker et al. 1997).

In the phase boundary potential model, the relationship between the phase boundary potential, E, and the activities of the ions in both phases is given by:

$$E = E^0 + \frac{RT}{zF} \ln \frac{k_1 a_m(aq)}{a_m(org)} \qquad 2.5$$

where, E^0 incorporates the constant potential contributions. a_m (aq) and a_m (org) are the activities of the ion with z charge in the aqueous and organic phase. The free energy for

Table 2.4 Typical Composition of the Carrier Based Membrane of Ion Selective Electrodes

Component	Composition
Ionophore	1 wt%
Plasticizer	65 wt%
Polymer	33 wt%
Lipophilic Additive	50 mol% (with respect to ionophore)

transfer of ion from the aqueous to the organic phase is incorporated into the constant term, k_1. R, T and F are the gas constant, the absolute temperature and Faraday constant respectively. Assuming that the membrane phase composition remains constant as the sample composition is varied and there are no interferences from the other sample ions, the above equation reduces to the Nernst equation:

$$E = E^0 + \frac{RT}{zF} \ln a_m(aq) \qquad 2.6$$

For a monovalent ion at 25 ^{0}C, the above equation reduces to:

$$E = E^0 + 59.2 \log a_m(aq) \qquad 2.7$$

Calibration curves are constructed by plotting the potential against the logarithm of the ionic activities. A typical calibration curve is shown in Figure 2.4. In the case of an asymmetric cellulose triacetate (CTA) potassium selective electrode, the slope of the calibration curve has been observed to be around 52 ± 3 mV/decade (Brooks et al. 1996). According to IUPAC recommendation, detection limits of ISEs can be obtained in two different ways (Buck and Lindner 1994). Minimum detectable concentration is the concentration corresponding to the potential which deviates from the average potential of the electrode in the linear region of the plot by a multiple of standard error. The second method of obtaining the detection limit involves the extrapolation of the two linear regions of the curve. The concentration or activity corresponding to the intersection of the two extrapolations constitutes the detection limit of the electrode. The latter method is illustrated in Figure 2.4.

Earlier studies have shown that incorporation of a confluent monolayer of human umbilical vein endothelial cells (HUVECs) onto the asymmetric CTA membrane resulted in inhibited response from the biosensor (May et al. 2005; May et al. 2004a) due to inhibition of potassium ion transfer by the cell monolayer. When the permeability across HUVECs is altered in the presence of histamine or VEGF, potassium ions can reach the membrane surface thereby leading to an increased sensor response (May et al. 2005; May et al. 2004b). The response thus obtained can be related to the concentration of these permeability modifying agents. In the present study, the mammalian cells used as the sensing device included HUVECs and porcine epithelial cells (LLC-PK1), and cell permeability dysfunction has been utilized to detect physiological toxins.

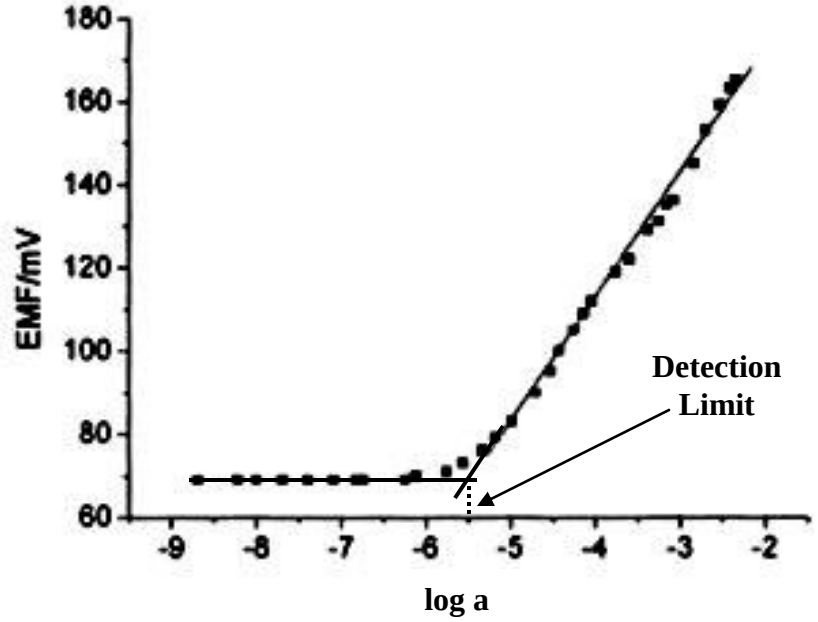

Figure 2.4 Typical calibration plot of an ISE. Modified from (Lazo et al. 2006)

Chapter 3 : Materials and Methods

Cell culture, membrane fabrication and evaluation of the electrode response are some of the techniques used throughout this study. This chapter describes the methods employed as well as the reagents required for these techniques. However, specific experimental methods and corresponding materials for particular studies have been described in respective chapters.

3.1 Cell Culture

Human umbilical vein endothelial cells (HUVECs) and porcine epithelial cell - line LLC-PK1 were cultured during the course of the research. Both cell types were cultured inside a sterile laminar flow hood and incubated in a humidified incubator maintained at 37 ^{0}C and 5% CO_2.

3.1.1 Reagents

HUVECs obtained from Cambrex Bioscience (East Rutherford, NJ) were cultured in EGM-2 media, supplemented with fetal bovine serum, hydrocortisone, insulin like growth factor, basic fibroblast growth factor, vascular endothelial growth factor, human epidermal growth factor, ascorbic acid, human fibroblast growth factor, gentamicine sulphate, amphotericin-B and heparin, also obtained from Cambrex Bioscience. Trypsin/EDTA, trypsin neutralizing solution (TNS) and HEPES buffered saline solution (HBSS) were also from Cambrex Bioscience.

LLC-PK1 cells obtained from ATCC (Manassas, VA) was cultured in Medium 199 (M 199) from Sigma Aldrich (Milwaukee, WI) supplemented with 3% fetal bovine serum (FBS). FBS and trypsin/EDTA were obtained from ATCC.

3.1.2 Culturing HUVECs

Upon arrival from Cambrex Bioscience, cells were stored in liquid nitrogen for future use. Before breaking cells out of freezing, HUVEC media was warmed for 45 min by placing it a water bath maintained at 37 ^{0}C. Ten milliliters of media was then aliquoted into a 75

cm^2 cell culture flask. The vials containing the frozen cells were then taken out of the liquid nitrogen tank, the caps of the vials turned to release pressure and the cells thawed by holding the vial inside the water bath maintained at 37 ^{0}C until the last piece of ice started to melt. The vials were then wiped with 10% bleach and sprayed with 70% ethanol before placing them inside the laminar flow hood. The cells were transferred to the cell flask using a sterile transferring pipette. The cell flask was then placed inside the incubator. Following the breaking of cells out of freezing, the cell media was changed every 24 h until the cells became confluent.

Once HUVECs were confluent, the media was aspirated and the cells were rinsed with 9 mL of HBSS. The cells were then incubated with 6 mL of trypsin/EDTA for 3 min. After the cells had detached from the cell culture flask, 12 mL of trypsin neutralizing solution was added. The cells were transferred to sterile centrifuge tubes and centrifuged for 5 min. Following centrifugation, the supernatant was removed, and the cells were resuspended in HUVEC media. The cells in each centrifuge tube were diluted in 10 mL HUVEC media and transferred to a different cell culture flask for further culturing.

To ensure ample cells for future use, some cells were frozen and kept inside a liquid nitrogen flask. For the purpose of freezing the cells, the confluent cells were detached from the culture flask similarly as described above. The cells were centrifuged and the supernatant decanted, and the cells were resuspended. A volume of 2 mL of freezing media, consisting of 10% FBS, 10% DMSO and 80% HUVEC media, was then used to dilute the cells in each tube. The diluted solution was then transferred to the cryogenic vials. The vials containing the cells were initially kept in the freezer at -80 ^{0}C for 24 h before storing in the liquid nitrogen tank.

3.1.3 Culturing LLC-PK1

The same protocol as described in case of HUVEC was followed for breaking LLC-PK1 out of freezing, except the media used was M199 supplemented with FBS. The media was changed twice a week, until the cells were confluent.

Once the cells were confluent, the media was removed, and the cells were rinsed with 3 mL of trypsin/EDTA solution. The solution was removed, and the cells were then incubated at 37 ^{0}C for 10-15 min with 3 mL of freshly added trypsin/EDTA solution.

Once the cells had detached, fresh media was added to the cells and the cells were diluted. The diluted cells were then transferred to different culture flasks for further culturing.

For the purpose of storing LLC-PK1 for future use, the cells were detached from the culture flask by incubating with trypsin /EDTA solution as described above. A volume of 7 mL of M199 media was then added to the culture flask and the cells were transferred to the centrifuge tubes. Following 5 min centrifugation, the supernatant was disposed off and the cells resuspended. A volume of 2mL freezing media consisting of 95% culturing media and 5% DMSO was used to dilute the cells in each centrifuge tube. As described for HUVECs, the diluted LLC-PK1 were then transferred to cryogenic vials and stored at -80 ^{0}C for 24 h prior to storing in a liquid nitrogen tank.

3.1.4 Counting Cells

Cells were counted with the hemacytometer to determine the cell density. For the purpose of counting cells, the cells were detached from the cell culture flask and transferred to the centrifuge tubes as described above. A volume of 0.5 mL of cell solution was aliquoted from the centrifuge tubes. The cells were then diluted 10 fold with HBSS in case of HUVECs and with M 199 in case of LLC- PK1 and transferred to both chambers of a hemacytometer. The number of cells in the square at the center as well as at the four corners of the chamber was counted in each chamber. Figure 3.1 shows a schematic of hemacytometer and describes the process of counting cells.

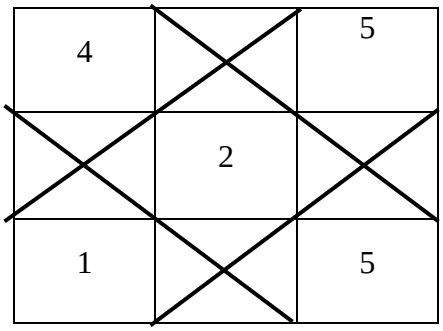

Total Number of cells = 17

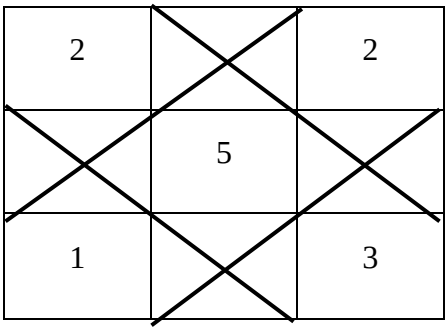

Total number of cells = 13

Each square of hemacytometer = 0.1 mm^3 = 10^{-4} c.c

Total number of cells = 17 + 13 = 30

Number of cells/ square = 30/10 = 3

Number of cells/mL = 3x 10 (dilution factor) x 10^4 (hemacytometer factor)

= 3 x 10^5

Figure 3.1 Counting cells using hemacytometer

3.2 Fabrication of Asymmetric Cellulose Triacetate Membrane

3.2.1 Reagents

Cellulose triacetate (CTA) pellets, methylene chloride, chloroform, 1,1,2,2 tetrachloromethane and all chloride salts were purchased from Aldrich (Milwaukee, WI). Valinomycin, the ionophore, was obtained from Calbiochem (San Diego, CA). The plasticizer *o*-nitrophenyl octyl ether (NPOE) and the lipophilic salt potassium tetrakis(chlorophenyl)borate (KTClPB) were from Fluka (Ronkonkoma, NY) whereas carbonyldiimidazole (CDI) and tris(hydroxymethyl)aminomethane (Tris) were from Sigma (St. Louis, MO). Deionized water obtained with a Milli-Q Water Purification System from Millipore (Bedford, MA) was used to prepare the aqueous solutions. The synthetic RGD peptide sequence (Gly-Arg-Gly-Asp-Ser (GRGDS)) was obtained from Bachem (King of Prussia, PA).

3.2.2 Membrane Fabrication

Earlier studies have demonstrated that hydrolysis of the asymmetric CTA membrane containing valinomycin as the ionophore facilitates further surface modification and biomolecule attachment (Brooks et al. 1996; Cha and M.E.Mayerhoff 1989; Cha et al. 1995; Koncki et al. 1997; Sakong et al. 1996). The procedure for preparation of the RGD modified CTA membrane was adapted from May and coworkers (May et al. 2004b).

Figure 3.2 and Figure 3.3 demonstrate the schematic of the membrane preparation procedure as well as the chemistry involved in various steps of membrane preparation. Initially, the base layer solution, consisting of 74 mg of CTA dissolved in 1.1 mL methylene chloride, 0.4 mL cholorform and 0.4 mL tetrachloromethane, was cast in a 31 m.m i.d. glass ring on a teflon plate. Following solvent evaporation, the bottom surface of the membrane was hydrolyzed by floating the membrane on 1.0 M sodium hydroxide solution for 4.5 hr. Next, the second layer consisting of the ionophore cocktail (35 mg CTA, 1 mg valinomycin, 0.42 mg KTClPB in 100 μL NPOE, 0.8 mL chloroform and 0.8 mL methylene chloride) was cast on the membrane, thereby making it sensitive to potassium ions. After solvent evaporation, when the two layers of membrane had fused to form a single asymmetric membrane, the surface of the membrane containing the

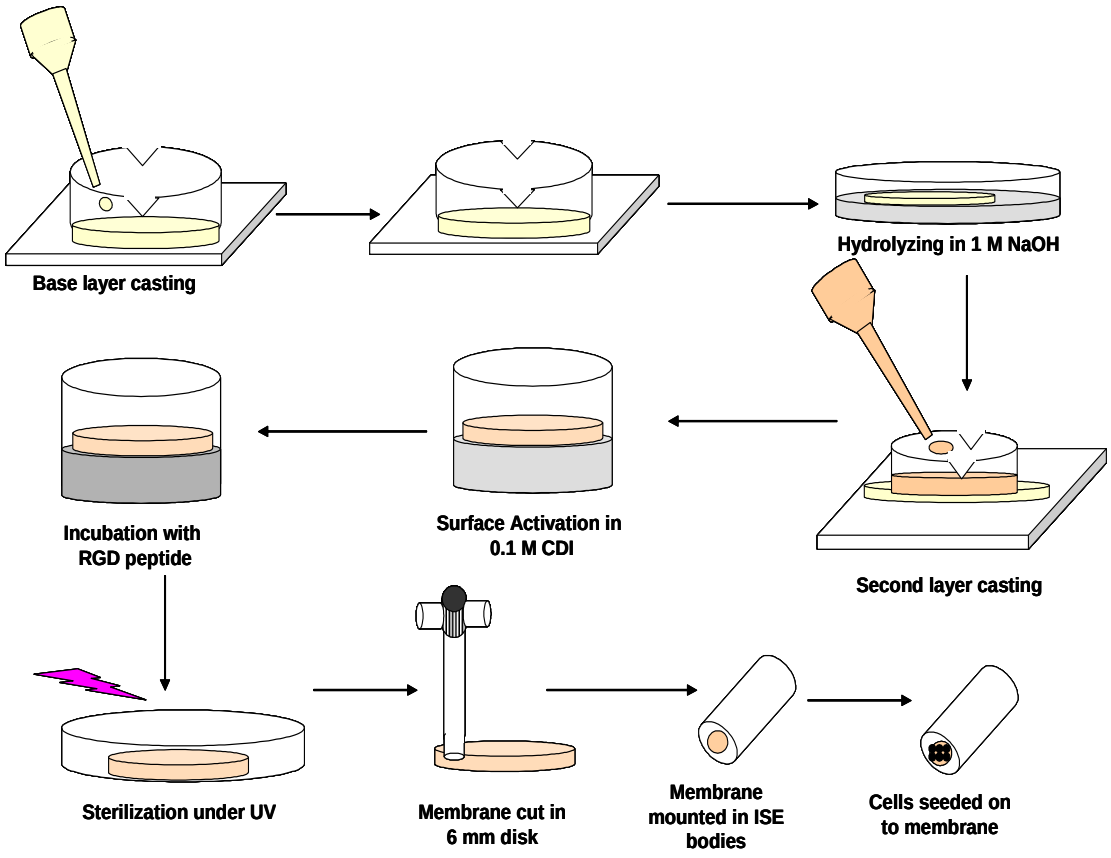

Figure 3.2 Fabrication of CTA membrane and seeding of cells

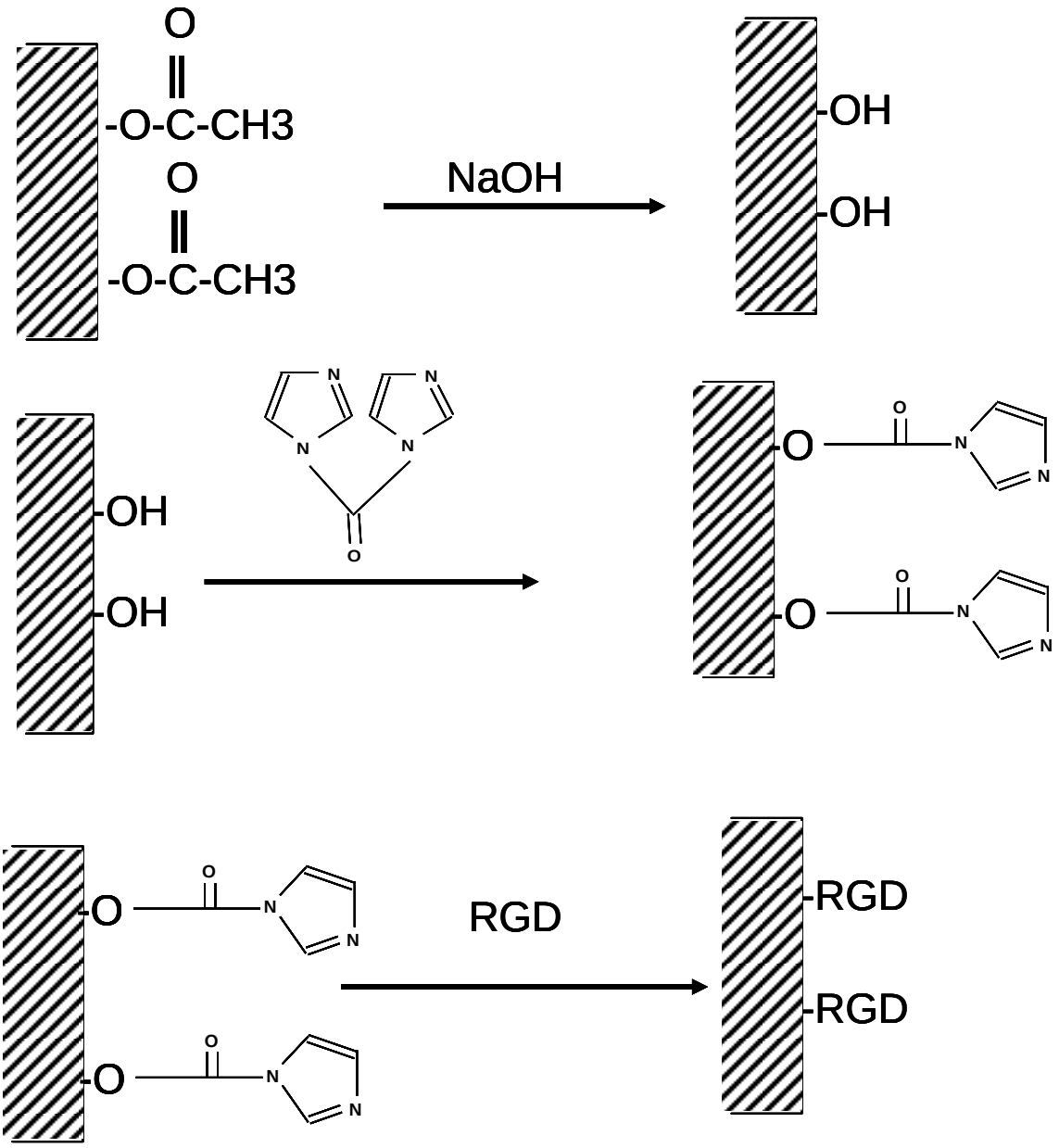

Figure 3.3 Chemistry involved in membrane preparation

hydroxyl groups was activated by incubating with 0.1 M CDI for 15 min. The surface activated membrane was then incubated overnight with 500 μg/mL RGD peptide in 0.1 M sodium carbonate solution (pH 9.5). This incubation facilitated the covalent coupling of the RGD peptide from the N-terminal amine to the membrane surface. Following incubation, the membrane was rinsed sequentially in 0.1 M sodium bicarbonate (pH 8.5), deionized water, acetate buffer (pH 4.0) and deionized water. The membrane was then exposed to germicidal UV overnight. The membranes were cut into 6 m.m i.d. disks and mounted into autoclaved ISE electrode bodies. Following conditioning in sterile 0.01 M KCl solution for 24 h, cells were seeded onto the membrane surface at a density of 1 x 10^5 cells/ml and incubated in a humidified incubator for 24 hr at 37 ^{0}C and 5% CO_2 to ensure confluent monolayer formation.

3.3 Evaluation of Electrode Response

Following confluent cell monolayer formation, the control membranes were tested for inhibited ion response. The schematic of the cell based biosensor set up is shown demonstrated in Figure 3.4. The internal reference electrode was Ag/AgCl, and the internal filling solution consisted of 0.01 M KCl. The external reference electrode consisted of a double junction Ag/AgCl electrode (Orion Model 90-02-00) with an Orion (90-02-02) internal filling solution and 0.1M Tris buffer (pH 7.5) in the outer compartment. Potentiometric responses were measured with a four channel high impedance amplifier interface (World Precision Instruments) connected to a Model 100 Instrunet A/D converter. Instrunet Software on a Macintosh Power PC was used to analyze the data. To obtain the ISE response, a series of incrementally sized sterile KCl aliquots were added to the stirred sterile buffer solution. The measured potential (mV) was plotted against the logarithm of the concentration of the potassium ions in the bulk solution to generate the calibration plots. Overall responses obtained at 0.1 M KCl solution for the membrane with cells were compared with the responses obtained for the membrane alone; 0.1 M KCl was used because it is close to physiological ionic strength.

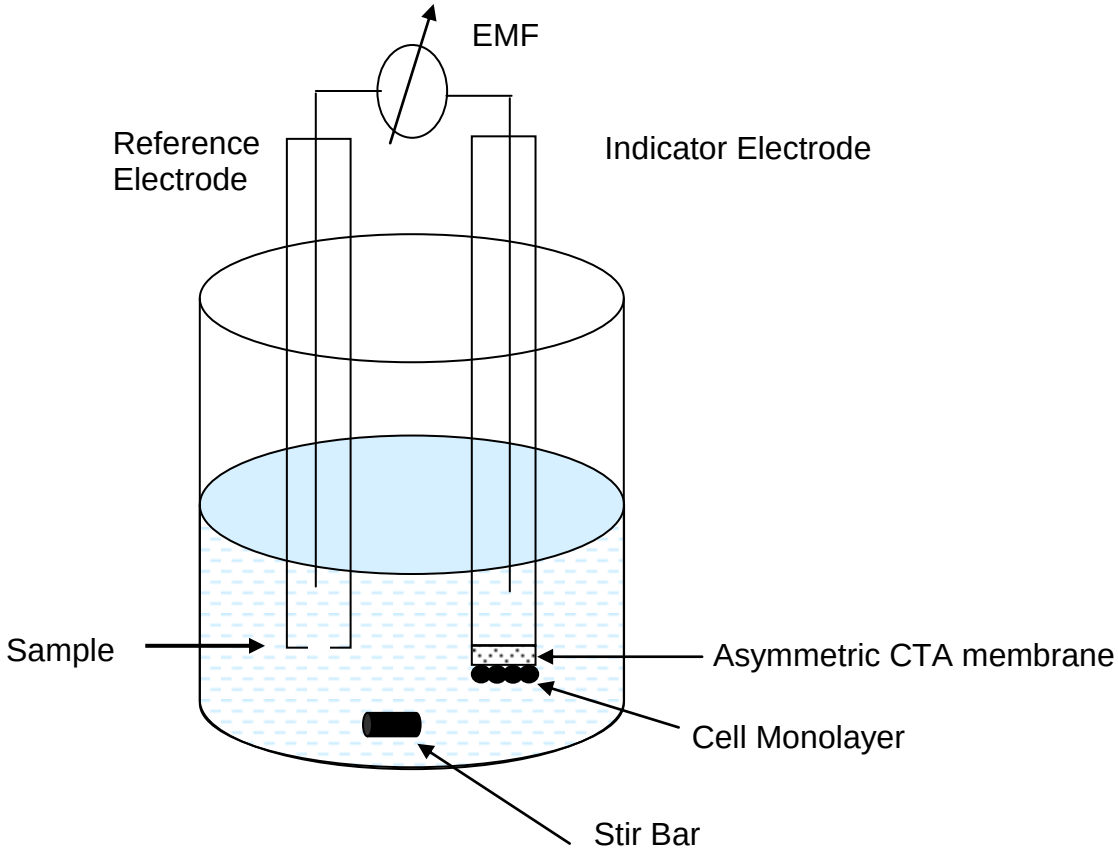

Figure 3.4 Schematic of cell- based biosensor set up

Chapter 4 ：Biosensor Incorporating Cell Barrier Architectures for Detecting *Staphylococcus aureus* Alpha Toxin

Based on studies published in: Ghosh, G., Bachas, L. G., Anderson, K. W. "Biosensor Incorporating Cell Barrier Architectures for Detecting *Staphylococcus aureus* Alpha Toxin" *Analytical and Bioanalytical Chemistry*, **2007**, 387, 567-574

4.1 Introduction

Staphylococcus aureus is one of the most common bacterial pathogens involved in various infections such as septicemia, endocarditis, osteomyelitis and septic arthritis. It is the major cause of postoperative infections and also infections associated with prosthetic devices by forming biofilms on catheters (Marrie and Costeron 1984) and pacemakers (Marrie et al. 1982). As a matter of fact, the recent years have seen a dramatic increase in the number of patients infected with sepsis related to *Staphylococcus aureus* infections with high mortality rate (Sista et al. 2004). Isolation and cultivation of the pathogen and the use of antibodies against different antigens of *S.aureus* (Christensson et al. 1983; Julander et al. 1983) are the current methods used for diagnosis of different staphylococcal diseases. The major disadvantages associated with these methods are the lack of sensitivity and the time consumption. Recent efforts have focused on identifying different antigens that would provide better sensitivity and hence early diagnosis.

Alpha toxin, a protein exotoxin produced by the majority (85-90%) of *S. aureus* strains (Mollby 1983), plays a critical factor in *S.aureus* induced pathogenicity. In fact, the presence of alpha toxin has been implicated as a necessary criterion for biofilm formation by *S.aureus* (Caiazza and O'Toole 2003). Alpha toxin is also believed to be largely responsible in *S. aureus* induced keratitis (O'Callaghan et al. 1997). This virulent factor of *S.aureus* exhibits haemolytic, cytotoxic, dermonecrotic as well as lethal effects on laboratory animals (Jonsson et al. 1985; Thelestam and Blomqvist 1988). The cytotoxicity of alpha toxin is attributed to its transmembrane pore forming ability leading to the leakage of ions and macromolecules, across the cell membrane, which eventually results in necrosis (Bhakdi S. 1991). Development of an enzyme immunoassay with

monoclonal antibodies (Soderquist et al. 1993a) as well as double antibody sandwich ELISA (Sarujballi and Fackrell 1984) for detection of staphylococcal alpha toxin has been reported. Depending on the methods employed, the assays require 6 h to overnight incubation for effective determination of alpha toxin (Sarujballi and Fackrell 1984; Soderquist et al. 1993a).

This study describes the detection of *Staphylococcal* alpha toxin using a whole cell based biosensor. The biosensor consists of a confluent monolayer of human umbilical vein endothelial cells (HUVECs) seeded on to the surface of an asymmetric cellulose triacetate (CTA) membrane of an ion-selective electrode (ISE) (May et al. 2004b). This sensor takes advantage of endothelial cell permeability dysfunction to detect the presence of small quantities of permeability modifying agents. Earlier studies with this electrode have shown that complete inhibition of ion transport across the membrane is observed when a confluent monolayer of HUVECs is formed (May et al. 2004b). This results in a reduced ISE response. Previous studies have shown that exposure of the biosensor to histamine and vascular endothelial growth factor (VEGF) resulted in an increased response from the biosensor, which can serve as an indirect measurement of the presence of these agents (May et al. 2005; May et al. 2004b).

Previous studies have demonstrated that exposing purified alpha toxin to endothelial cell monolayers leads to the rounding up of cells (Menzies and Kourteva 2000) and increase in permeability (Dorsch et al. 1999; Suttorp et al. 1985). Hence, it is hypothesized that this sensor can be used to measure the presence of alpha toxin. The aim of the present study was to determine the response of the sensor to the various concentration of alpha toxin. It was also our objective to determine the effect of exposure to alpha toxin on the integrity of cell-cell contacts, cell shape as well as on the interendothelial gaps formation. For the later purpose, the borders of HUVECs were stained with silver nitrate. Silver staining technique had been previously used to successfully determine the shape of cells (Killackey et al. 1986), neutrophil transmigration (Burns et al. 1997), and leukocyte attachment as well as to quantify the gap size and number (Hirata et al. 1995; McDonald 1994).

4.2 Experimental Section

4.2.1 Reagents

Purified *Staphylococcal* alpha toxin was purchased from List Biological Laboratories. (Campbell, CA). Glutaraldehyde, for fixing cells during silver staining, as well as silver nitrate was obtained from Sigma (St. Louis, MO). Cells were washed with Dulbecco's phosphate buffered saline (D-PBS) from Invitrogen (Carlsbad, CA). Mowiol 4 -88, the mounting reagent, was from Calbiochem (San Diego, CA). HUVECs used during the experiments, were cultured as described in Chapter 3. Membrane materials and sensor preparation had also been described in Chapter 3.

4.2.2 Evaluation of Electrode Response

Following confluent cell monolayer formation, the control membranes were tested for inhibited ion response. After the confirmation of the inhibited ion response due to the formation of the confluent monolayer, the cell-seeded membranes were exposed to varying concentrations (ranging from 0.1 ng/ml to 1000 ng/ml) of *Staphylococcal* alpha toxin solution (pH 7.2) in PBS for 20 min. The response of the sensor was measured after 20 min.

At a final concentration of 0.1M KCl, the electrode response was measured for the following conditions: (a) the membrane without cells and without alpha toxin to obtain the baseline response of the sensor (b) membranes without cells and with 1000 ng/ml alpha toxin to test the effect of the maximum concentration of alpha toxin on the sensor alone (c) membranes with cells and without alpha toxin to confirm the inhibited response of the sensor due to the confluent monolayer of cells and (d) membranes with cells and with alpha toxin at concentrations ranging from 0.1 ng/ml to 1000 ng/ml. To optimize the exposure time, the cell based membranes were exposed to alpha toxin for 10, 20, 30, 60 and 90 min.

4.2.3 Data Analysis

To account for slight variations between fabricated membranes, the final data are reported as the ratio of the response obtained at 0.1 M KCl for the ISEs with HUVECs

and alpha toxin to the response obtained for the same membrane without HUVECs and alpha toxin. Data are reported as mean ± SEM of three replicates. Multiple pairwise comparisons were carried out using one-way ANOVA and the Student-Newman-Keuls test for post-hoc comparisons of the means with $P<0.05$. SigmaStat v3.1 software was used for this purpose.

4.2.4 Silver Staining of HUVEC monolayers

To examine the effect of alpha toxin on the morphology of HUVECs, the cell monolayers were fixed and borders were stained following the method adapted from Burns and coworkers (Burns et al. 1997). Briefly, HUVECs were seeded on glass chamber slides at a density of $1x10^5$ cells/ml and cultured till confluency were reached. The confluent cell monolayers were treated with alpha toxin at concentrations varying from 0.1 to 1000 ng/ml for 20 min, the exposure time required by the sensor to detect the presence of the toxin. After the incubation period the toxin solutions were aspirated and the monolayers were fixed in 0.05% glutaraldehyde in PBS for 10 min at room temperature. This was followed by washing with D-PBS for three times. The cells were then exposed to the aqueous solution of 0.25% silver nitrate for 40 s. Following the incubation with the silver solution, the cells were washed again with D-PBS for three times. The silver stain was developed by exposing the cells to UV for 15 min. Cells were then mounted using Mowiol 4-88 and viewed under Zeiss IM 35 microscope. In each study, three independent images were photographed from randomly selected fields of view. The dimensions of endothelial cells, silver lines, number and size of silver deposits were measured using AxioVision 4 software. Gap size was determined by subtracting two times the thickness of the silver lines from diameter of the silver deposits (Baluk et al. 1997).

Average values of the dimensions of cells and number and size of silver deposits are presented as mean ± SEM of three experiments. As mentioned earlier statistical analysis were carried out using one-way ANOVA and the Student-Newman-Keuls test for post-hoc comparisons of the means with $P<0.05$. SigmaStat v3.1 software was used for this purpose.

4.3 Results and Discussion

Earlier studies have demonstrated that the immobilization of RGD peptide on the ISE membrane surface does not give rise to a mass transfer resistance and affects the sensor response minimally (May et al. 2004b). It had also been shown that with the growth of cells, the overall ISE response decreases, eventually leading to an almost completely inhibited response upon formation of a complete confluent monolayer after 24 h (May et al. 2004b) After the inhibited ion response was obtained, experiments were conducted with cells and alpha toxin.

4.3.1 Optimization of Exposure Time

Initially, experiments were performed to optimize the exposure time by exposing cell - based ISE membranes to 1000 ng/ml alpha toxin solution for 10, 20, 30, 60 and 90 min. It became important to optimize the exposure time such that not only an increased overall response would be obtained but also no damage would be caused to the cells seeded on the membrane. Calibration plots for potassium were constructed using these ISEs. An increase in the sensor response was observed with increasing exposure time (Fig. 4.1). Microscopic studies revealed that prolonged exposure to alpha toxin, at this concentration, led to detachment of cells. These results are consistent with the other studies in literature demonstrating that direct application of 5 nM alpha toxin to cultured endothelial cell monolayers for 24 h caused detachment of cells followed by apoptosis (Menzies and Kourteva 2000). Moreover, it had been also shown that application of 5 -40 ng/ml alpha toxin in isolated rabbit lung for 40-120 min led to condensation of nuclei of the endothelial cells and eventually, detachment of cells from the basal lamina (Seeger et al. 1990). Upon exposing the cultured HUVECs to 1000 ng/ml alpha toxin for varying length of time, it was observed that no damage was induced to the cells when HUVECs were exposed to alpha toxin for 20 min. In addition, a significant difference in sensor response was observed at this time when compared to the response with cells only. Hence forth, all experiments with the sensor were carried out by exposing it to alpha toxin solution for 20 mins.

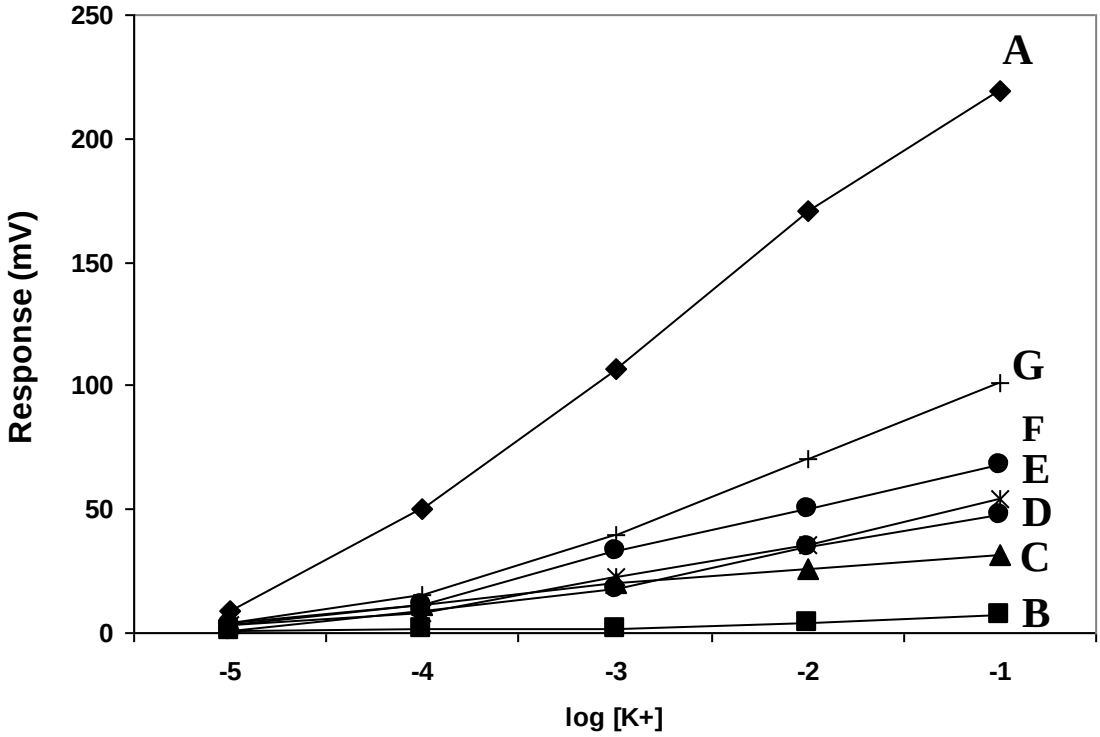

Figure 4.1 Calibration plots corresponding to (A) control, (B) cells only, (C - G) ISE electrodes with confluent monolayer of HUVECs were exposed to 1000 ng/ml alpha toxin for (C) 10 min, (D) 20 min, (E) 30 min, (F) 60 min, and (G) 90 min.

4.3.2 Evaluation of the Response from the Biosensor

Since the highest concentration of alpha toxin used in this study was 1000 ng/ml, control experiments were first performed without cells to confirm that alpha toxin does not affect the sensor response by itself. Figure 4.2 reveals that the response profile obtained from the sensor upon exposure to the toxin for 20 min matches closely with that of the control. When the overall response obtained at 0.1 M KCl for the membrane exposed to toxin for 20 min was compared with that obtained for control, it was observed that 98% of the sensor response had been recovered indicating minimal protein adsorption on the sensor surface.

The cell based membranes were then exposed to different concentrations of alpha toxin for 20 min and the response of the sensor to the presence of the toxin was measured. Figure 4.3 illustrates the overall response ratio with increasing alpha toxin concentration. The overall response ratio of the sensor increased from 0.07 to 0.20 on varying the alpha toxin concentration from 0.1 to 1000 ng/ml. TableCurve 2D v 5.01 was used to fit the experimental data to the following equation ($R^2 = 0.994$):

$$\text{Response Ratio} = 0.0417 + 0.0433 \times [\text{Alpha Toxin}]^{0.182} \qquad \text{(Equation 2.1)}$$

The above equation was used to determine the detection limit of this biosensor for alpha toxin.

4.3.3 Determination of Detection Limit

Figure 4.4 shows a plot of the total response ratio vs. logarithm of alpha toxin concentration. This is a standard curve used for determining the detection limit of alpha toxin using IUPAC recommendations (Buck and Lindner 1994). The detection limit obtained from the intersection of extrapolated parts of two linear regions of the curve is approximately 0.05 ng/ml of alpha toxin. The detection limit was also determined by using equation 2.1. Minimum detectable concentration of alpha toxin by the biosensor was considered to be the concentration at which the response deviates from the average response of the sensor in the linear region by three times the standard error. By substituting this response ratio value in equation 1, the detection limit of the sensor for alpha toxin was found to be approximately 0.1 ng/ml.

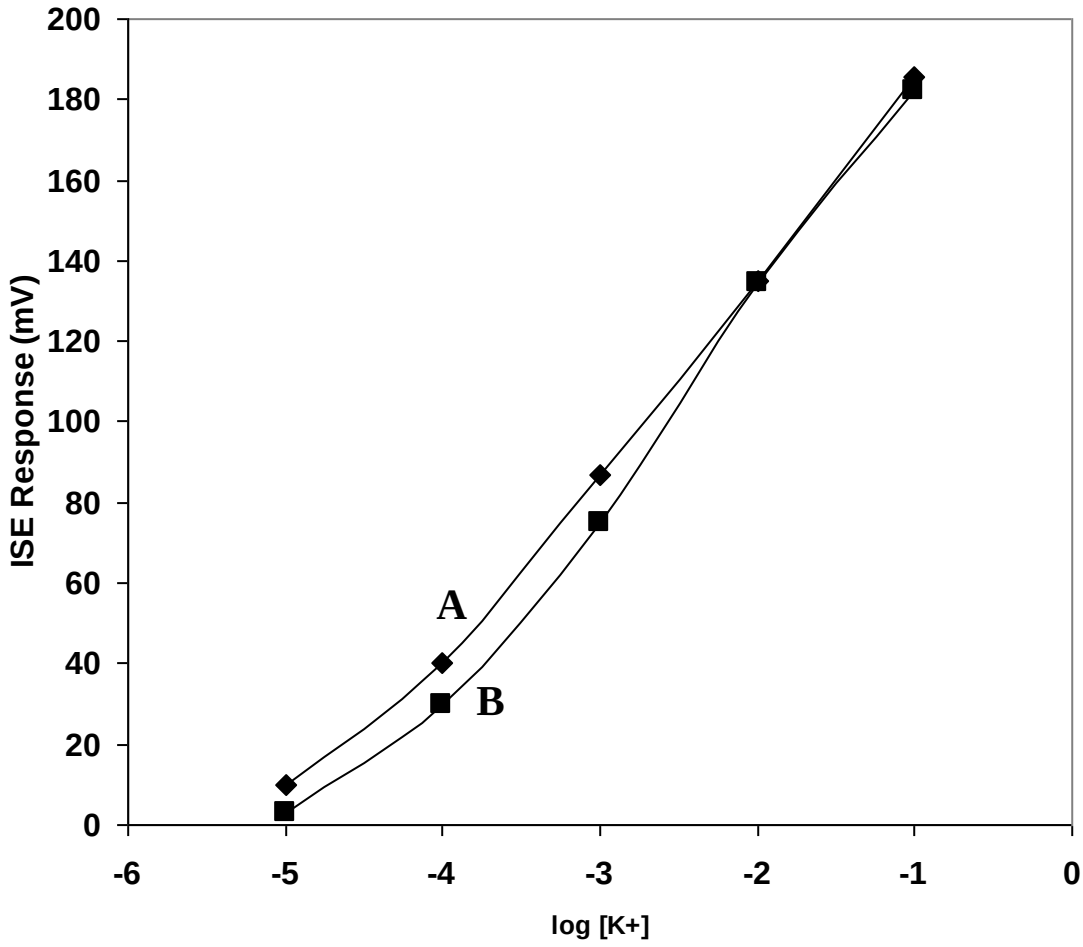

Figure 4.2 Calibration plot for the ISE membranes (A) without cells and without alpha toxin and (B) without cells and exposed to 1000 ng/ml alpha toxin for 20 min. This plot represents one experiment. The experiment was repeated two more times giving similar results

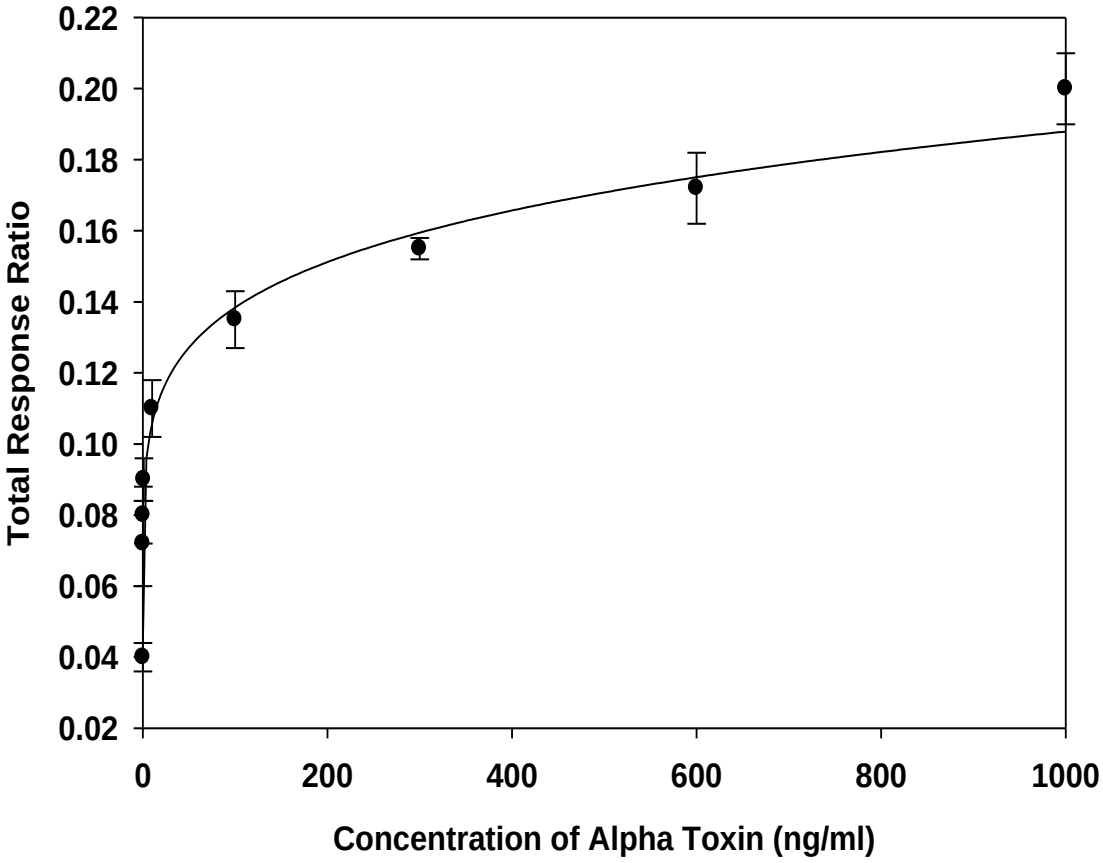

Figure 4.3 Plot of the ratio of ISE response obtained at 0.1 M KCl following exposure to alpha toxin concentration ranging from 0.1-1000 ng/ml to ISE response obtained at 0.1 KCl for the membrane without cells and without alpha toxin. (Error bars represent SE N=3)

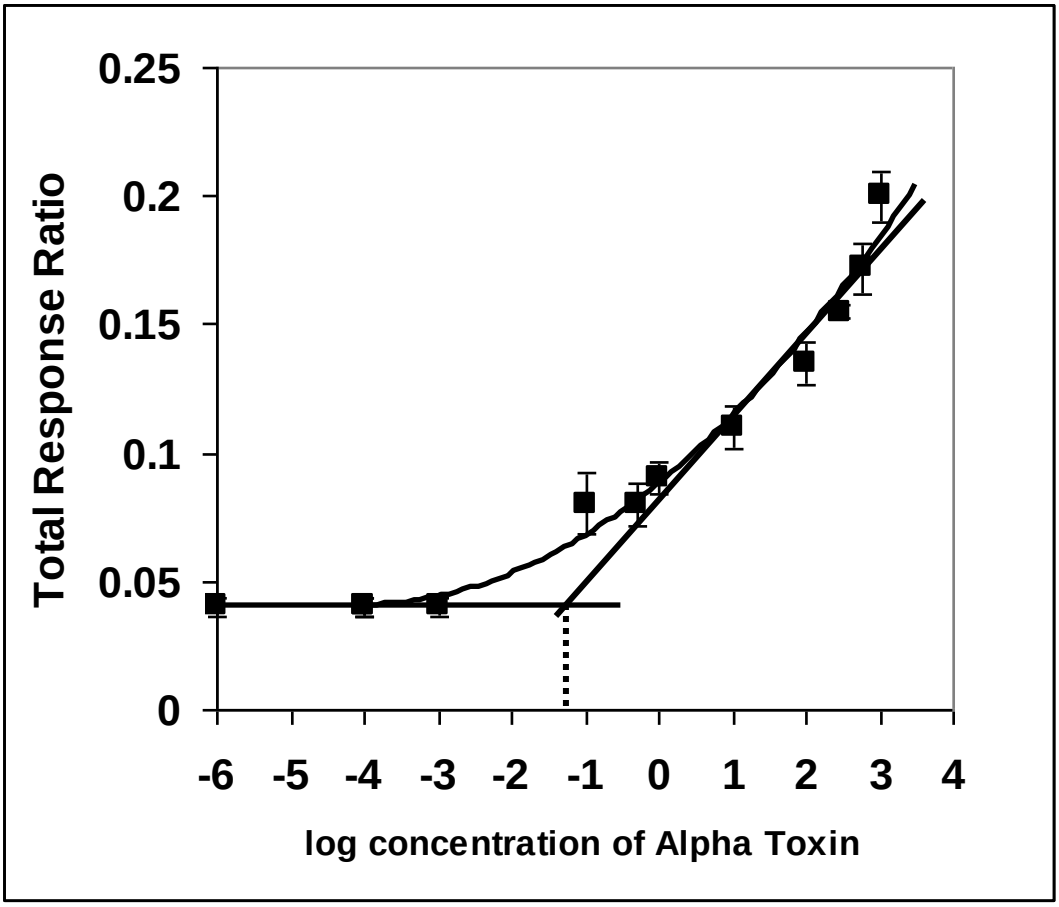

Figure 4.4 Detection limit was obtained from the point of intersection of the extrapolated parts of two linear regions as indicated

Considering the fact that the acute toxic concentration of alpha toxin in human is 100-250 ng/ml of whole blood [Bhakdi 1989], it is proposed that the sensor can be used to detect alpha toxin in the serum of patients infected with staphylococcal diseases.

4.3.4 Changes in Morphology of HUVECs

Silver staining was used to investigate changes in HUVEC morphology due to exposure to alpha toxin and the results are summarized in Table 4.1. Without alpha toxin, it was observed that the confluent monolayer of HUVECs was stained consistently along the contours of the cell borders. The number of intercellular gaps was quantified from the number of silver deposits (dots) along the stained borders of the cells. In the absence of alpha toxin treatment, few dots (0.4 ± 0.08/endothelial cell) were observed along the cell borders (Fig. 4.5A), even though numerous silver dots were seen on the cell surface. Other studies have also reported the presence of such silver granules on the surfaces of cells (Hirata et al. 1995; McDonald 1994).

With the stimulation of HUVEC monolayers with alpha toxin, a significant increase in the number of silver deposits were observed along the border of the cells (Fig. 4.5 B and C). When increasing the alpha toxin concentration from 0.1 ng/ml (Fig. 4.5B) to 1000 ng/ml (Fig. 4.5C), the number of silver deposits increased from 0.8 ± 0.18 to 4.4 ± 0.31 per cell. The thickness of the silver stained border (silver line) between the cells was determined to be 0.58 ± 0.05 μm (N = 20). Silver dots consist of approximately circular depositions of silver, at the intercellular gaps, surrounded by the silver lines as shown in Figure 4.6. The gap diameter was calculated by subtracting twice the silver line thickness (2 X 0.58 μm) from the diameter of silver dots. Almost no significant difference was observed in the gap size, as reflected from the average gap diameter of 0.9 ± 0.02 μm and 0.92 ± 0.08 μm for cells exposed to 0.1 ng/ml and 1000 ng/ml alpha toxin respectively. Gap area, expressed as percentage of total area, increased from 0.04 ± 0.007 for control to 0.41 ± 0.02 μm^2 for cells treated with 1000 ng/ml alpha toxin. Exposing the confluent monolayer to alpha toxin had a little effect on cell shape as shown in Table 4.1. However, the small change in shape index (Shape Index = $4*\pi*A/P^2$ where A is area and P is the perimeter) from 0.48 for control to 0.56 for cells exposed to 1000 ng/ml for 20 min, indicated a tendency for cells to round up.

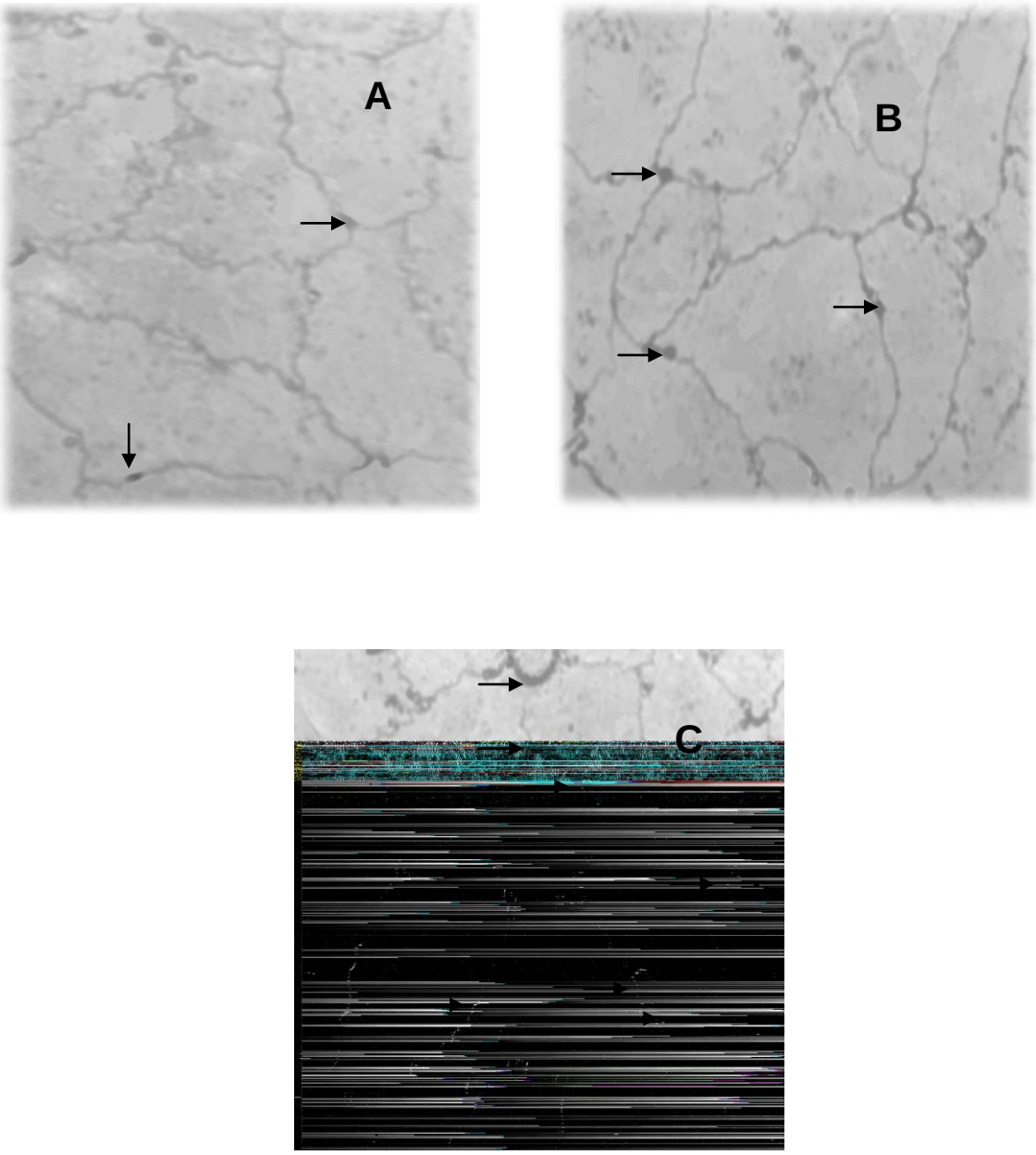

Figure 4.5 Silver staining of HUVECs monolayer (512 X magnifications) (A) untreated or (B) treated with 0.1 ng/ml and (C) 1000 ng/ml alpha toxin. In case of control (A), few silver deposits (pointed with arrow) were found around the cells, while this number significantly increased in case of treated cells (B, C)

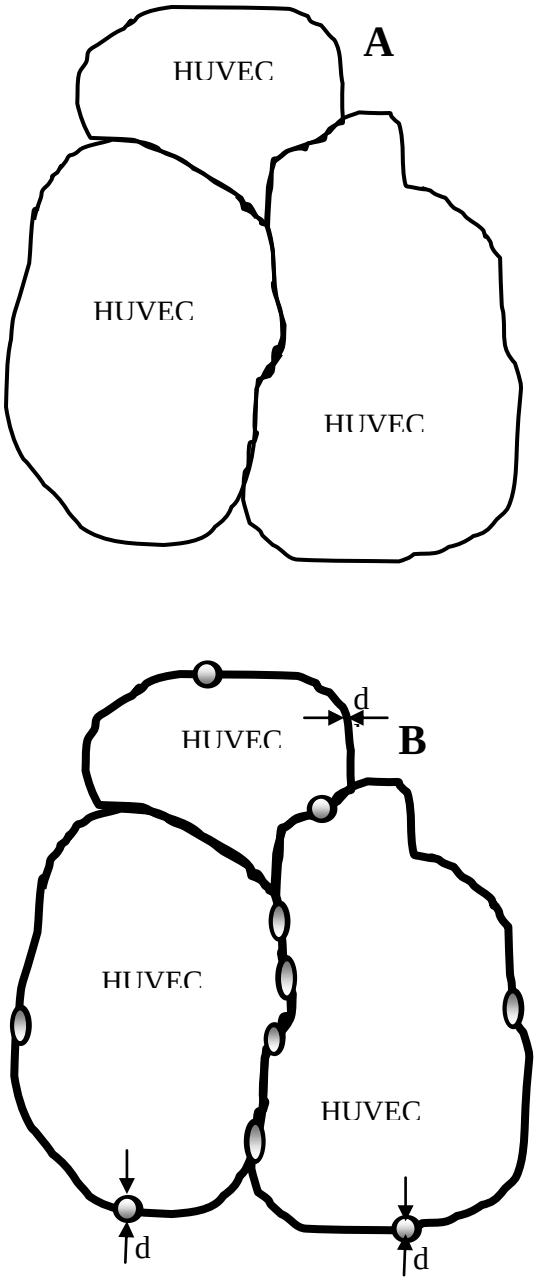

Figure 4.6 Schematic diagram showing the HUVEC monolayers prior to staining (A) and after staining along the contours of cell borders as well as the silver dots (B). To simplify, the gap area and the surrounding silver lines are shown in different colors. For the purpose of calculating the gap diameter (dg), two times the thickness of silver lines (dl) is subtracted from the diameter of silver deposit (ds)

Table 4.1 Effect of 20 min Exposure to Alpha Toxin on the Morphology of HUVECs.

	Control	**Cells treated with alpha toxin for 20 min**	
		0.1 ng/ml	**1000 ng/ml**
Cell Diameter (μm)	33.28 ± 0.85	33.1 ± 0.84	33.4 ± 0.66
Cell Perimeter (μm)	149.7 ± 4.14	147.2 ± 4.12	142.3 ± 3.08
Cell Area (μm^2)	859.5 ± 47.25	881.3 ± 47.98	919.33 ± 35.74
Shape Index	0.48 ± 0.01	0.51 ± 0.01	0.56 ± 0.008
Minor Axis/Major Axis	0.21 ± 0.006	0.23 ± 0.007	0.27 ± 0.005
# of Silver Deposits/ Cell	0.435 ± 0.08	0.84 ± 0.184	4.44 ± 0.314
Gap Area (% of Total Area)	0.04 ± 0.007	0.086 ± 0.008	0.41 ± 0.02

Values are means ± SEM. For each condition, three set of experiments were carried out. During each of the studies, three independent images were photographed from randomly selected fields of view. Overall 90 cells (15 cells per image) were measured for each condition to calculate the mean values.

Figure 4.7 reveals a strong positive correlation between the sensor response and gap area (% of total area). The response of the biosensor to the presence of alpha toxin can thus be attributed to the formation of intercellular gaps upon exposure of cells to alpha toxin. Evidence of gap formation leading to the increased permeability of water and albumin on exposing confluent endothelial –cell monolayers to low doses of alpha toxin had been documented (Suttorp et al. 1985). Moreover, staphylococcal alpha toxin induced endothelial barrier function in isolated perfused rabbit lung and isolated rat ileum had also been reported (Brell et al. 2005; Seeger et al. 1990). Redistribution of junctional VE-cadherin and occludin as well as slight F-actin stress fiber formation had been shown to accompany the intercellular gap formation when HUVECs were incubated with staphylococcal alpha toxin (Hocke et al. 2006). Other studies had reported that the initial binding of alpha toxin to the target cells in the water-soluble monomeric form is followed by oligomerisation to the heptameric structures. This leads to the formation of transmembrane pores (Bhakdi and J. 1991; Gouaux et al. 1994). These pores not only lead to the leakage of small molecules but also to an influx of calcium ions, which in turn trigger the arachidonate cascade (Bhakdi and J. 1991; Seeger et al. 1990; Suttorp et al. 1985; Suttorp et al. 1987). It had been proposed that influx of calcium ions can initiate an interaction between the actin and myosin filament, which eventually leads to the contraction of the cells (Suttorp et al. 1988).

4.4 Discussion

The conventional method for detection of *Staphylococcus aureus* induced diseases involves the isolation and cultivation of the pathogen. Even though the method is reliable, it is time consuming. Moreover, the method lacks sensitivity once the antibiotic treatment has been initiated [12, 38]. Methods involving the detection of antibodies against staphylococcal antigens have been used for a long time. A more recent study performed ELISAs to measure the IgG antibodies against different antigens namely peptidoglycan, teichoic acid, alpha toxin, lipase, capsular polysaccharide, *S. aureus* ultrasonicate and whole *S. aureus* cells both separately and in combination. The aim was to evaluate their

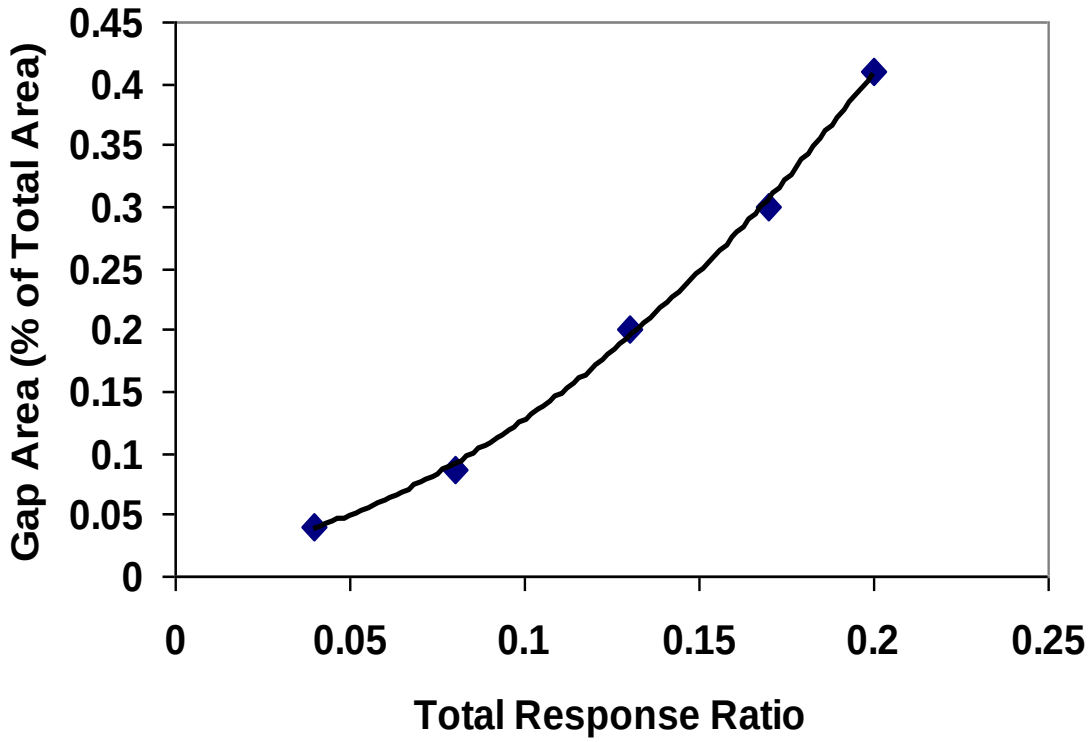

Figure 4.7 Regression analysis between the gap area (% of total area) and the response obtained from the sensor upon exposure to different concentrations of alpha for 20 min

capability in distinguishing between uncomplicated and complicated *S. aureus* bacterimea, between *S. aureus* and non- *S. aureus* bacterimea and between *S. aureus* and non- *S. aureus* endocarditis (Ryding et al. 2002). No single assay was found to be suitable for the purpose. Two different combinations of ELISAs involving whole cells, teichoic acid, alpha toxin, lipase and capsular polysaccharide were only able to differentiate between *S. aureus* and non- *S. aureus* endocarditis (Ryding et al. 2002). There are many problems associated with antibody detection. Since the healthy individuals have antibodies against many staphylococcal antigens (Julander et al. 1983), detecting antibodies in the blood of patients is not sufficient. It is therefore important to detect unusually high levels of antibody titers for proper diagnosis. Hence, there is a requirement to define a cut off limit of the titer values to differentiate between a healthy individual and a patient. However, it had been observed that some patients having low titer values at the early stages of the disease showed a tendency of not generating high titers even with the progression of the disease (Mollby 1994). The other drawback associated with the antibody detection method is that a rise in serum antibodies against *S. aureus* antigens occurs after 7 – 30 days of onset of the infection (Christensson et al. 1983; Julander et al. 1983).

On the contrary, staphylococcal antigens can be detected in the serum at the onset of the illness and also in the serum having low titer of antibodies. Detection of antigens can thus act as a valuable tool for the diagnosis of staphylococcal infections at the initial stages. Different assays have been employed to detect staphylococcal antigens like teichoic acid, muramic acid, alpha toxin, toxic shock syndrome toxin -1, various exo and enterotoxins and others (Christensson et al. 1989; Gehron et al. 1984; Loeffler et al. 1988; Rosten et al. 1987; Sarujballi and Fackrell 1984; Soderquist et al. 1993b). Alpha toxin, a protein exotoxin produced by the majority (85-90%) of *S. aureus* strains (Mollby 1983), plays a critical role in the pathogenicity induced by *S. aureus*. As a matter of fact, it had been established, in animal models, that alpha toxin mutant or deficient *S. aureus* have diminished effect in inducing brain abscesses and keratitis (Kielian et al. 2001; Wu et al. 2005c). Moreover, it had also been shown that immunization to alpha toxin can protect cornea from damaging during *S. aureus* keratitis (Hume et al. 2000). Studies describing

the physiological effects of alpha toxin had been reported (Bhakdi et al. 1988; Gemmell et al. 1982).

In this study, we reported the detection of staphylococcal alpha toxin using an endothelial cell based biosensor. The sensor is capable of detecting the presence of as low a concentration of alpha toxin as 0.1 ng/ml after only a 20 min exposure time. The response of the sensor can be attributed to the gap formation upon exposure of confluent HUVECs monolayer to varying concentration of alpha toxin. In fact, a strong positive correlation has been obtained between the sensor response and the area of the gap formed. The fact that this sensor requires only 20 min to measure the presence of alpha toxin together with its very low detection limit of 0.1 ng/ml bolsters its potential to act as a diagnostic tool during the onset of staphylococcal infections.

Chapter 5 ：Measuring Permeability with a Whole Cell- Based Biosensor as an Alternate Assay for Angiogenesis: Comparison with Common *in vitro* Assays

Based on studies published in: Ghosh, G., Mehta, I., Cornette, A., Anderson, K. W. "Measuring Permeability with a Whole Cell – Based Biosensor as an Alternate Assay for Angiogenesis: Comparison with Common *in vitro* Assays" *Biosensors and Bioelectronics*, 2007, in Press

5.1 Introduction

Angiogenesis, sprouting of new blood vessels from the existing ones, under regulated conditions occurs in physiological functions like reproduction, wound repair as well as in muscle remodeling. Under pathological conditions, uncontrolled angiogenesis is observed in cancer, diabetes, arthritis, ocular neovascularization and several other diseases (Carmellet and Jain 2000; Folkman 1990; Reynolds et al. 1992). The angiogenic cascade consists of several distinct steps. Degradation of the basement membrane and extracellular matrix (ECM) and migration and proliferation of endothelial cells is followed by the organization of cells into three dimensional structures to form new capillaries as shown in Figure 5.1. Increased permeability plays an initial critical role in angiogenesis. Permeability increase results in the leakage of plasma proteins into the extracellular matrix thereby fostering the deposition of fibrin gel. Remodeled ECM further supports and helps in the development of new blood vessels (Bates et al. 2002; Dvorak et al. 1995).

Angiogenesis is regulated by the balance between pro and anti angiogenic molecules as shown in Figure 5.2. Several molecules have been classified as angiogenic factors based on their biologic activities (Folkman and Shing, 1992). Vascular endothelial growth factor (VEGF), basic fibroblast growth factor (bFGF), hepatocyte growth factor (HGF) and tumor necrosis factor- alpha (TNF-α) are some of the common potential regulators of angiogenesis, and these cytokines act simultaneously to activate angiogenesis *in vivo* (Asahara et al. 1995; Bond et al. 1998; Xin et al. 2001). These angiogenic molecules are known to regulate different steps of angiogenesis by modulating permeability, proliferation, migration and tube formation of endothelial cells

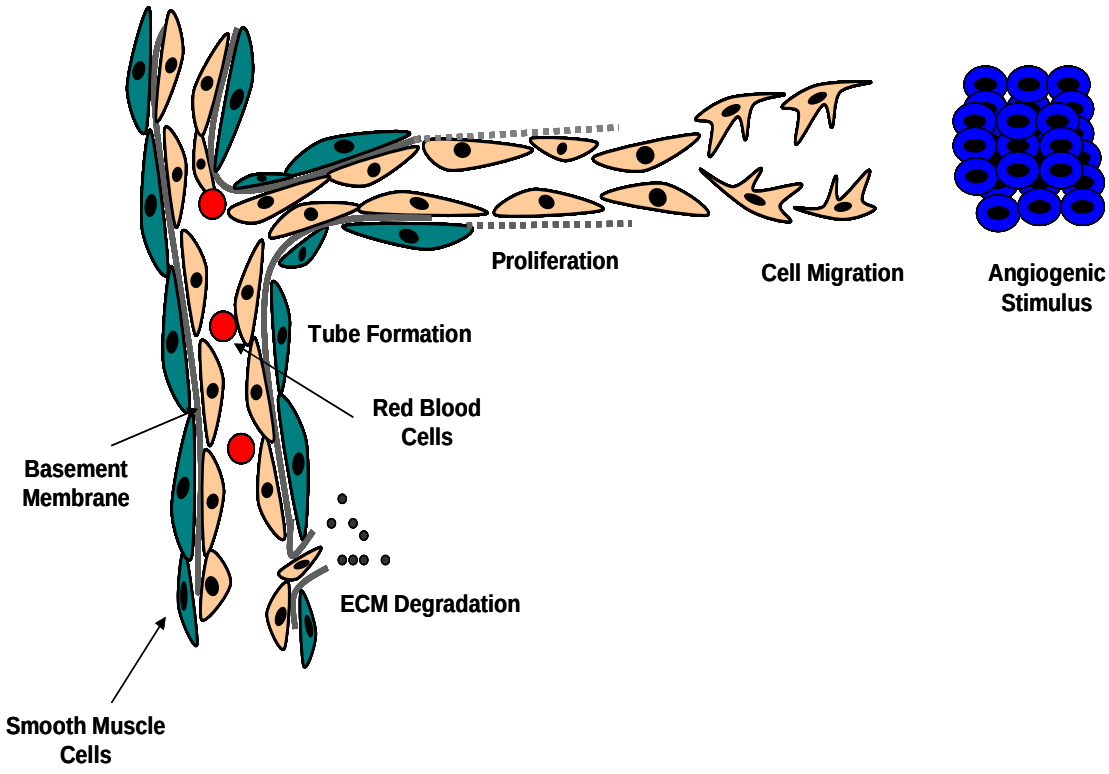

Figure 5.1 Schematic of the angiogenic cascade. In response to the stimulus (cancer, wound healing etc), endothelial cells are activated leading to ECM degradation, cell migration and proliferation and eventually formation of capillaries. Modified from (Torry and Rongish 1992)

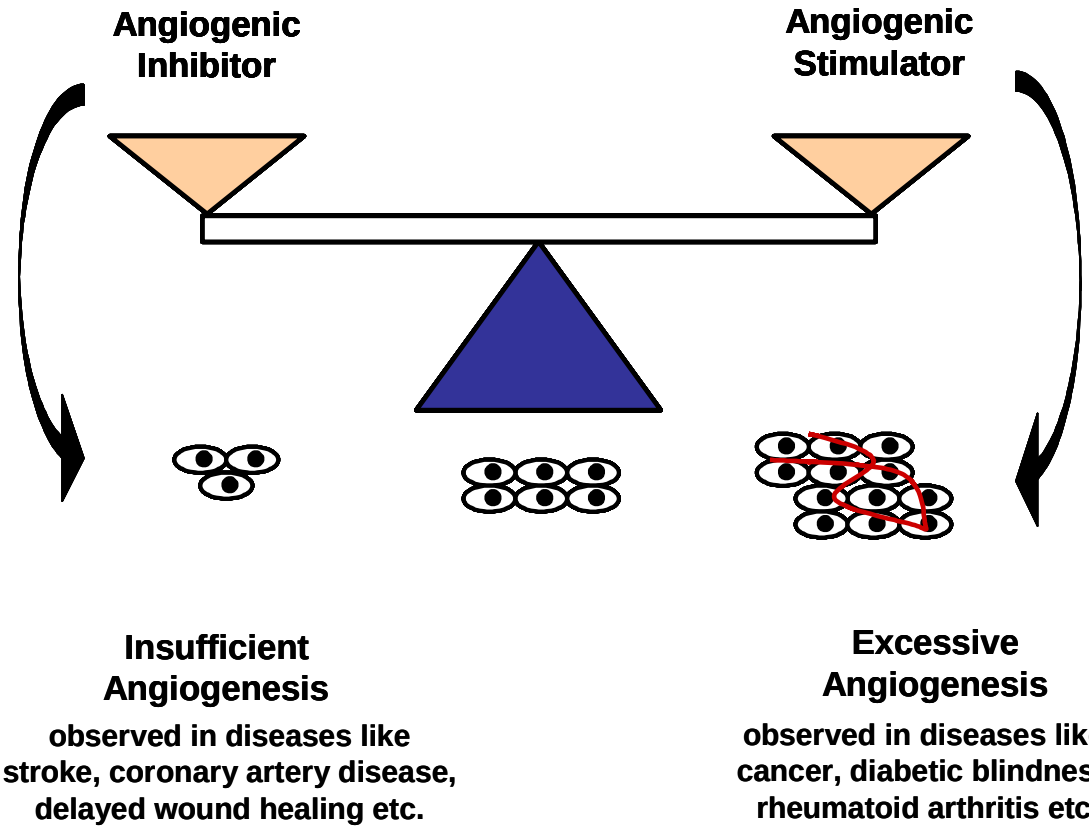

Figure 5.2 Angiogenesis is regulated by angiogenic inhibitor and stimulator.Disturbance in this equilibrium leads to different diseases

(Jiang et al. 1999; Lal et al. 2001; Morimoto et al. 1991; Naik et al. 2003; Nooteboom et al. 2000; Patterson et al. 1996; Rousseau et al. 2000; Wu et al. 2000).

One of the most important challenges in the study of angiogenesis is the selection of an appropriate method for assessing this process. While angiogenesis is best studied using *in vivo* assays, *in vitro* assays are preferred for initial screening of both pro-angiogenic and anti-angiogenic molecules. Common *in vitro* assays include analysis of cell migration, proliferation, and differentiation (Auerbach et al. 2003; Staton et al. 2004). Because increased cell permeability also plays a role in angiogenesis, the present study focused on the use of the whole cell-based biosensor that detects changes in cell monolayer permeability as an additional assay for quantifying angiogenesis.

This study investigates the response of the sensor to both individual and combined cytokines that are known to stimulate angiogenesis, and this response is compared to other commonly used *in vitro* angiogenic assays including cell migration, cell proliferation and tube formation assays.

5.2 Experimental Section

5.2.1 Reagents

Purified carrier free $VEGF_{165}$, bFGF, HGF and TNF-α were purchased from R&D Systems (Minneapolis, MN). The cytokines were dissolved in 0.1% bovine serum albumin (BSA) in Dulbecco's phosphate-buffered saline (PBS) (GIBCO^{TM}). Different concentrations of the cytokines studied were VEGF (1000 pg/ml), HGF (2000 pg/ml), bFGF (40 pg/ml) and TNF-α (100 pg/ml). These concentrations correspond to those found in serum of cancer patients (Dirix et al. 1997; Sezer et al. 2001). Basal medium consisted of EGM-2 supplemented with fetal bovine serum (FBS), ascorbic acid and gentamicin sulfate. Tube formation assay kit was purchased from Cell Biolabs Inc (San Diego, CA). HUVECs used during the experiments, were cultured as described in Chapter 3. Membrane materials and sensor preparation have also been described in Chapter 3.

5.2.2 Evaluation of Electrode Response for Permeability Studies

Following confluent cell monolayer formation, the control membranes were tested for inhibited ion response. After the confirmation of the inhibited ion response due to the formation of the confluent monolayer, the cell-seeded membranes were exposed to different cytokine solutions containing individual and combinations of cytokines in PBS (pH 7.2), and the response of the sensor was measured.

At a final concentration of 0.1M KCl, the electrode response was measured for the following conditions: (a) the membrane without cells and without cytokines to obtain the baseline response of the sensor, (b) membranes without cells and with the cytokines to test the effect of these angiogenic factors on the sensor alone, (c) membranes with cells and without cytokines to confirm the inhibited response of the sensor due to the confluent monolayer of cells, and (d) membranes with cells and with cytokines.

To account for slight variations between fabricated membranes, the final data are reported as the ratio of the response obtained at 0.1 M KCl for the ISEs with HUVECs and cytokines to the response obtained for the same membrane without HUVECs and cytokines.

5.2.3 Evaluation of Cell Migration

HUVECs were cultured in 24 well plates in complete medium and allowed to reach confluence. Once confluent, a wound was inflicted on the cell monolayer by scraping it with a sterile 200 µL pipette tip. The cell monolayer was washed three times, and the cells were then exposed to basal media with or without cytokines. Pictures were taken for times varying from t = 0 to t = 10 hrs to calculate the wound area using a Zeiss IM 35 microscope. The percentage of wound closure was calculated as follows:

$$\%\ Wound\,Closure = \frac{A_{w,t=0} - A_{w,t=t}}{A_{w,t=0}}\, x\, 100$$

where A_w = area of wound

Using the available software, AxioVision 4, the area of the wound was measured at different times. Three independent sets of experiments were carried out for each condition. Each experiment was replicated in two wells. Figure 5.3 demonstrates a schematic of the wound formation assay.

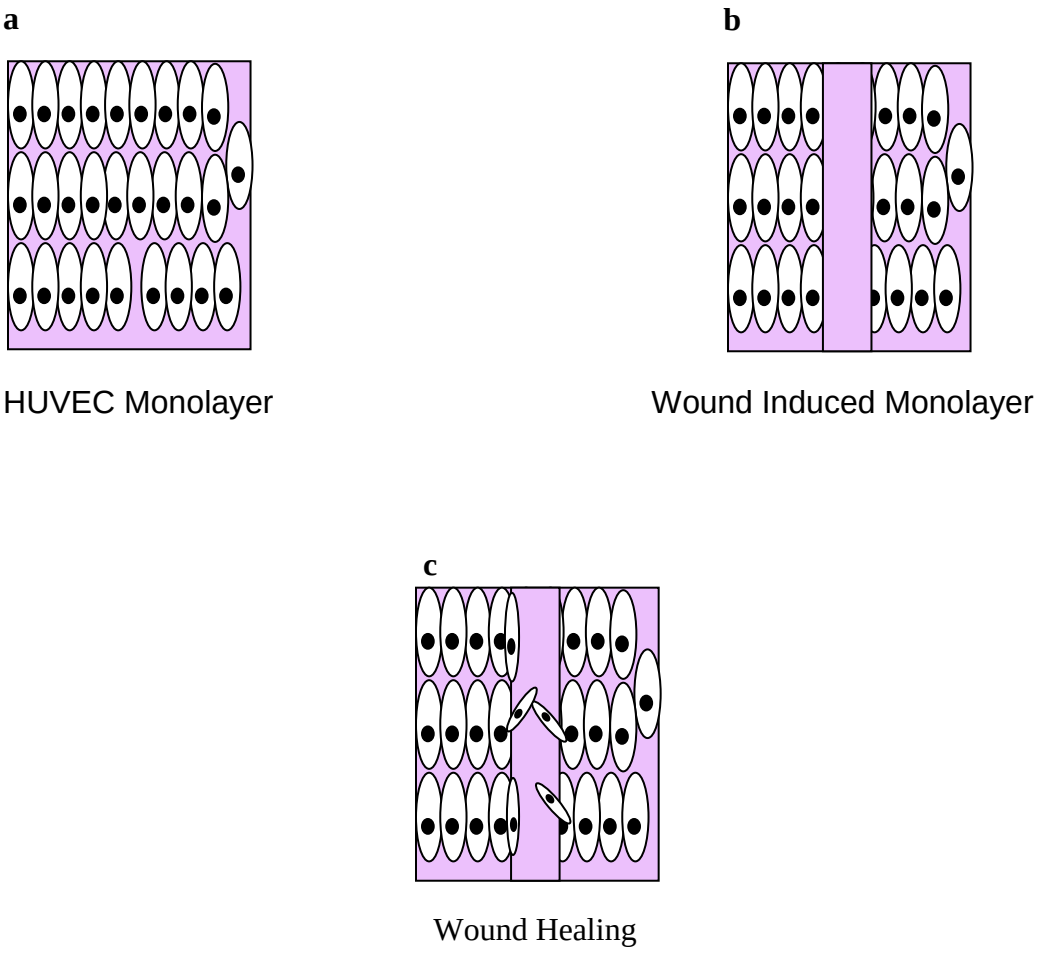

Figure 5.3 Schematic of the wound healing technique. As described in the procedure the confluent cell monolayer (a) was wounded by scraping (b) and then exposed to the angiogenic factors. The migration of the cells in the denuded area (c) led to the healing of wounds

5.2.4 Cell Proliferation Analysis

HUVECs seeded at cell density of $1x10^5$ cells/mL were cultured in complete media in 25 cm^2 culture flasks. After 24 h, the media was replaced by basal media with or without the cytokines. Following 48 h incubation, the cells were counted in a hemacytometer. Three independent sets of experiments were carried out for each condition.

5.2.5 Tube Formation Assay

Tube formation experiments were carried out as directed by the kit manufacturer. Briefly, 50 µL of ECM gel was added to each well of the sterile 96 well plate and incubated for 30-45 min. A volume of 150µL of cell solution in basal media with or without cytokines was then added to each well. The cell density was maintained at $1x10^5$ cells/well. After 11h, the extent of tube formation was examined under a Zeiss IM 35 microscope and tube length was measured using Axiovision 4 software. Two independent sets of experiments were carried out for each condition. Each experiment was replicated in two wells. Figure 5.4 demonstrates a schematic representation of the tube formation assay.

5.2.6 Statistical Analysis

For all experiments, data are reported as mean ± SEM. Statistical analyses were carried out using one-way ANOVA and the Student-Newman-Keuls test for post-hoc comparisons of the means with $P<0.05$. SigmaStat v 3.1 software was used for these analyses.

5.3 Results

5.3.1 Sensor Response to Individual Cytokines and Optimization of Exposure Time

An important part of this investigation was to determine how long the sensor should be exposed to cytokines to obtain the optimum response. To do this, the cell based ISE membranes were first exposed to 1000 pg/ml VEGF in PBS for times ranging from 30

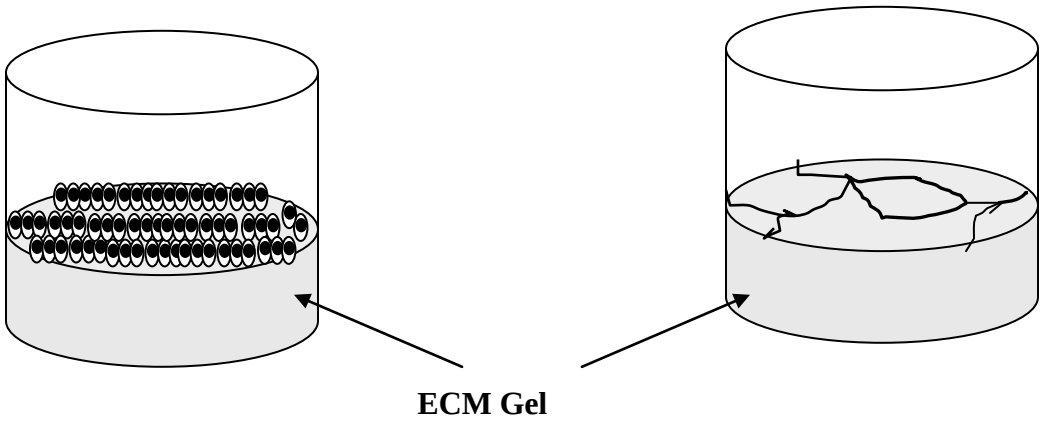

Figure 5.4 Schematic representation of the tube formation assay. Cells seeded onto the ECM gel in 96 well plates (a) formed tubes (b) after 11 hrs of incubation with angiogenic factors

min to 10 h and the response of the sensor to the presence of the VEGF was measured. Figure 5.5 illustrates the increase in overall response ratio with the increasing exposure time. The overall response ratio of the sensor increased from 0.08 to 0.43 on varying the exposure time from 30 min to 10 h. The results indicate that VEGF induced increase in HUVEC monolayer permeability initiated within 30 min of its addition and longer exposure times up to 10 h, resulted in further permeability enhancement. The cell based biosensor was then exposed to 100 pg/ml TNF-α in PBS for times ranging from 30 min to 10 h. As shown in the figure, upon increasing the exposure time from 30 min to 3 h, the sensor response increased from 0.07 to 0.16. However, further exposure of the sensor to TNF-α resulted in a decrease in sensor response, indicating a decline in permeability of HUVEC monolayers. This result is consistent with a previous study which demonstrated a gradual decrease in HUVEC monolayer permeability after 6 h of exposure to TNF-α (Nooteboom et al. 2000). As shown in Figure 5.5, the sensor response dropped to 0.12 after 5 h and 0.06 after 10 h. Thus, with TNF-α, permeability enhancement initiated after 30 min of exposure with maximal change occurring after 3 h.

Since, the response of the sensor decreased after 3 h for TNF-α, it was decided that henceforth all the experiments would be carried out with a maximal exposure time of 3 h. In addition, 30 min exposure time was eliminated since the sensor response to TNF-α and VEGF was minimal at this time compared to the response with cells only. As shown, the response from the sensor to the presence of 2000 pg/ml HGF in PBS increased from 0.08 to 0.16 as the exposure time increased from 1 to 3 h. The cell based ISE membranes were then exposed to 40 pg/ml bFGF in PBS for 1 and 3 h. The sensor response increased from 0.07 to 0.1. These results agree with a previous study that demonstrated bFGF induced increase in HUVEC monolayer permeability (Stockton et al. 2004).

To ensure that these cytokines do not affect the response of the sensor without cells, control experiments were performed where the ISE membranes without cells were exposed to cytokines for 3 h at the same concentration. When the overall response obtained at 0.1 M KCl for the membrane exposed to the cytokines for 3 h was compared with that obtained for control, it was observed that more than 95% of the sensor response had been recovered as shown in Figure 5.6, indicating minimal protein adsorption on the sensor surface.

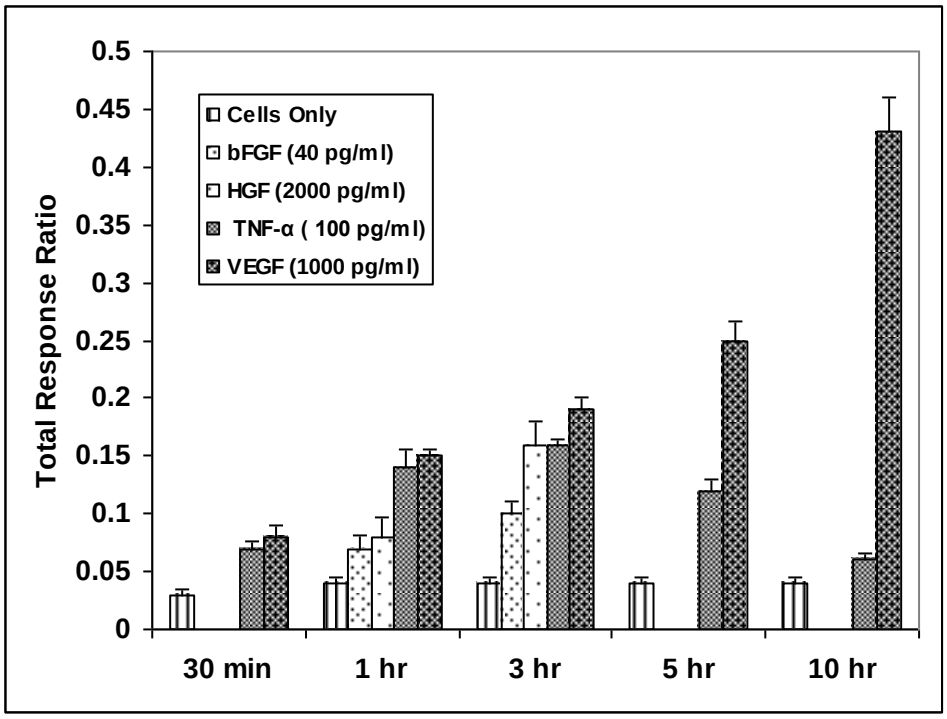

Figure 5.5 Ratio of ISE response obtained at 0.1 M KCl following exposure of the cell based sensor to different cytokines to ISE response obtained at 0.1 M KCl for the membrane without cells and without cytokines. (Error bars represent SE, N=3)

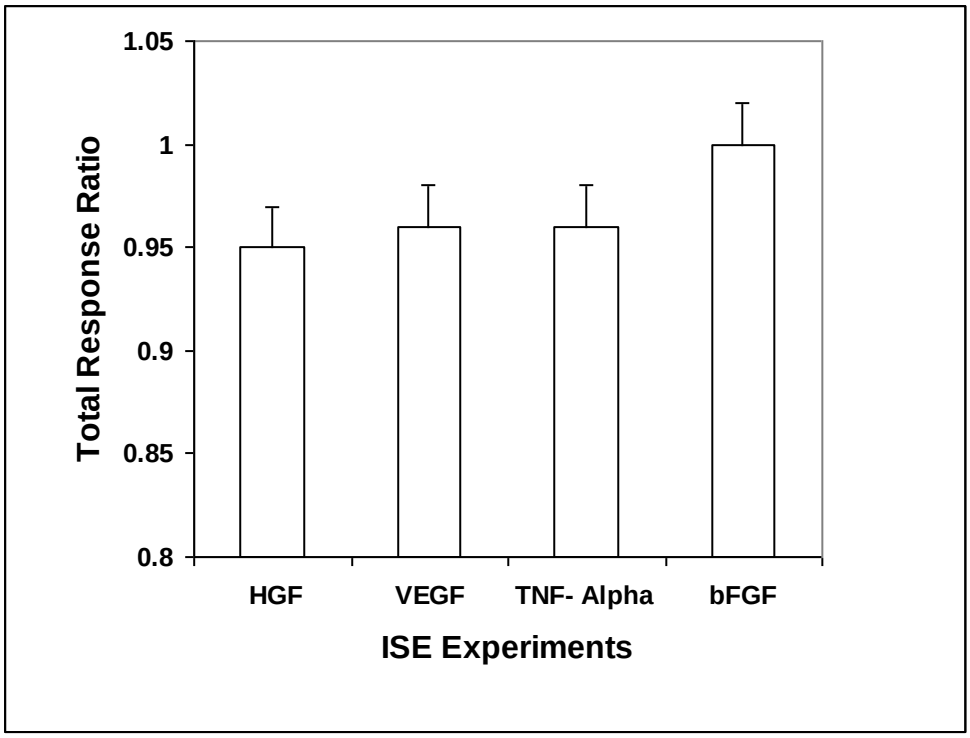

Figure 5.6 Ratio of ISE response obtained at 0.1 M KCl following exposure of the sensor to different cytokines in absence of cells to ISE response obtained at 0.1 M KCl for the membrane without cells and without cytokines. (Error bars represent SE, N=3.)

5.3.2 Sensor Response to Combination of Cytokines

Once the response of the sensor to the presence of the individual cytokines had been measured, the biosensor was exposed to a combination of VEGF and TNF- α for 1 and 3 h. Figure 5.7 illustrates the increase in sensor response indicating the modulation of monolayer permeability by the combination of cytokines. Even though an additive effect was not observed, the sensor response increased to 0.22 and 0.26 for the combined cytokines, as compared to 0.15 and 0.19 for VEGF and 0.14 and 0.16 for TNF- α, when exposed for 1 and 3 h, respectively.

The biosensor was then exposed to VEGF, TNF-α and HGF simultaneously for 1 and 3 h. As shown in Figure 5.7, addition of HGF does not significantly change the response of the sensor from that obtained for the VEGF and TNF-α combination. Similar responses were obtained when the sensor was exposed to the combination of VEGF, TNF-α and bFGF, indicating that the addition of the third cytokine does not effectively improve the modulation of HUVEC monolayer permeability.

Next, the cell based ISE membranes were exposed to all four cytokines for 1 and 3 h. Figure 5.7 illustrates the increase in sensor response indicating the enhancement of HUVEC monolayer permeability due to the combination of all four cytokines. The sensor response increased to 0.32 and 0.42 for an exposure time of 1 and 3 h, respectively.

5.3.3 Effect of Cytokines on Cell Migration

Investigation of cell migration was carried out over times ranging from 0 to 10 h using the wound healing assay. Figure 5.8 shows the microscopic images of wound healing of cells when exposed to all four angiogenic factors. Figure 5.9A shows the increased percent wound closure with the increased exposure time. Significant difference in values between control and that induced by the individual or combination of cytokines was observed only after 10 h.

Figure 5.9B further illustrates the % wound closure when exposed to different cytokines for 10 h. Unlike TNF-α and VEGF, percentage wound closure induced by bFGF and HGF increased significantly as compared to the control. Combination of VEGF and TNF-α resulted in enhanced % wound healing compared to that induced by them individually. A previous study also reported a stimulatory effect of TNF-α on

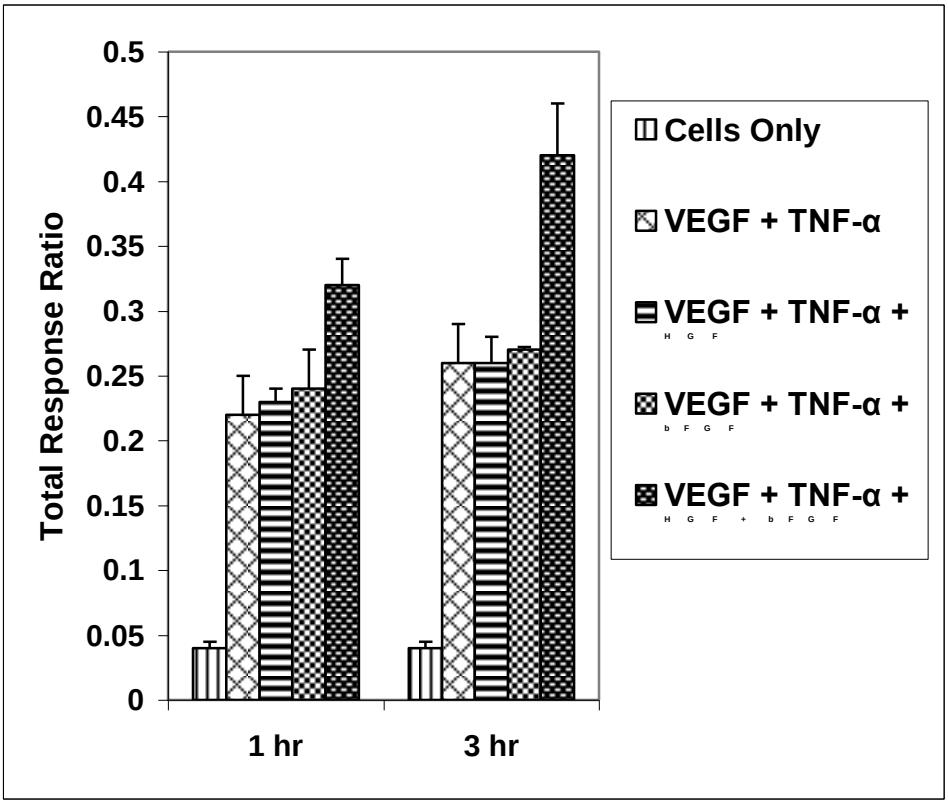

Figure 5.7 Ratio of ISE response obtained at 0.1 M KCl following exposure of the cell based sensor to combinations of different cytokines for 1 and 3 hr to ISE response obtained at 0.1 M KCl for the membrane without cells and without cytokines. (Error bars represent SE, N=3.)

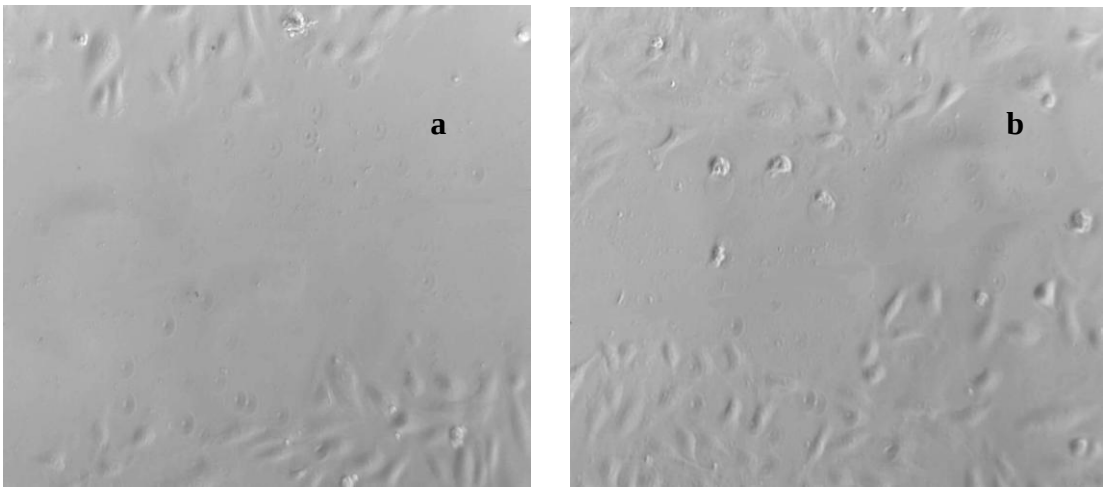

Figure 5.8 The microscopic images of wound induced in cells at time t = 0 (a) and healing of wound upon exposure to all four angiogenic factors after 10 hr (b)

A:

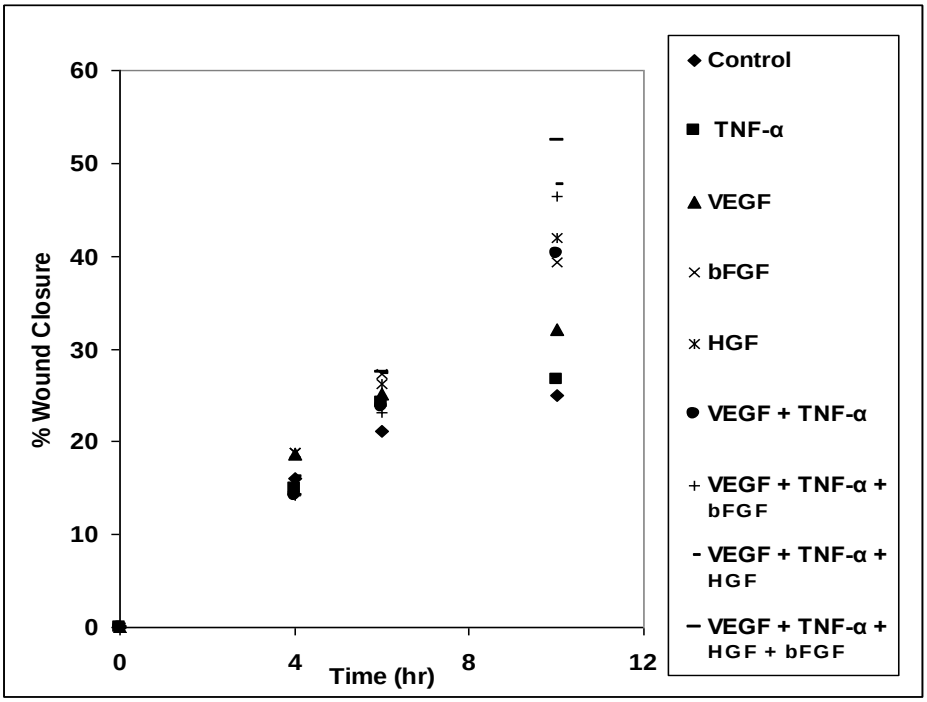

B:

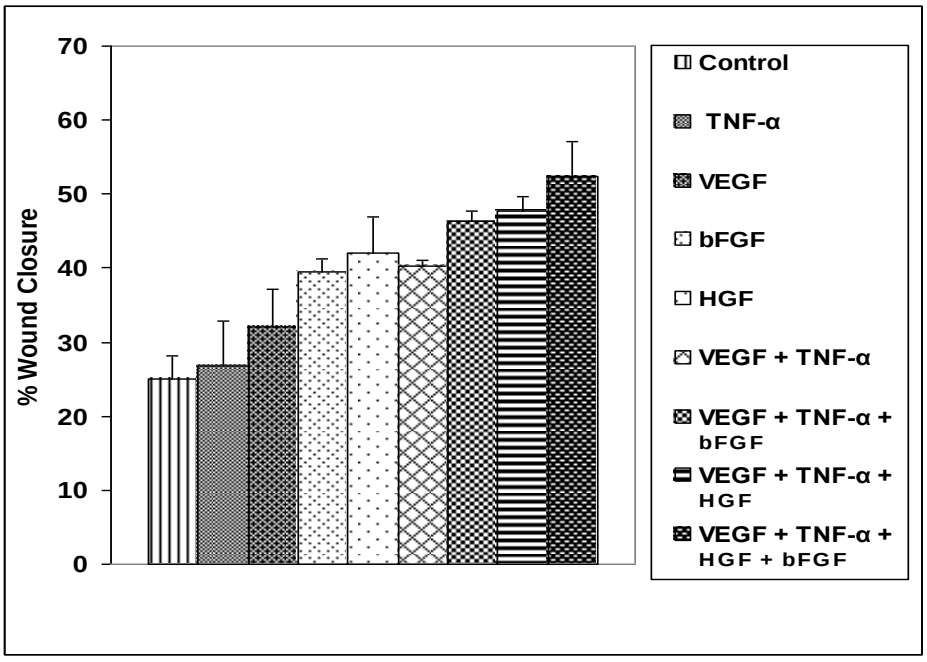

Figure 5.9 (A) Percent of wound closure, incurred in HUVEC monolayers, in response to individual as well as combination of cytokines over the time ranging from 0 to 10 hr. (B) Comparisons of the effects of cytokines on wound healing after 10hr. (Error bars represent SE, N=3.)

VEGF induced wound healing (Giraudo et al. 1998). Addition of the third cytokine in the form of bFGF or HGF increased the % wound healing from that obtained when exposed to the combination of VEGF and TNF- α. However, no significant difference was observed between the combination of VEGF, TNF-α, bFGF and VEGF, TNF-α, HGF. When the cells were exposed to all four cytokines, a more profound closure of wound was observed. Exposure to all four cytokines more than doubled the % wound healing when comparing with the control.

5.3.4 Effect of Cytokines on Cell Proliferation

The effects of the four cytokines on cell proliferation are shown in Figure 5.10. The results showed that while bFGF showed no effect on proliferation, exposing the cells to VEGF and HGF for 48 h significantly increased cell proliferation. However, TNF- α actually inhibited proliferation. In addition, it was observed that when HUVECs were incubated with both VEGF and TNF-α, TNF-α inhibited the effect of VEGF on HUVEC proliferation. The inhibitory effect of TNF-α and its ability to downregulate the mitogenic activity of VEGF has previously been documented in other studies (Frater-Schroder et al. 1987; Nakagami et al. 2002; Patterson et al. 1996). Adding bFGF and HGF to the VEGF/TNF- α solution did not significantly effect proliferation. A previous study documented a synergistic effect of bFGF and VEGF in stimulating proliferation of bovine endothelial cells (Goto et al. 1993). However, our results show that in the presence of TNF-α, this synergistic effect does not occur indicating the TNF-α still inhibits the effects of VEGF on proliferation even in the presence of bFGF. It is interesting to note, however, that when the cells were exposed to all four cytokines, a significant increase in proliferation is observed.

5.3.5 Effect of Cytokines on Tube Formation

The effects of the four cytokines on cell differentiation were investigated using the tube formation assay. Figure 5.11 shows the microscopic images of tube formation in the control studies (a) and when the HUVECs were treated with all four cytokines (b).Figure 5.12 illustrates average length of tubes when the cells were exposed to both individual and combination of cytokines for 11 h. Stimulating cells with these individual cytokines

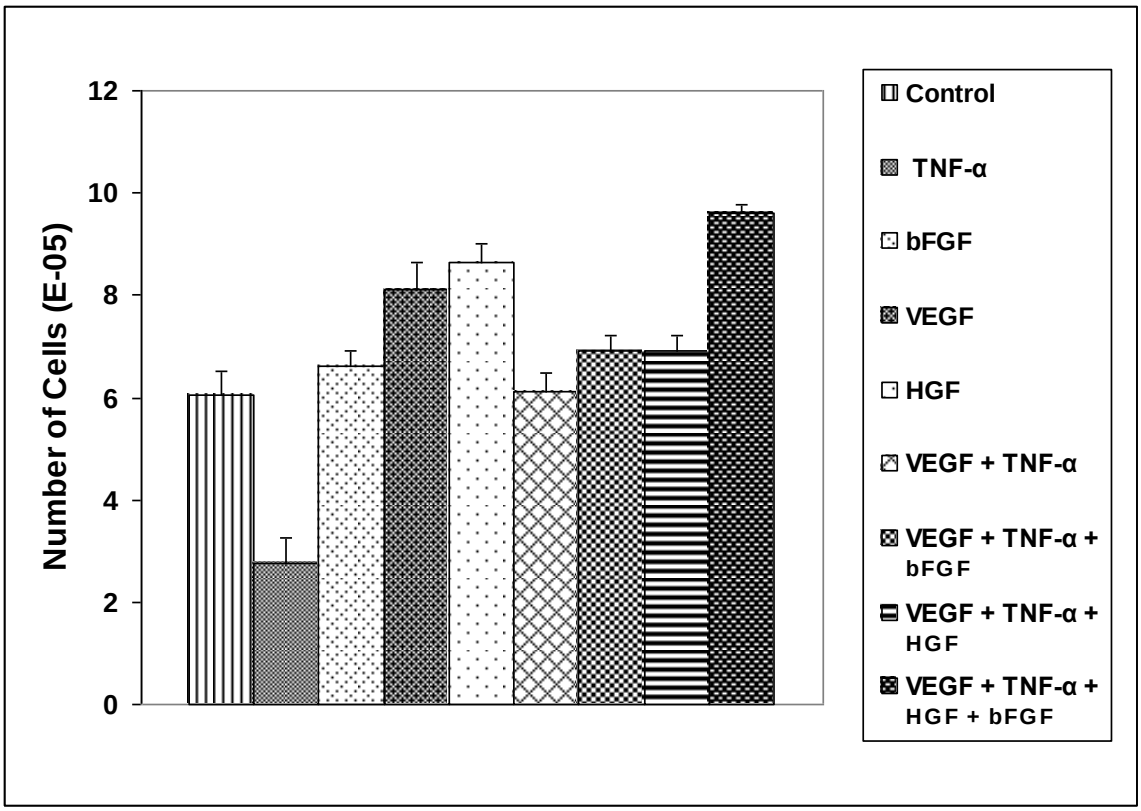

Figure 5.10 Proliferation of HUVEC in response to individual as well as combination of the cytokines. (Error bars represent SE, N=3.)

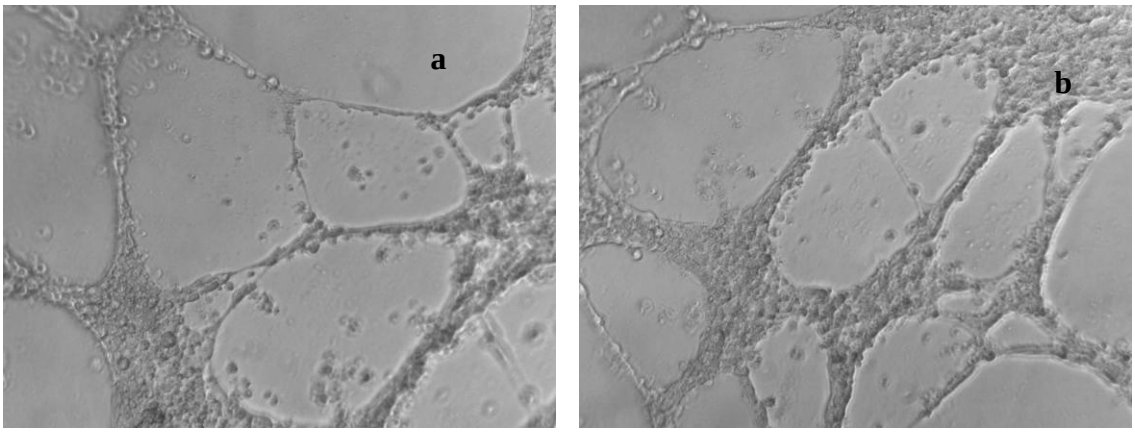

Figure 5.11 Microscopic images of tube formation in control studies (a) and after the cells are treated with all four angiogenic factors (b)

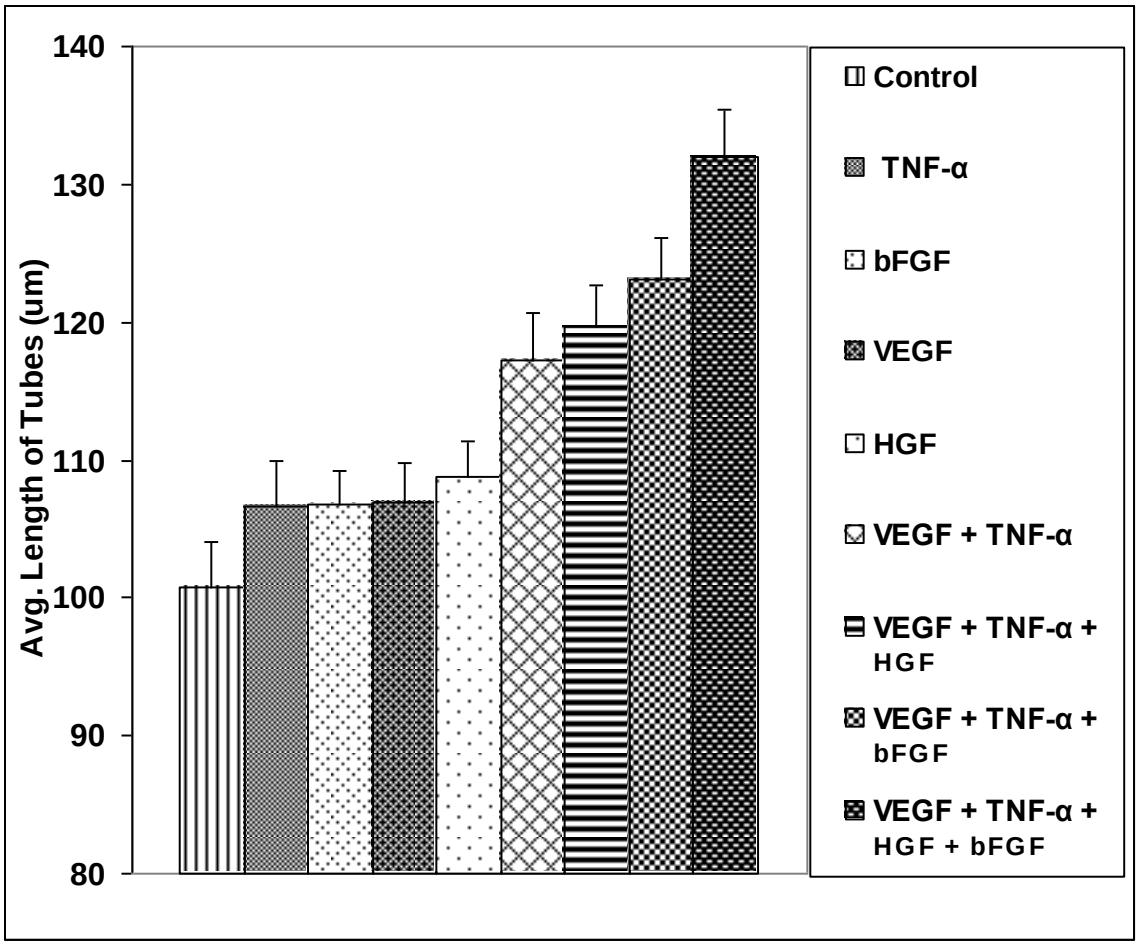

Figure 5.12 Average length of tubes formed upon exposing HUVEC to individual as well as combination of different cytokines for 11 h. (Error bars represent SE, N=2.)

did not result in significant increases in the length of tubes as compared to the control studies. However, a significant increase in tube length was observed when HUVECs were cultured with both VEGF and TNF-α. Adding bFGF or HGF to the VEGF/TNF-α solution did not increase the lengths of the tubes as compared to VEGF/TNF-α alone. Previous studies have reported a synergistic effect of VEGF and bFGF as well as the cooperative effect of VEGF, TNF-α and bFGF in inducing tubular structures in vitro (Koolwijk et al. 1996; Pepper et al. 1992). The difference in observation can be attributed to the difference in the cell lines used for the experiments. However, adding both bFGF and HGF to the VEGF/ TNF-α solution significantly increased the length of the tubes.

5.3.6 Comparison Among Different Assays

In order to carry out quantitative comparison among the different angiogenic assays, the responses of HUVECs to different cytokines were normalized. The normalized response is represented as the ratio of the responses to the stimulant to the responses obtained for control in that particular assay. The exposure time, at which significant difference in responses to the stimulant were obtained, were different for each assay. In the case of cell monolayer permeability studies, the relative increase in sensor response was determined from the ratio of the overall sensor response after 1 h exposure to different cytokines to the response obtained from the untreated monolayers. In case of cell migration, proliferation and tube formation study responses after 10 h, 48 h and 11 h were considered, respectively. Figure 5.13 shows the normalized responses of the different assays when exposed to the individual cytokines and combinations of the cytokines. As demonstrated, a maximum of 1.75-fold increase in cell monolayer permeability was induced by bFGF. In other assays, it stimulated HUVECs to increase cell migration, proliferation and tube formation by 1.6, 1.1 and 1.06-fold the control value. Hence, at the concentrations studied, bFGF has almost an identical effect on all the steps of angiogenesis. Treating HUVECs with HGF resulted in increases of 2, 1.7, 1.4 and 1.08-fold the control in permeability, migration, proliferation and tube formation respectively. Both TNF-α and VEGF showed a much greater effect on cell monolayer permeability as compared to the other steps of angiogenesis (3.2 and 3.75 times the control, respectively). Effects on the other steps of angiogenesis ranged from a decreased

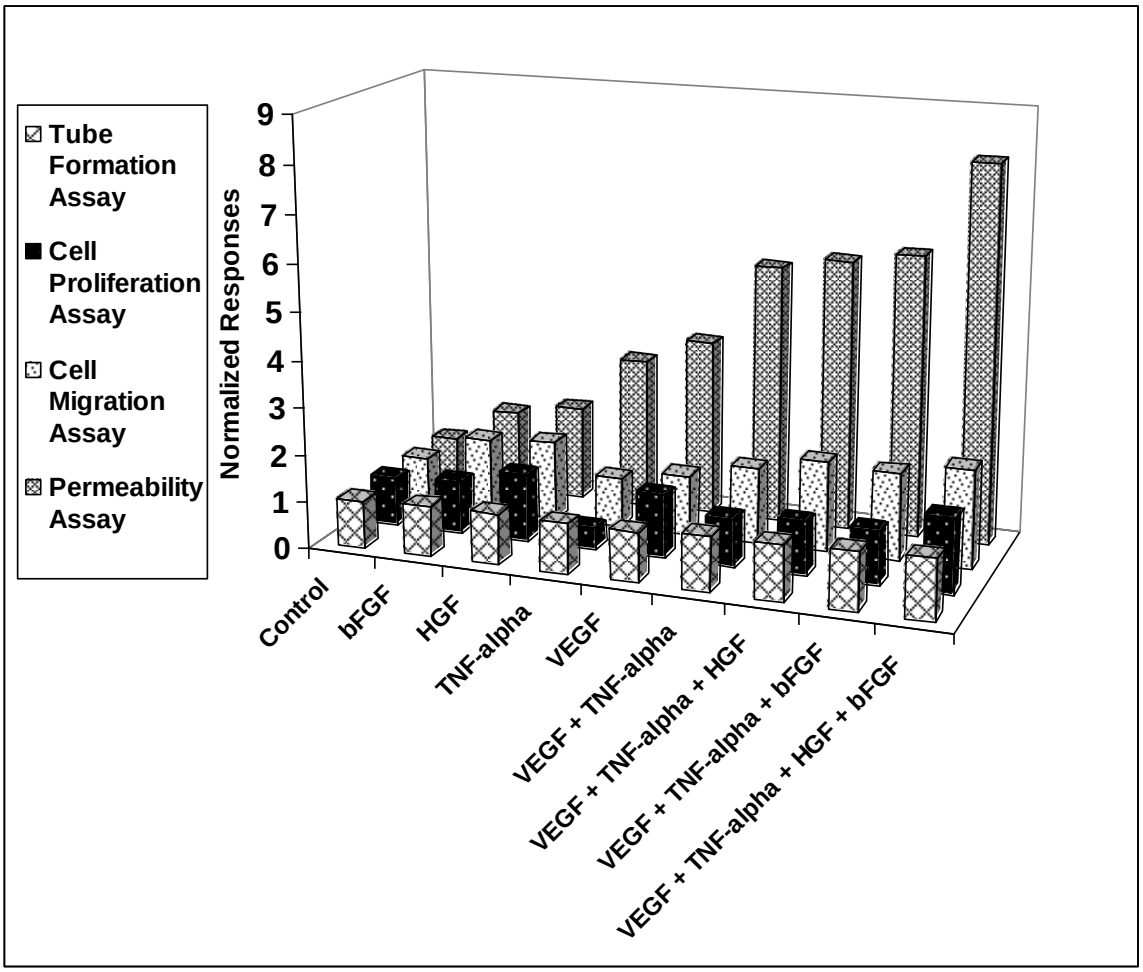

Figure 5.13 Relative increase, compared to control, of cell migration, proliferation, tube formation and permeability in response to individual as well as combination of different cytokines. The exposure time, at which significant difference in responses to the stimulant were obtained, are different for each assay. In the case of cell monolayer permeability studies, the relative increase in sensor response was determined from the ratio of the overall sensor response after 1 h exposure to different cytokines to the response obtained from the untreated monolayers. In case of cell migration, proliferation and tube formation study responses after 10 h, 48 h and 11 h were considered, respectively

in cell proliferation when exposed to TNF-α to a 1.3-fold increase in cell proliferation and migration when exposed to VEGF. Finally, combination of cytokines also showed large changes in cell monolayer permeability compared to the other steps of angiogenesis. For example, when exposed to all four cytokines, the permeability increased by 8-fold whereas tube formation, cell proliferation and cell migration only increased by 1.3, 1.6, and 2.1-fold, respectively. When comparing these assays, it is important to remember that the exposure time at which significant differences in response to the stimulant were obtained differed for each assay. However, the results clearly demonstrate that the permeability assay provided the most significant response in the quickest amount of time (only 1 h).

5.4 Discussion

Angiogenesis involves formation of new blood vessels from the existing ones. Pro- and anti-angiogenic molecules act in tandem to regulate angiogenesis. In diseases, it is this balance between the stimulators and inhibitors of angiogenesis that is disturbed. Several molecules have been classified as angiogenic factors based on their biological activities (Folkman and Shing 1992). Generally, multiple angiogenic factors are released in vivo and if one factor is insufficient in inducing any particular event of angiogenesis by itself, it can act in conjunction with other factors. In addition, it has been shown that some factors can enhance the ability of other factors to induce the event. Different studies have demonstrated the combined effect of different growth factors on angiogenesis *in vivo* (Asahara et al. 1995; Bond et al. 1998; Xin et al. 2001). However, while *in vivo* analyses provide the most accurate representation of angiogenesis inside the body, it is not feasible to use *in vivo* analyses for initial screening of pro- and anti-angiogenic molecules. One of the most important challenges in the study of angiogenesis is the selection of appropriate *in vitro* methods for assessing this process. Investigators have accepted the fact that a combination of assays is needed to truly assess the entire angiogenic process (Staton et al. 2004).

Cell proliferation is one of the most common methods employed for assaying *in vitro* angiogenesis. Results from this investigation demonstrated that bFGF, HGF and

VEGF enhanced cell proliferation while TNF-α inhibited it. Upon incubating HUVECs with both VEGF and TNF-α, it was observed that TNF-α downregulated the ability of VEGF to stimulate cell proliferation. Previous studies had also reported similar observations (Frater-Schroder et al. 1987; Nakagami et al. 2002; Patterson et al. 1996). Even though incubating HUVECs with three different cytokines did not increase the proliferation in significant amount, incubation with all the four cytokines resulted in a significant increase in the mitogenic activity.

Another *in vitro* technique commonly used to analyze angiogenesis is cell migration. Experiments with individual cytokines demonstrated that at the concentrations tested, bFGF and HGF produced maximum migration, followed by VEGF and TNF-α after 10 h. Incubating cells with combination of VEGF and TNF-α resulted in increased migration of HUVECs. Another study had also demonstrated wound healing induced by VEGF was enhanced by TNF-α (Giraudo et al. 1998). Profound wound healing was observed upon stimulating the cells with all four cytokines.

Finally, morphogenesis or organization of cells into tubular structures is commonly used to assay angiogenesis. This investigation showed that exposing HUVECs to individual cytokines at the concentrations studied produced no significant changes in their ability to induce tube formation. However, previous studies had shown that unlike HGF, at higher concentrations (0.1 to 100 ng/ml) bFGF and VEGF stimulated tube formation (Kumar et al. 1998). Incubating cells with combination of VEGF and TNF-α resulted in significant increase in the average length of tubes. Further addition of the third cytokine did not increase the tube length significantly. Synergistic effect of VEGF and bFGF as well as the cooperative effect of VEGF, TNF-α and bFGF in inducing tubular structures in human microvascular endothelial cells have been reported previously (Koolwijk et al. 1996; Pepper et al. 1992). However, incubating cells with all four cytokines enhanced tube formation.

Another key initial step in the process of angiogenesis is increase in vascular permeability. The effects of growth factors on endothelial cell permeability have been studied previously; however, the use of permeability as an assay for angiogenesis has not been investigated. The present study focused on the use of a cell-based biosensor that detects changes in cell monolayer permeability as a possible assay for quantifying

angiogenesis. Results demonstrated that the biosensor responded to the presence of VEGF as early as 30 min, and the overall sensor response increased with increasing exposure time up to 10 h. However, it was observed that exposing the sensor to TNF-α beyond 3 h resulted in a reduced sensor response indicating a decrease in cell monolayer permeability. This result is in agreement with another study which also reported a decrease in permeability after 6 h stimulation of HUVEC with TNF- α (Nooteboom et al. 2000). The decrease in cell monolayer permeability can be either due to the internalization of cell surface receptors thereby resulting in reduced number of receptors for TNF-α to bind or due to release of phosphatases upon prolong exposure to TNF-α which thereby prevents phosphorylation of different signaling pathways (Lum and Malik 1994). Even though bFGF and HGF were able to induce an increase in monolayer permeability, as evident from the increased sensor response, the responses of HUVEC monolayers to these growth factors were much less compared to that obtained for VEGF and TNF-α.

Exposing the cell based sensor to the combination of VEGF and TNF-α resulted in an increased response from the sensor indicating the modulation of cell monolayer permeability by the combined effect of these two cytokines. However, addition of third factor in the form of bFGF or HGF did not increase the sensor response. When the sensor was exposed to the combination of all the four cytokines, a profound increase in sensor response was observed. To the best of our knowledge, only one study had previously been reported which investigated the effect of combining TNF-α, IFN-gamma and interleukin-1 alpha/beta on HUVEC monolayer permeability (Burke-Gaffney and Keenan 1993).

The changes in cell monolayer permeability and hence the increase in sensor response can be due to the weakening of cellular junctions leading to gap formation in the cell monolayer or can be due to the formation of caveolae like structure within cells which act as transcellular channels. Study directed towards elucidating the mechanism behind increased biosensor response has been described in Chapter 6.

To compare the permeability assay with the other commonly used *in vitro* assays, the responses obtained from each assay were normalized with respect to the control values. This comparison demonstrated that the relative change in the permeability assay

in the presence of cytokines compared to the control was far greater than the relative change observed in other assays, especially when the cells were exposed to combinations of cytokines. These results indicate that a permeability assay may be an alternative or at least additional method for screening both pro- and anti-angiogenic factors and may provide better sensitivity at lower concentrations of angiogenic factors. In addition, while other *in vitro* angiogenic assays can take up to 10 - 48 h to complete, the cell based biosensor provided a response in only 1 h, bolstering its potential to act as a quick screening tool for angiogenesis.

Chapter 6 : Comparing the Effect of Different Cytokines on Endothelial and Epithelial Cell Architectures

6.1 Introduction

Epithelia as well as endothelia act as a selectively permeable barrier, whereby permitting the passage of water and nutrients while preventing the passage of pathogens. During several pathological conditions such as cancer, diabetes, Crohn's disease and inflammatory bowel disease, the permeability properties of these cells are compromised (Clayburgh et al. 2004; Irvine and Marshall 2000; Rak et al. 2007; Scalia et al. 2007). Different angiogenic molecules such as vascular endothelial growth factor (VEGF), basic fibroblast growth factor (bFGF), hepatocyte growth factor (HGF) and tumor necrosis factor – alpha (TNF-α) are known to induce increased permeability across cell monolayers (Lal et al. 2001; Martin et al. 2002; McKay and Baird 1999; Mullin and Snock 1990; Nusrat et al. 2000; Stockton et al. 2004; Walsh et al. 2000; Wang et al. 2005). This modulation of permeability can be attributed either to the altered rate of transport of solutes across the cells through transcellular channels (transcellular permeability) or through the gaps formed due to the disintegration of cell barrier architectures (paracellular permeability). Also, both pathways can contribute simultaneously to enhanced permeability across the cell monolayer. Figure 6.1 shows a schematic of these pathways which may be involved in increased permeability. Epithelial and endothelial cells maintain their flattened shape by counteracting the centrifugal tension generated by cellular junctions, focal adhesions and microtubules with the centripetal tension created by actinomyosin (Dudek and Garcia 2001; Mehta and Malik 2006) as shown in Figure 6.2. The disruption of cell barrier integrity during increased paracellular permeability leads to changes in cell shape due to the disturbance of the equilibrium between the forces that help the cells maintain their morphology. Stimulation of cells with different cytokines has been shown to increase actin stress fiber formation and induce cell contraction (Dowrick et al. 1991; Morales-Ruiz et al. 2000; Petrache et al. 2003; Stockton et al. 2004). Even though studies had shown that various actin binding proteins interact with intercellular junctional proteins as well as the cell - matrix binding

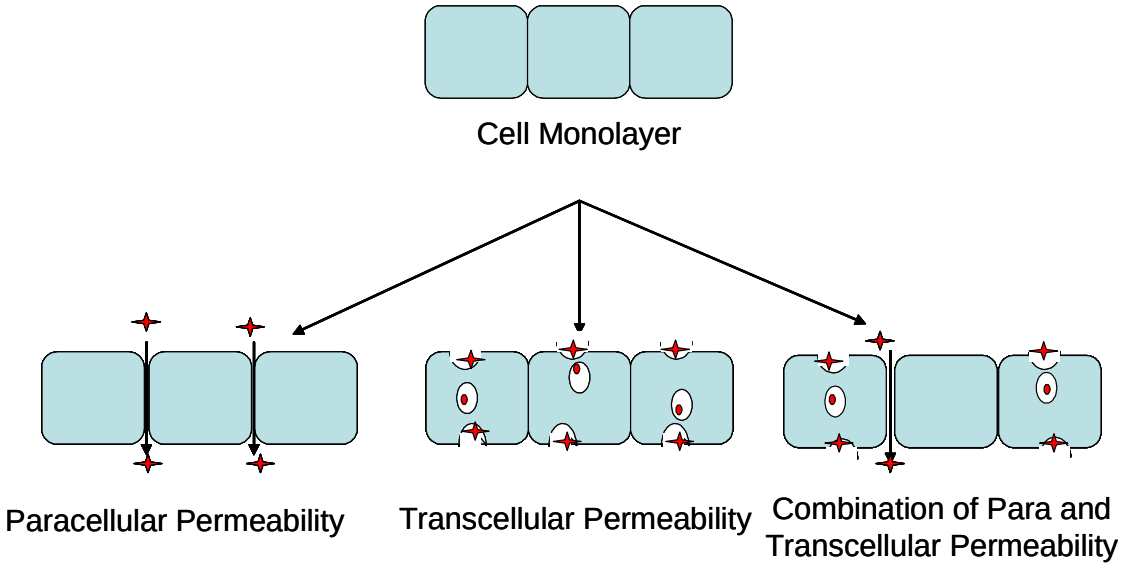

Figure 6.1 Schematic showing different permeability pathways. Permeability across cell monolayer can involve transcellular, paracellular or both pathways

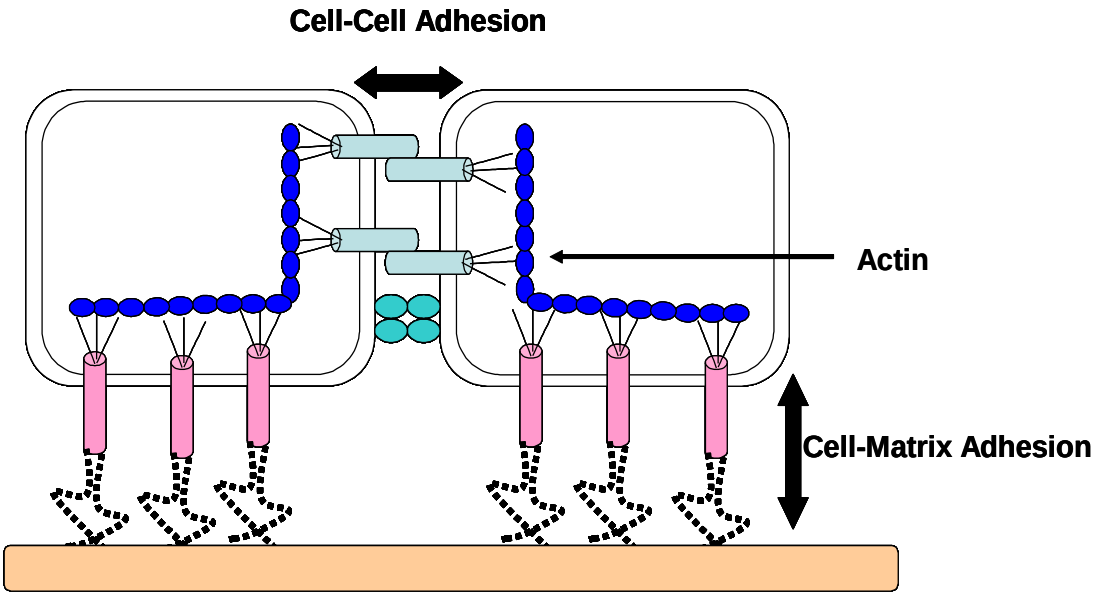

Figure 6.2 Schematics showing cell-cell and cell- matrix adhesion

proteins, the effect of these agents on cell-substrate adhesion has not been studied in detail (Dudek and Garcia 2001; Lum and Malik 1994; Mehta and Malik 2006). The present study is carried out with the aim of i) investigating the effects of the above mentioned cytokines, individually and in combination, on the permeability properties of epithelial cells and comparing the effects with those on endothelial cells, ii) determining the mechanism (transcellular vs. paracellular) responsible for the changes in permeability and iii) studying the effect of these cytokines on cell – substrate adhesion.

To compare the effects of VEGF, HGF, bFGF and TNF-α in inducing permeability across epithelial cell monolayers with those across endothelial cell monolayers, a confluent monolayer of LLC-PK1 was grown on the ISE membrane surface. LLC-PK1 is a well characterized porcine epithelial cell line having physiological properties very similar to the renal proximal tubule (Mullin and Kleinzeller 1985). Inflammatory cytokines like TNF-α had been shown to increase the permeability of LLC-PK1 by altering the cell barrier integrity (Mullin and Snock 1990). This study is directed towards investigating the permeability modifying effects of both the individual and combined cytokines on the LLC-PK1 monolayer by measuring the responses from the LLC-PK1 based biosensor under these conditions and comparing these responses to those obtained from the HUVEC based biosensor. Further, to investigate whether the paracellular and transcellular pathway is involved in the induced permeability across the cell monolayer, the effect of these cytokines on the formation intercellular gaps as well as transcellular structures was studied for both the LLC-PK1 monolayer and the HUVEC monolayer.

Studies have demonstrated that binding of cytokines to their respective cell receptors results in the activation of the signaling cascade eventually leading to increased permeability. Pathways implicated for increased permeability include the Raf-1-MEK-ERK1/2 pathway and the NOS involved pathway (Breslin et al. 2003; Hu et al. 2005; Lal et al. 2001; Wu et al. 1999). As demonstrated in Figure 6.3, while protein kinase C (PKC) is the direct upstream mediator of Raf-1, both the PKC and Phosphatidylinositol 3 – Kinase (PI3-K) pathway are involved in NO induced permeability. PKC and PI3-K signaling pathways have been reported to regulate the cell – cell junctional proteins and have thus been implicated to play integral roles in cytokine mediated increase in

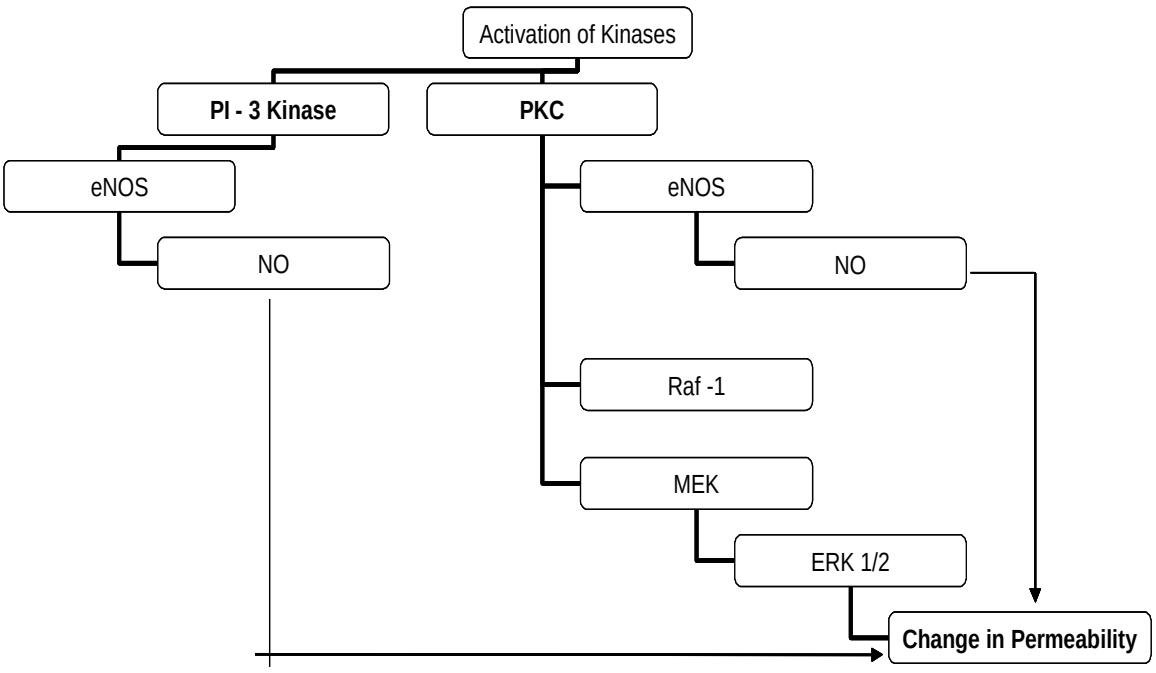

Figure 6.3 Schematic of signaling pathways. Binding of cytokines to the respective receptors leads to the activation of PI-3K and PKC. In turn, PKC can induce permeability by Raf1-MEK-ERK1/2 pathway or by activation of eNOS. PI-3K activation leads to the involvement of Akt –eNOS pathway for induction of permeability

paracellular permeability [Mullin 1990, Lal 2001, Breslin 2003, Hu 2005, Wu 1999]. The present study also investigated the effect of blocking PKC and PI3-K, with LY294002 and Bisindolylmaleimide I (BIM I) respectively on the sensor response and the intercellular gap area for both the cell lines.

6.2 Experimental Section

6.2.1 Reagents

Purified carrier free $VEGF_{165}$, bFGF, HGF and TNF-α were purchased from R&D Systems (Minneapolis, MN). The cytokines were dissolved in 0.1% bovine serum albumin (BSA) in Dulbecco's phosphate-buffered saline (PBS) (GIBCO^{TM}). HUVECs and LLC-PK1 cells used during the experiments were cultured as described in Chapter 3. Membrane materials and sensor preparation have also been described in Chapter 3.

6.2.2 Evaluation of Electrode Response

Following confluent cell monolayer formation, the control membranes were tested for inhibited ion response. After the confirmation of the inhibited ion response, the cell-seeded membranes were exposed to different cytokine solutions containing individual and combinations of cytokines (pH 7.2) in PBS for 3 h, and the response of the sensor was measured.

At a final concentration of 0.1M KCl, the electrode response was measured for the following conditions: (a) the membrane without cells and without cytokines to obtain the baseline response of the sensor, (b) membranes with cells and without cytokines to confirm the inhibited response of the sensor due to the confluent monolayer of cells, and (c) membranes with cells and with cytokines.

To account for slight variations between fabricated membranes, the final data are reported as the ratio of the response obtained at 0.1 M KCl for the ISEs with cells and cytokines to the response obtained for the same membrane without cells and cytokines.

6.2.3 Determination of Transcellular Structures

To determine whether caveolae like structures leading to transcellular channels were formed in the cells upon exposure to the cytokines, the cells were examined under transmission electron microscope. For this purpose, the cells (both HUVECs and LLC-PK1s) were cultured till confluency in petri dishes. Once confluent, the cells were treated with the combination of all four cytokines for 3 h. The cells were then rinsed with 0.1 M Sorenson's phosphate buffer and fixed in 3.5% glutaraldehyde in 0.1 M Sorenson's phosphate buffer for 45 min at 4 ^{0}C. Then, the cells were washed with 5% sucrose in 0.1 M Sorenson's buffer and post fixed with osmium tetra oxide in buffer for 45 min at 4 ^{0}C. The cells were then dehydrated in graded ethanol from 50% to 100% at room temperature. Next, they were embedded in resin, which was polymerized for 36 h at 60 ^{0}C. After hardening, thin sections (60 – 80 nm) were cut on a Reichert Ultracut E ultramicrotome with a diamond knife. They were stained initially with uranyl acetate for 5 min and then with lead citrate for 3 min and then examined with a Philips Tecnai 12 transmission electron microscope.

6.2.4 Determination of Intercellular Gap Area

Gap area determination by staining cells with coomassie blue had been described previously (Geldhof et al. 2002; Stockton et al. 2004). Briefly, a confluent monolayer of cells, cultured in 24 well plates, was treated with individual and different combinations of cytokines for 3 h. Cells were then rinsed with PBS and fixed for 30 min in 3% PFA in PBS. Following fixation, the cells were rinsed and stained with 0.25% coomassie blue in 1:1:2 volume ratio of methanol: glacial acetic acid: deionized water for 10 min. The cells were then rinsed thoroughly with PBS. The air-dried cells were then examined under a Zeiss IM 35 microscope. The stained cells appeared dark and the intercellular gaps appeared white. For the purpose of determining the gap area using the Scion Image software, the images were inverted. As a result, the gap between the cells appeared black while the cells were white. The pixel values of the image ranged from 0 for white to 255 for black. The total pixels corresponding to the image were counted. At different regions of the image, the threshold pixel value i.e. the pixel value corresponding to the beginning of gap area was determined. Total pixels greater than this value were then counted. From

this two pixel count, percent gap area was determined. Three independent set of experiments were carried out for each condition. Each experiment was replicated in two wells.

6.2.5 Determination of the Effect of Blocking PKC and PI3-K Pathways

To further investigate the role of the paracellular pathway in modifying permeability, the PI3-K and PKC pathways were blocked with 0.01 nM LY294002 and 10 μM BIM I, respectively. Studies have shown that BIM I and LY294002 at these concentrations can effectively block the PKC and PI3-K pathways effectively without inhibiting other protein kinases (Breslin et al. 2003; Lal et al. 2001). For this purpose, the effect of these inhibitors on sensor response as well as on the intercellular gap area was determined. To investigate the effect of blocking the pathways on sensor response, the electrode response was measured at a final concentration of 0.1 M KCl for the following conditions: (a) membranes with cells (HUVECs or LLC-PK1) and inhibitors but without cytokines, and (b) membranes with cells (HUVECs or LLC-PK1) and with cytokines and inhibitors.

To study the effect of blocking these pathways on paracellular permeability, intercellular gap area was determined as described earlier after treating the cells with inhibitors with or without the combination of all four cytokines.

6.2.6 Determination of Cell- Substrate Adhesion

To determine the effects of different cytokines on cell – substrate adhesion, cell surface area was measured following the method developed by Alexander and coworkers (Alexander et al. 2001). Briefly, confluent monolayers of cells, cultured in 24 well plates, were treated with individual and different combination of cytokines for 3 h. Following the treatment, the cells were rinsed and incubated with 0.1% trypsin in PBS for 5 min. The cells were rinsed again and fixed with 3% PFA for 30 min. Following fixation, the cells were rinsed and stained with coomassie blue for 10 min. To remove the excess dye, the cells were then rinsed and the air-dried cells were examined under a Zeiss IM 35 microscope. The surface areas of the cells were then measured using Axio Vision 4 software. Trypsinization leads to rounding up of cells resulting in reduced surface area. When the cell-substrate adhesion is increased, the cells resist rounding up following the

treatment with trypsin resulting in higher surface area (Alexander et al. 2001). Thus alteration in the cell-substrate adhesion is reflected in the altered surface area of cells.

Three independent set of experiments were carried out for each condition. Each experiment was replicated in two wells.

6.2.7 Statistical Analysis

For all experiments data are reported as mean ± SEM. Statistical analyses were carried out using one-way ANOVA and the Student-Newman-Keuls test for post-hoc comparisons of the means with $P<0.05$. SigmaStat v 3.1 software was used for these analyses.

6.3 Results

6.3.1 Optimization of the Seeding Times

In the case of the LLC-PK1 cell-based biosensor, the sensor response was initially evaluated as a function of seeding times of LLC-PK1. For this purpose calibration curves were constructed as shown in Figure 6.4. It was observed that increasing the seeding time from 5 h to 18 h resulted in reduced response from the sensor. However, further increasing the seeding time to 24 h, resulted in an increase in sensor response. Microscopic studies revealed that a confluent cell monolayer was formed within 18 h of seeding. Further incubation led to the cell death and detachment. Henceforth, for all the sensor experiments with epithelial cells, the incubation period of 18 h was maintained.

6.3.2 Sensor Response in the Presence of Cytokines

To evaluate the response from the sensor in the presence of different cytokines, the LLC-PK1 cell-based sensor was exposed to four cytokines individually for 3 h. As seen in Figure 6.5, the response from the sensor significantly increased in the presence of these cytokines. When LLC-PK1 based biosensor was exposed to VEGF a response of 0.15

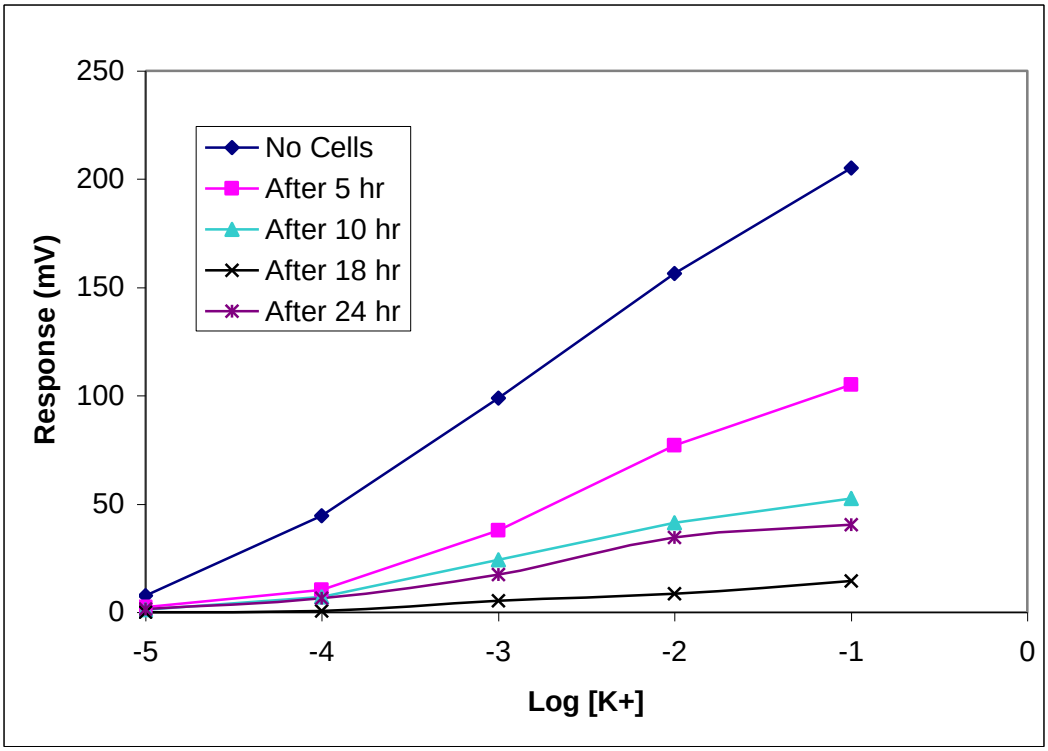

Figure 6.4 Calibration plots as a function of cell seeding times

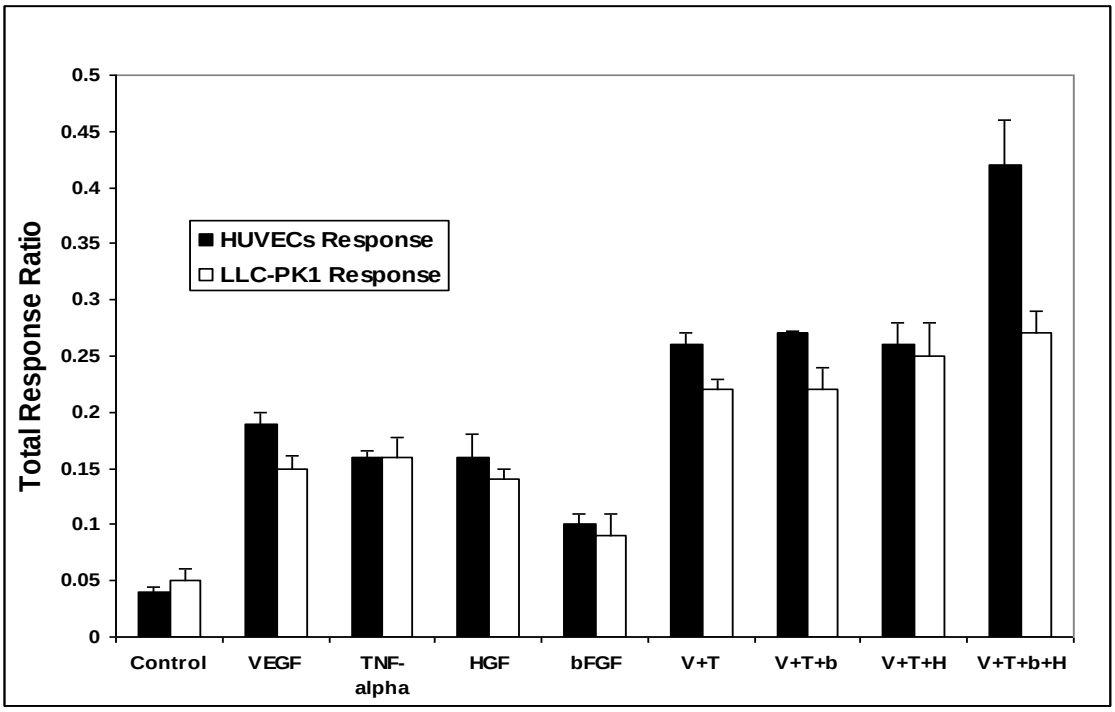

Figure 6.5 Ratio of ISE response obtained at 0.1 M KCl following exposure of the cell based (HUVECs or LLC-PK1) sensor to the individual as well as combination of different cytokines for 3 hr to ISE response obtained at 0.1 M KCl for the membrane without cells and without cytokines. (Error bars represent SE N=3.)

was obtained. In case of TNF-α, HGF and bFGF the responses were 0.16, 0.14 and 0.09 respectively. Next, the cell based sensor was exposed to different combination of these cytokines. Initially, upon exposing the sensor to the combination of VEGF and TNF-α (V+T) for 3 h, an enhanced response (0.22) from the sensor was obtained. Even though the response was not additive, it was significantly different from the responses obtained upon exposing the sensor to these cytokines individually. The sensor responses to the presence of the combinations of VEGF, TNF-α and HGF (V+T+H), VEGF, TNF-α and bFGF (V+T+b) and all four cytokines (V+T+b+H) were next evaluated. As demonstrated in Figure 6.4, the responses, 0.25, 0.22 and 0.27, respectively, were not significantly different from the response obtained for the combination of VEGF and TNF- α.

Upon comparing the epithelial cell based sensor with that of endothelial cell based sensor, no significant difference in the responses were observed when the cell based sensors were exposed to different cytokines individually. Thus while a response of 0.15 was obtained from LLC-PK1 based biosensor in the presence of VEGF, the response from HUVEC based sensor was 0.19. In case of TNF-α, HGF and bFGF while for epithelial cell based biosensor the responses were 0.16, 0.14 and 0.09, respectively, the responses from HUVEC based sensor are 0.16, 0.16 and 0.1, respectively. However, when the responses to the combination of cytokines were compared, responses obtained from HUVEC based sensor was significantly greater than that obtained from LLC-PK1-based sensor except in the case of combination of VEGF, TNF-α and HGF (V+T+H). For example, in the presence of all four cytokines, while a response of 0.42 was obtained from HUVEC based sensor, the response from the LLC-PK1 based sensor was 0.27.

6.3.3 Determination of Permeability Pathway

Since we observed differences in the responses from the endothelial and epithelial cell based sensors, the next focus of this study was to determine the mechanisms behind the altered permeability in HUVEC as well as in LLC-PK1 monolayers. Increased permeability can be due to the disintegration of intercellular junctions leading to the gap formation between cells or due to the formation of caveolae acting as the transcellular channels. It is also possible that the passage of ions is due to both pathways acting simultaneously.

6.3.3.1 Determination of Caveolae

Since, we obtained the maximum response from both the sensors in the presence of all the four cytokines, we decided to examine whether there is any caveolae formation when the cells were treated with the combination of all four cytokines. As observed in Figure 6.6A, the number of caveolae in treated epithelial cells was much more than that observed in the control. However, as shown in Figure 6.6B, increases in the number of caveolae like structures were not observed in treated HUVECs as compared to the control.

6.3.3.2 Determination of Intercellular Gap Area

To observe the effect of different cytokines on intercellular gap formation, the cells were exposed to individual and combined cytokines for 3 h and gap area was determined. Figure 6.7 shows percent gap area upon exposing HUVEC and LLC-PK1 monolayers to different cytokines. With HUVECs, a 6% gap area was observed in the control. Exposing HUVECs to individual cytokines, except bFGF, resulted in significant increase in gap area. Treating with HGF and TNF-α individually caused a gap area of 16.5% and 16.9% respectively whereas treating with VEGF caused a gap area of 22%. When the cells were exposed to the combination of cytokines, percent gap area increased significantly as compared to individual cytokines. Treating with V+T, V+T+H and V+T+b caused gap areas of 26.2%, 26.5% and 27.4%, respectively, whereas a profound increase in gap area to 43% was observed when HUVEC monolayer was treated with the combination of all the four cytokines.

In the case of LLC-PK1 cells, however, changes in gap area were not as profound. No significant difference in percent gap area from control was observed when the cells were treated with the cytokines individually. Thus, while a 2.4% gap area was observed in control, treating cells with VEGF, HGF, bFGF and TNF-α caused gap area of 3.99%, 4.05%, 3.13% and 6.28% respectively. Exposure of cells to combinations of cytokines resulted in increase in gap area as compared to control. Treating the cells with V+T, V+T+H, V+T+b and V+T+H+b caused gap area of 7.15%, 7.04%, 7.52% and 8.5%, respectively.

A

Control

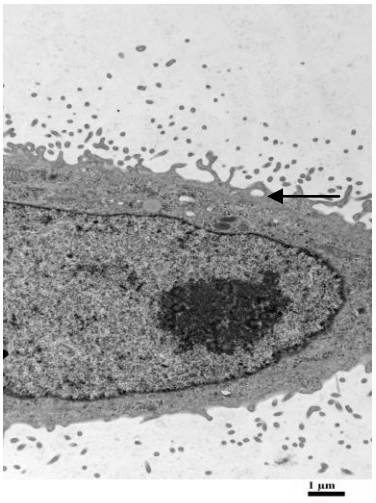

Treated

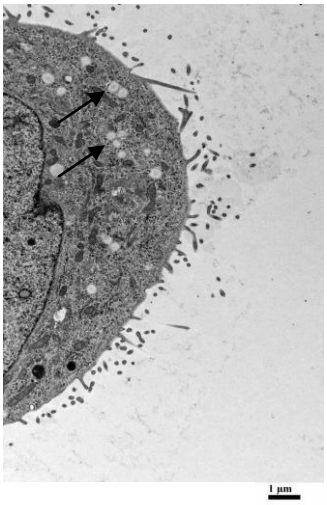

B

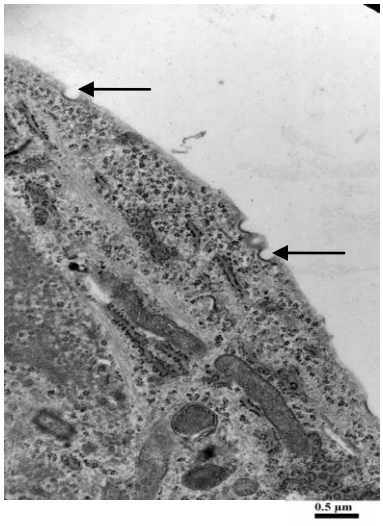

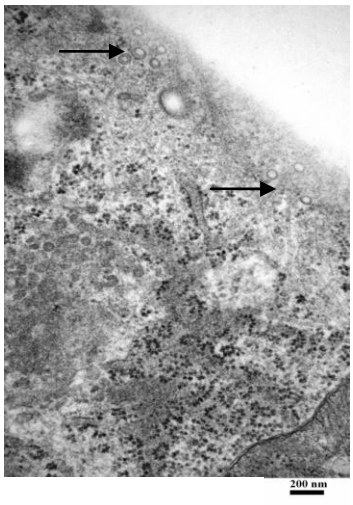

Figure 6.6 Electron micrograph of LLC-PK1 (A) and HUVEC (B) cells with or without exposure to the combination of all four cytokines. A significant increase in the density of caveolae like structures observed in treated LLC-PK1 as compared to control. In case of HUVEC, caveolae like structure formation did not increase significantly following treatment

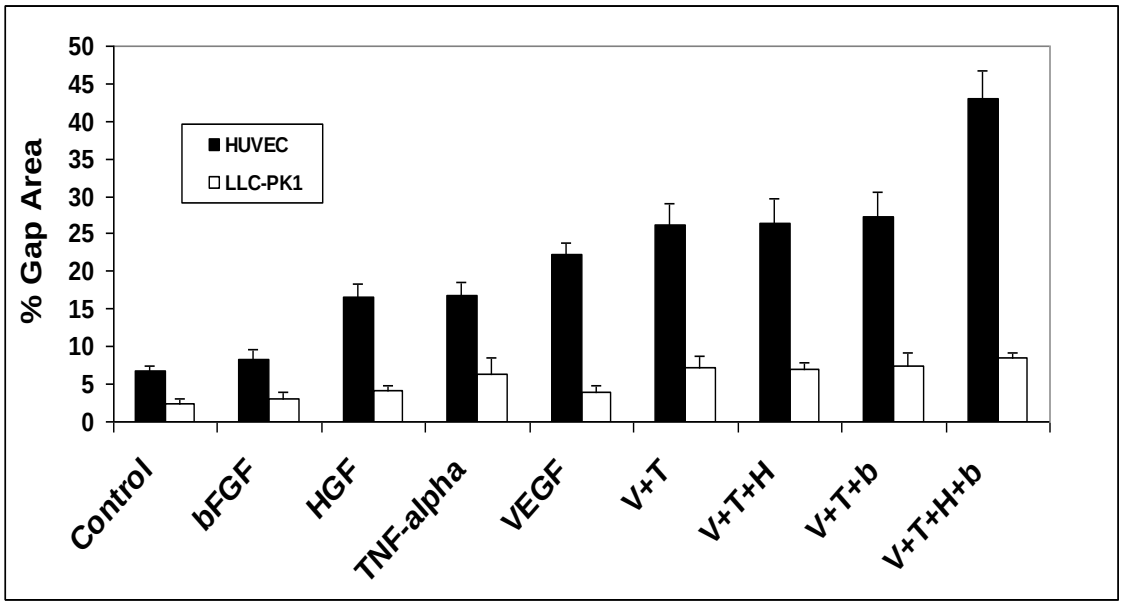

Figure 6.7 Percent gap area formed in HUVEC and LLC-PK1 monolayer upon exposing to different individual and combination of cytokines for 3 h. (Error bars represent SE N=3.)

6.3.3.3 Correlating Percent Gap Area with Sensor Response

In Figure 6.8 the correlation between percent gap area and sensor response is shown. In the case of HUVECs, a strong positive correlation was obtained indicating that the sensor response can be attributed primarily to the formation of intercellular gaps. However, with LLC-PK1 cells, even though a positive correlation was observed it was not as great as that observed with the HUVECs indicating that the sensor response was not entirely due to the gaps formed between cells. These results also agree with the previous results showing more caveolae formed when treating LLC-PK1 cells indicating increases in transcellular permeability play a bigger role than increases in paracellular permeability when treating these cells with cytokines. In contrast, changes in paracellular permeability play a bigger role when treating HUVECs with these cytokines.

6.3.3.4 Effect of Blocking Signaling Pathways on Sensor Response

Studies have reported that the cytokines have the ability to activate PI3-K and PKC in different cell lines. The activation leads to a series of downstream signaling which ultimately regulates intercellular proteins (Breslin et al. 2003; Hu et al. 2005; Lal et al. 2001; Mullin and Snock 1990; Wu et al. 1999). Studies have also demonstrated that blocking PI3-K and PKC resulted in decrease in paracellular permeability induced by different cytokines across cell monolayers (Breslin et al. 2003; Hu et al. 2005; Lal et al. 2001; Mullin and Snock 1990; Wu et al. 1999). The next part of this study was to observe the effect of blocking PI3-K by LY294002 and PKC by BIM I individually and then in combination on the sensor response. Figure 6.9 shows the effects of exposing the HUVEC based sensor to the inhibitors with or without the cytokines. When exposing the HUVEC based sensor to 0.1 nM LY294002 and 10 μM BIM I individually and in combination, in the absence of the cytokines the responses were not significantly different from the response obtained without inhibitors. When exposing the cell based sensor to the combination of all four cytokines for 3 h in the presence of BIM I, a significant decrease in sensor response was obtained. A significant decrease in sensor response was also obtained when exposing the cells to LY294002 in the presence of cytokines. The responses thus obtained were 0.13 and 0.15 in the presence of BIM I and

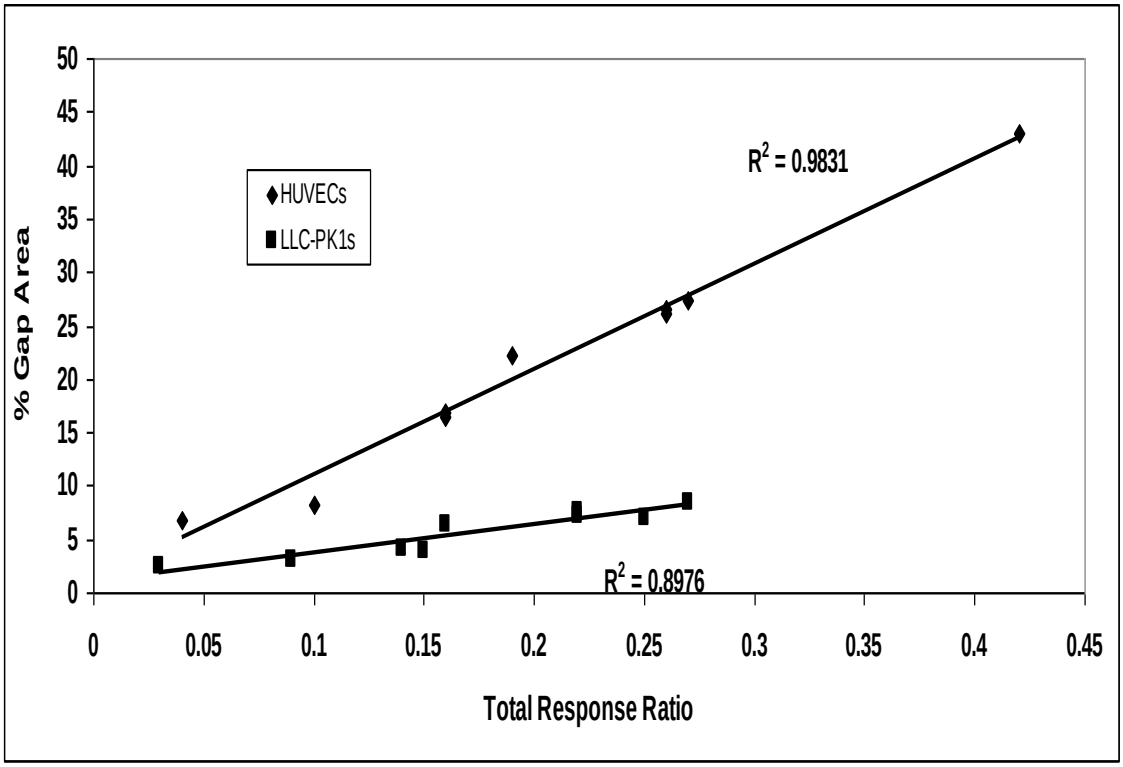

Figure 6.8 Correlation between percent gap area and sensor response for HUVEC and LLC-PK1

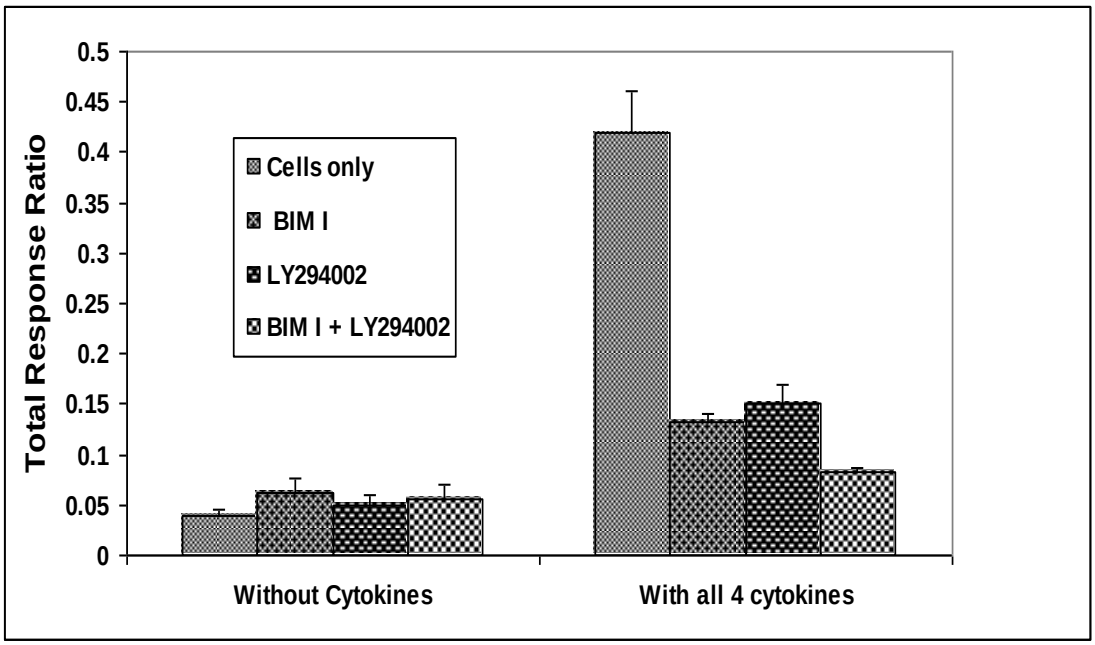

Figure 6.9 Ratio of ISE response obtained at 0.1 M KCl following exposure of the HUVEC based sensor to the individual as well as combination of inhibitors with or without all four cytokines for 3 h to ISE response obtained at 0.1 M KCl for the membrane without cells and without cytokines. (Error bars represent SE N=3.)

LY294002 respectively. When exposing the HUVEC based sensor to all four cytokines in the presence of both these inhibitors, the response from the sensor decreased further and was comparable with the responses obtained for the controls. This indicates that both PI3-K and PKC signaling pathways are simultaneously involved in the induction of permeability by these cytokines in HUVECs. This further supports our hypothesis that the increased response from the HUVEC based biosensor in the presence of cytokines is due to increased passage of potassium ions through the paracellular route.

Figure 6.10 shows the effect of exposing the LLC-PK1 cell based sensor to the inhibitors with or without the cytokines. Similar to that observed with the HUVEC based sensor, no significant difference was observed in the responses when no cytokines were present. Upon exposing the sensor to BIM I in the presence of all four cytokines, the sensor response decreased significantly to 0.13, indicating that the PKC signaling pathway is involved in inducing permeability across the LLC-PK1 monolayer. Exposure to LY294002 led to a reduced response from sensor also, but it only reduced to 0.19. When exposing the sensor to all four cytokines in the presence of both inhibitors, the response (0.12) was not significantly different from that obtained upon exposing the sensor to BIM I alone. Hence, these observations indicate that the PKC signaling pathway is primarily involved in modulating permeability across the epithelial cell line. In addition, these results further support our hypothesis that in case of epithelial cells, both paracellular and transcellular pathways are simultaneously involved.

6.3.3.5 Effect of Blocking Signaling Pathways on Intercellular Gap Area

To ensure that the attenuated sensor response in the presence of the inhibitors is due to reduced passage of ions through the paracellular route, the cell monolayers were exposed to these inhibitors with or without cytokines to observe their effect on gap formation. Figure 6.11 shows the effect of the inhibitors individually and in combination, on the percent gap area of the HUVEC monolayers. In the absence of the cytokines, the gaps formed between the cells in the various controls were not significantly different. Exposing the cells to the BIM I and LY294002 individually and both inhibitors simultaneously in the presence of all four cytokines reduced gap area significantly to

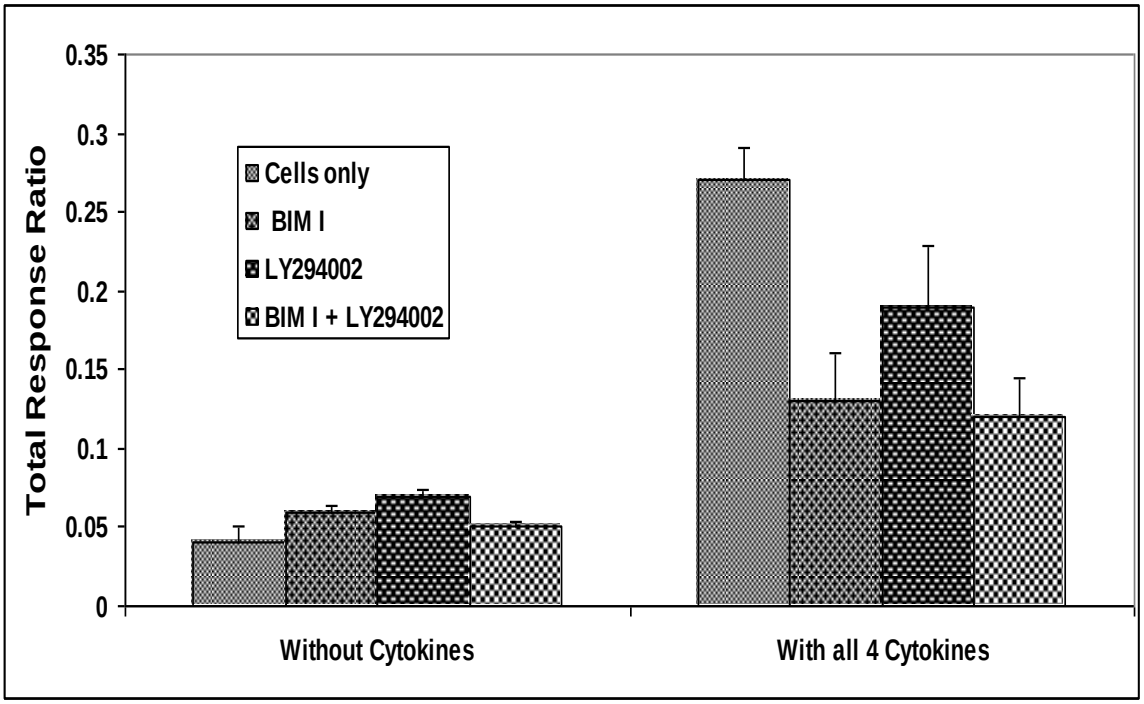

Figure 6.10 Ratio of ISE response obtained at 0.1 M KCl following exposure of the LLC-PK1 based sensor to the individual as well as combination of inhibitors with or without all four cytokines for 3 h to ISE response obtained at 0.1 M KCl for the membrane without cells and without cytokines. (Error bars represent SE N=3.)

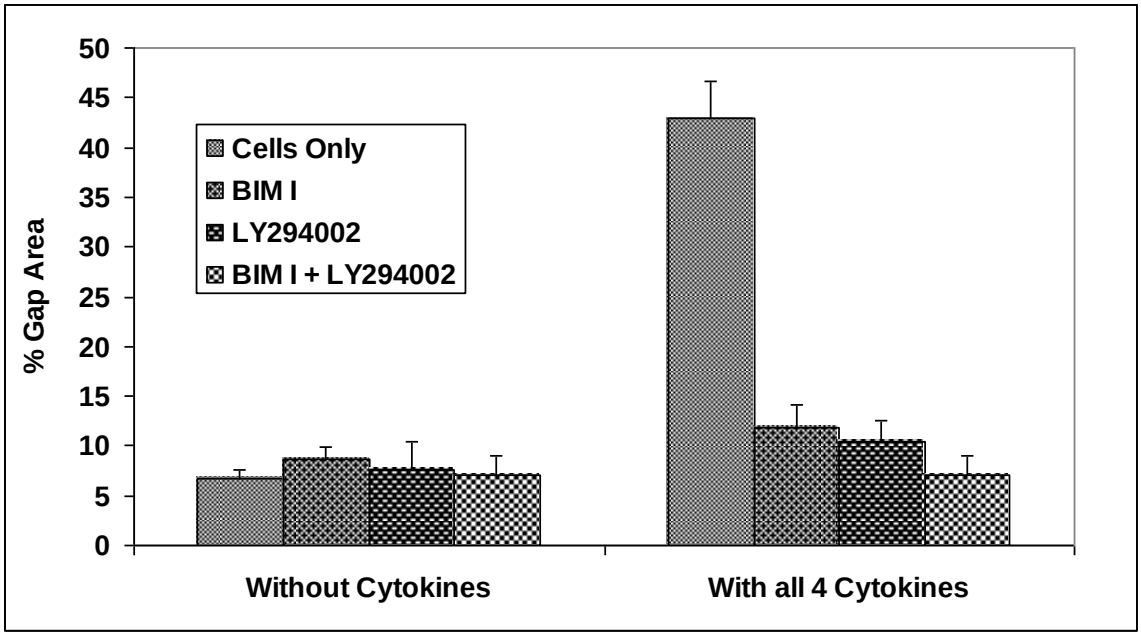

Figure 6.11 Percent gap area formed in HUVEC monolayer upon exposing to individual as well as combination of inhibitors with or without all four cytokines for 3 h (Error bars represent SE N=3.)

11.9%, 10.4 % and 7%, respectively, as compared to the 43% gap area obtained by treating the cells with these four cytokines in the absence of inhibitors. As observed, the gap area obtained in the presence of both the inhibitors and all four cytokines was not significantly different from that obtained in the control studies.

Similarly in case of LLC-PK1 cell monolayers, significantly reduced gap area was observed in the presence of the inhibitors as observed in Figure 6.12. The gap areas obtained in the presence of the inhibitors and the cytokines were comparable to that obtained in controls.

6.3.4 Determination of Cell- Substrate Adhesion

In the case of both HUVEC and LLC-PK1 cells, the formation of gaps was observed between the cells indicating disruption of cell barrier integrity. This indicates that the balance between the tensile and contractile force that maintains the cell shape is disturbed. To determine whether the cell-substrate adhesion is altered to counteract the reduced cell-cell adhesion, we observed the effect of these cytokines on the surface area of trypsinized cells.

Figure 6.13 shows the effects of different cytokines on the surface area of the cells. Trypsinization results in rounding up of the cells which is evident from the reduced surface area of trypsinized as compared to the non-trypsinized cells in the absence of any cytokines. Treating cells with the individual cytokines, except TNF-α, for 3 hr did not significantly change the cell surface area of either the HUVEC or LLC-PK1 cells. However, when the cells were treated with the combination of cytokines, a significant increase in cell surface area was observed when compared to the control. As observed, the surface areas of trypsinized cells that had been treated with all four cytokines were 836 and 797.8 μm^2 for the HUVEC and LLC-PK1 cells and significantly higher than the respective trypsinized cells (670.6 and 654.5 μm^2) in the absence of cytokines, indicating increased cell – substrate adhesion.

To determine whether the change in surface area correlates with the change in the intercellular gap area, percent increase in gap area was plotted against percent increase in surface area as shown in Figure 6.14. In both the cell types, a strong positive correlation was obtained between the two.

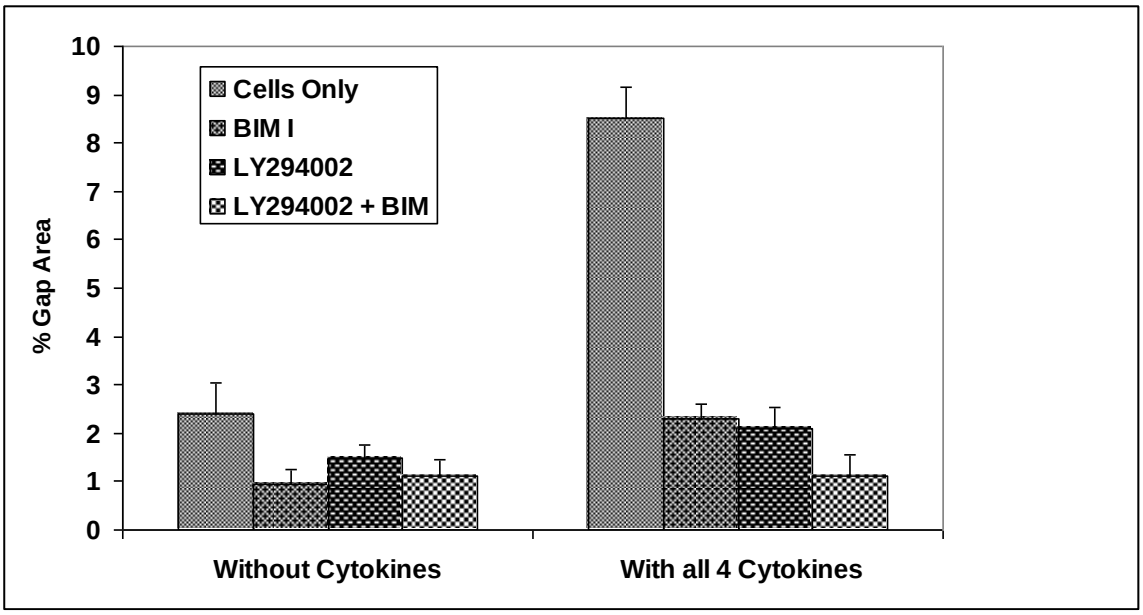

Figure 6.12 Percent gap area formed in LLC-PK1 monolayer upon exposing to individual as well as combination of inhibitors with or without all four cytokines for 3 h (Error bars represent SE N=3.)

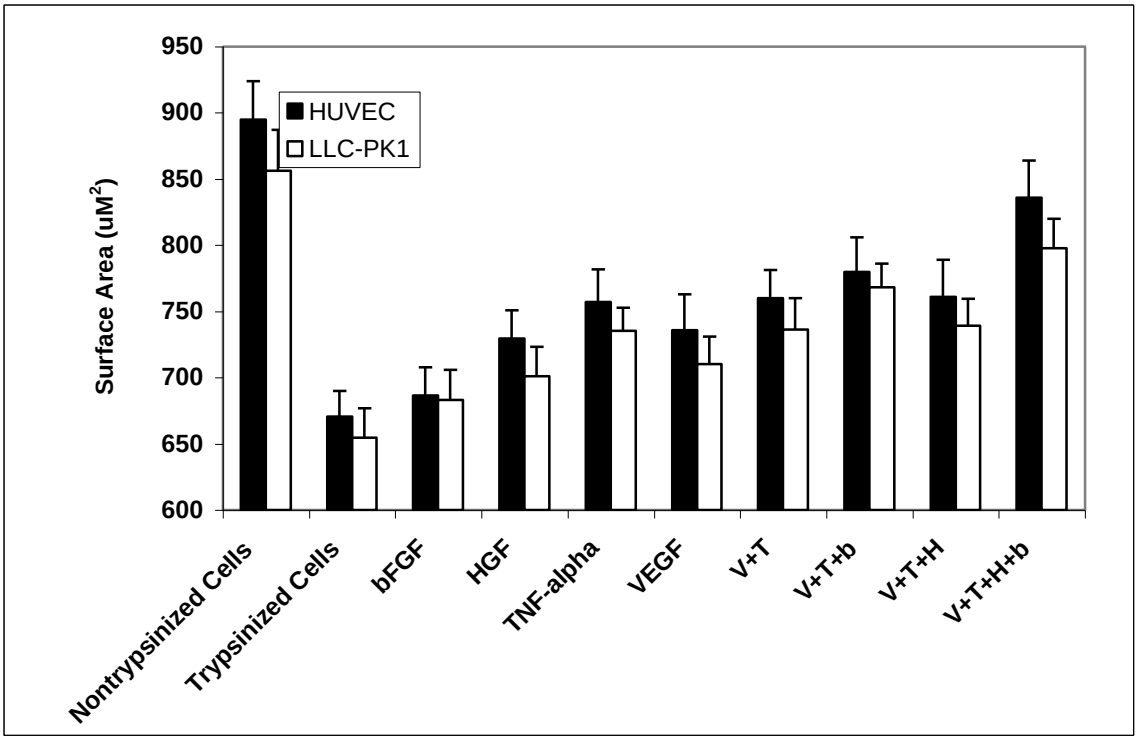

Figure 6.13 Surface area of HUVEC and LLC-PK1 cells upon exposing to different individual and combination of cytokines for 3 h. (Error bars represent SE N=3.)

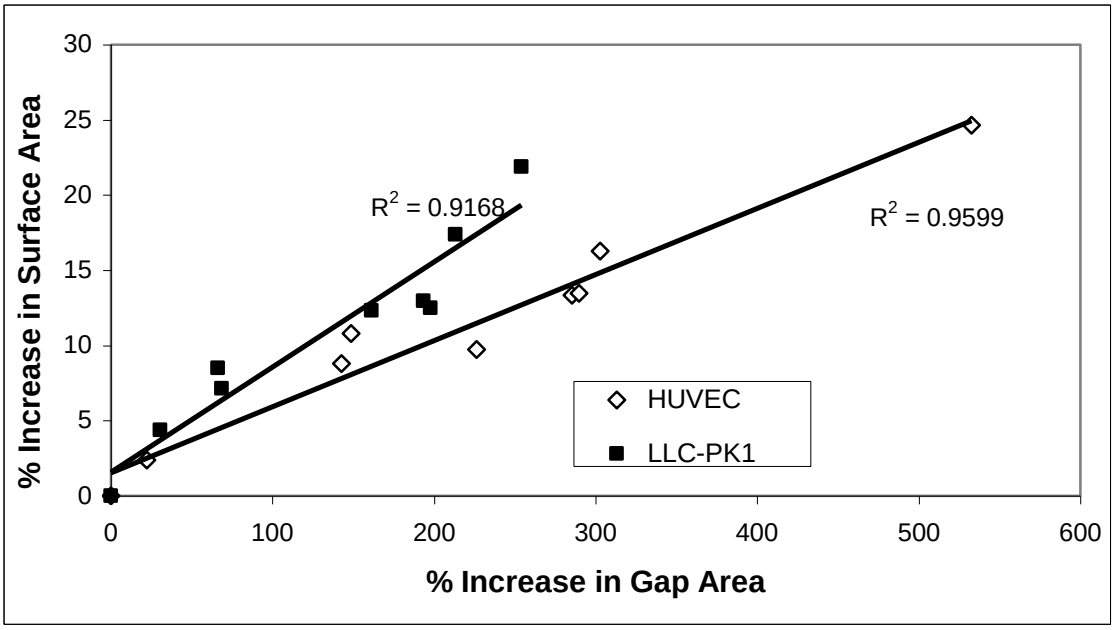

Figure 6.14 Correlation between percent increase in gap area and percent increase in surface area for HUVEC and LLC-PK1

6.4 Discussion

The present study investigated the effect of different cytokines on the permeability across LLC-PK1 monolayers using a cell based biosensor and compared the responses with those obtained from HUVEC based biosensor. Previous study with HUVEC based sensor showed that the sensor responded to the presence of VEGF, TNF-α, HGF and bFGF (Ghosh et al. 2007b). When the sensor was exposed to the combination of these cytokines, the responses from the sensor increased especially when exposed to the combination of all four cytokines (Ghosh et al. 2007b). Other studies have shown disruption of cell barrier integrity of different epithelial cells by different cytokines such as TNF-α, HGF, IL-13 and IFN- γ leading to induction of increased permeability across the cell monolayer (McKay and Baird 1999; Mullin and Snock 1990; Nusrat et al. 1994; Nusrat et al. 2000; Sanders et al. 1995; Walsh et al. 2000; Wang et al. 2005). The barrier properties of LLC-PK1, the porcine epithelial cell line with properties very similar to the renal proximal tubule (Mullin and Kleinzeller 1985), are altered by different permeability modifying agents (Mullin and O'Brien 1986; Mullin and Snock 1990). The present study demonstrated that exposure of the epithelial cell based sensor to VEGF, TNF-α, HGF and bFGF resulted in enhanced sensor response indicating increase permeability across the LLC-PK1 cell monolayer. Exposing the sensor to different combinations of cytokines led to enhanced response from the sensor, indicating increased permeability in response to combination of cytokines. This observation is at par with an earlier study which had also demonstrated that IFN- γ and TNF-α can synergistically disrupt the cell barrier integrity of Caco-2 cell monolayers (Wang et al. 2005).

When comparing the epithelial cell based biosensor to the endothelial cell based biosensor it was shown that the responses obtained with the LLC-PK1 cells were less than that obtained with the HUVECs. The response from the sensor is due to the modulation of permeability by these cytokines. The differences in the sensor responses indicate that increased permeability induced across LLC-PK1 and HUVEC monolayer due to the cytokines is less with the LLC-PK1 cells as compared to the HUVECs. The mechanisms for increased permeability may involve either a transcellular pathway, paracellular pathway or both.

Caveolae, invaginations of plasma membrane, have been observed in most type of cells (Stan 2005) and different permeability modifying agents like VEGF and bFGF have been shown to increase the density of caveolae like structures both *in vivo* and *in vitro* (Chen et al. 2002; Esser et al. 1998b; Feng et al. 1999; Roberts and Palade 1997). The caveolae are then internalized and fuse together to form vesicles. The caveolae can thus act as transcellular channels for the transport of solutes or marker molecules. The electron microscopic study in the present case revealed an increased number of caveolae in LLC-PK1 exposed to all four cytokines as compared to the control. The number of caveolae in HUVEC treated with same cytokines did not increase. This observation indicates that in the case of the epithelial cells, increase in permeability due to cytokines can be mediated through the transcellular pathway, however, in case of HUVECs, the increase in permeability may not involve the transcellular route.

Significant increases in intercellular gap area were observed in the HUVEC monolayers treated with the cytokines as compared to control, indicating that the increase in permeability is mostly modulated through the paracellular pathway. Correlation between the sensor response and the percent gap area further confirms that the response from the sensor can be attributed to the formation of the gaps between cells in the presence of these cytokines. Other studies have also reported the formation of gaps in between the HUVECs leading to increased permeability, when treated with cytokines (Kevil et al. 1998; Nwaraiku et al. 2002; Stockton et al. 2004). Immunofluorescent staining of junctional proteins of HUVECs treated with VEGF or TNF-α revealed significant loss of VE – cadherin and occludin at the cell – cell junctions (Kevil et al. 1998; Nwaraiku et al. 2002). Disorganization of the junctional proteins led to the formation of gaps between the cells. Another study suggested that the tyrosine phosphorylation of adherens junctional components resulted in weakening of cell-cell adhesions (Esser et al. 1998a). In the case of the LLC-PK1 monolayer, gap formation was also observed indicating the possibility of increased paracellular permeability. Previous studies had shown that increased permeability induced in LLC-PK1 by different stimulants like TNF-α and TPA occurs through paracellular pathway (Mullin and O'Brien 1986; Mullin and Snock 1990). However, correlation between sensor response and gap

area was not great, indicating the gaps formed between LLC-PK1 cells are not solely responsible for increased sensor response.

Binding of cytokines to their respective receptors on the cell surface results in stimulation of several intercellular kinases like PI3-K and PKC. Activation of PI3-K and PKC triggers a series of reactions leading to the stimulation of downstream targets which eventually leads to the relaxation of tight junctions (Breslin et al. 2003; Hu et al. 2005; Lal et al. 2001; Mullin and Snock 1990; Potempa and Ridley 1998; Wu et al. 1999). Disintegrated cellular junctions results in an increase in paracellular permeability (Breslin et al. 2003; Hu et al. 2005; Lal et al. 2001; Mullin and Snock 1990; Wu et al. 1999). Exposure of the HUVEC based sensor to the combination of all four cytokines in the presence of each inhibitor resulted in significant reduction in sensor response. This observation matches closely with other studies which have demonstrated that blocking PI3-K and PKC by their respective inhibitors had abolished the enhancement of permeability induced by the stimulators (Breslin et al. 2003; Lal et al. 2001; Wu et al. 1999). When the sensor was exposed to the cytokines in the presence of both the inhibitors, the response obtained was comparable to that obtained in the control. This shows that the permeability induced across HUVECs by the cytokines are mediated by both the PI3-K and PKC pathways and further supports our hypothesis that the response from the sensor can be attributed to the increase in paracellular permeability across HUVECs. Other studies have reported simultaneous activation of these pathways with VEGF and HGF induced permeability across endothelial cells [Lal 2001, Clermont 2006]. In the case of the LLC-PK1 based sensor, blocking the PKC pathway resulted in a significantly attenuated sensor response. Upon blocking the PI3-K pathway, the sensor response was not reduced as much as seen when blocking the PKC pathway. Blocking both pathways by treating with both inhibitors simultaneously did not significantly alter the response from that obtained when only PKC pathway was blocked. This observation demonstrates that in the case of LLC-PK1 cells, the increase in permeability induced by these cytokines is mostly mediated through PKC pathway. Other studies have also revealed that TNF-α and TPA induced permeability across LLC-PK1 monolayer is regulated by the PKC pathway (Clarke et al. 2000; Mullin and Snock 1990). The observation that the response obtained from the sensor in the presence of both the

inhibitors was significantly different from the control, further indicates that in case of LLC-PK1, permeability is not only mediated through the transcellular pathway but also the paracellular pathway. Moreover, treating the cells with the inhibitors of PKC and PI-3K reduced the formation of gaps between cells indicating that the attenuated sensor response in the presence of the inhibitors was due to the reduction in gap area. With the HUVECs, both the gap area and the sensor response decreased to values comparable to the control when exposed to the cytokines and both inhibitors. This suggests that only the paracellular pathway is involved in increased permeability. However, with the LLC-PK1 cells, even though the gap area reduced to that of control upon treating cells with both the inhibitors and all four cytokines, the sensor response was significantly different from the control. This further supports our hypothesis that cytokine induced increases in permeability are mediated through both the paracellular and the transcellular pathway.

Increase in intercellular gap area induced by the cytokines correlated well with the increase in cell surface area indicating that the cell barrier integrity is inversely related to the cell – matrix adhesion. Studies have also reported similar observations with lung microvascular endothelial cells treated with H_2O_2 (Alexander et al. 2001). Integrity of the cell monolayer is maintained by balancing the tensile cellular adhesion force with the contractile force generated by actin-myosin (Clayburgh et al. 2004; Irvine and Marshall 2000). When the cell-cell adhesion is loosened, the equilibrium between the forces is disturbed. Cytokines have been reported to induce actin stress fiber formation in cells (Dowrick et al. 1991; Mehta and Malik 2006; Morales-Ruiz et al. 2000; Petrache et al. 2003) as well as disruption of intercellular junctions (Esser et al. 1998a; Martin et al. 2002; Mehta and Malik 2006; Nwaraiku et al. 2002). The cells maintain their morphology by counteracting the decrease in cell – cell adhesion force as well as the increase in actin generated contractile force by an increase in cell – matrix adhesion. This prevents cells from detaching from the substrate.

In summary, our studies revealed that VEGF, HGF, TNF-α and bFGF can induce permeability across the LLC-PK1 monolayer, both individually and in combination. The modulated permeability can take place through a combination of trans and paracellular routes. Moreover, paracellular permeability is primarily regulated by the PKC pathway. However, the change in permeability HUVECs by the cytokines is due to the formation

of the gaps and is regulated separately by PI3-K and PKC signaling pathways. Subjecting the cells to the cytokines, resulted in an increase in cell – matrix adhesion.

Chapter 7 : Biosensor Incorporating Cell Barrier Architectures on Ion Selective Electrodes for Early Screening of Cancer

7.1 Introduction

Millions of people die every year due to cancer all over the world, making it the second leading cause of death after heart disease. Such huge numbers of deaths can be attributed to the fact that in the absence of quick screening tools for cancer, in major cases, cancer is not diagnosed until the later stages of the disease. This, as a result, reduces the chances of successful therapy. According to American Cancer Society, early screening of cancer can reduce cancer related deaths by 50% by diagnosing an individual at the early stages of cancer and also by detecting individuals showing inclination to develop cancer. As a matter fact, mammography screening has been implicated for significant decrease in deaths of women suffering from breast cancer (Tabar et al. 2003). Moreover, recent years have witnessed profound decreases in mortality associated with uterine cancer due to increased screening using the Papanicolaou (Pap) test (Greenlee et al. 2000). Besides specificity and sensitivity, another factor that plays a critical role in screening cancer is the willingness of people to participate in a screening program. Increasing participation is generally observed in tests which are easy to perform and safe as compared to the complicated tests or tests which are uncomfortable and painful (Zitt et al. 2007). According to American Cancer Society, while 79% of American women 18 yr or older undergo PAP tests and 70% of women older than 40 yr undergo mammogram examination, only 40% of American women and men aged 50 yr or more take part in endoscopic screening, and only 20% participate in the fecal occult blood test (FOBT). Hence, recent research has been directed towards developing non-invasive techniques for early detection of cancer.

Simplicity associated with the collection of blood samples has facilitated the development of diagnostic assays by using serum or plasma biomarkers. One such method is the detection of circulating tumor cells (CTC) in the peripheral blood of cancer patients. Studies demonstrated that detecting CTCs can be correlated with disease progression and therapeutic response (Denis et al. 1997; Muller et al. 2005; Nakagawa et

al. 2007; Sher et al. 2005). One major problem associated with this method is the discrepancies associated with the detection rates, which in turn may be due to the differences in the methods used for enrichment and detection of CTCs. Another non-invasive method of cancer detection involves detection of DNA in the blood samples (Herrera et al. 2005; Silva et al. 2002). Studies have demonstrated the detection of genetic alterations such as mutations in the oncogenes and tumor suppressor genes, alterations in loss of heterozygosity (LOH) and microsatellite instability (MI), present in tumors, in the circulating DNA (Anker and Stroun 2001; Mulcahy et al. 1998; Shaw et al. 2000; Silva et al. 1999). Another simpler approach involves the detection of total DNA concentration in plasma. Studies reported the increase in total DNA concentration in the plasma of cancer patients as compared to healthy individuals (Leon et al. 1977). However, posttranslational modifications which may be important in oncogenesis, can not be detected by this method of cancer detection (Kopf and Zharhary 2007). Since cancer is associated with altered expression of proteins and signaling pathways and eventually to altered levels of protein secretion in blood, detecting proteins in blood is a popular screening tool for cancer (Haab 2005; Kopf and Zharhary 2007; Nedelkov et al. 2006; Srinivas et al. 2002; Zangar et al. 2006). Some of the common and successful biomarkers include prostate specific antigen (PSA), cancer antigen 125 (CA-125) and carcinoembryonic antigen (CEA) mostly for prostate, breast and colorectal cancer. Detection and validation of these protein biomarkers depend mostly on traditional immunoassay methods such as ELISA or protein microarrays. These methods can be used to assay multiple proteins simultaneously and require less sample volumes. However, protein arrays are intrigued with several problems such as i) protein immobilization, ii) protein instability and denaturation, iii) need for highly specific antibodies and iv) problems associated with non specific binding (Sanchez-Carbayo 2006).

One biological characteristic common to most cancers irrespective of origin is angiogenesis. To sustain beyond 2-3 mm size and to progress from benign to malignant state, tumors must recruit blood vessels from existing vasculature (Folkman 1995; Gimbrone et al. 1972). This in turn facilitates the metastasis or the spreading of cancer (Holmgren et al. 1995). Research has suggested that angiogenesis occurs during the

premalignant phase of tumor growth and inhibition leads to dormancy and ultimately death of cancer cells (Folkman 1985; Hanahan and Folkman 1996). Angiogenesis is regulated by the balance between pro and anti angiogenic molecules. Tumor angiogenesis is believed to stem from increased secretion of different angiogenic molecules such as vascular endothelial growth factor (VEGF), basic fibroblast growth factor (bFGF), hepatocyte growth factor (HGF) and tumor necrosis factor- alpha (TNF- α) by tumor cells (Dunlop and Campbell 2000; Oppenheim and Fujiwara 1996). Increased secretion results in elevated levels of these molecules in the serum of cancer patients as compared to healthy individuals (Cronauer et al. 1997; Dirix et al. 1997; Granato et al. 2004; Heer et al. 2001; Marci et al. 2006; Premkumar et al. 2007; Sezer et al. 2001; Sheen-Chen et al. 1997; Sliutz et al. 1995; Szlosarek et al. 2006; Ueno et al. 2001; Yoshida et al. 2002).

Since angiogenesis is not only common to most cancers but also occurs during the premalignant stage of cancer, we hypothesized that any physiological instrument having the ability to measure angiogenesis can act as a screening tool for cancer. A human umbilical vein endothelial cell (HUVEC) based biosensor has been developed in our laboratory, which takes the advantage of endothelial permeability dysfunction to detect small quantities of permeability modifying agents (Ghosh et al. 2007a; May et al. 2005; May et al. 2004a). The biosensor consists of a confluent monolayer of HUVEC seeded across the asymmetric cellulose triacetate (CTA) membrane of an ion selective electrode (ISE). In the presence of the confluent monolayer the passage of the marker ion, potassium, to the membrane surface is prevented, resulting in inhibited response from the sensor. When the permeability of the cell monolayer is altered by different permeability modifying agents, potassium ion reaches the membranes surface and hence the response from the sensor increased. The responses thus obtained can be related to the concentration of these agents (Ghosh et al. 2007a; May et al. 2005; May et al. 2004a). Earlier studies with this biosensor have shown that it has the potential to act as an alternate assay for measuring angiogenesis (Ghosh et al. 2007b). The study demonstrated that the biosensor responded to the presence of the above mentioned angiogenic molecules, both individually and in combination, at concentrations observed in the serum of cancer patients (Ghosh et al. 2007b).

The present study is focused on measuring the responses of the sensor when exposed to the serum from healthy individuals and patients of different types and at different stages of cancer to explore the possibility of this biosensor to act as a quick screening tool for cancer.

7.2 Experimental Section

7.2.1 Reagents

Purified carrier free $VEGF_{165}$, bFGF, HGF and TNF-α were purchased from R&D Systems (Minneapolis, MN). The cytokines were dissolved in 0.1% bovine serum albumin (BSA) in Dulbecco's phosphate- buffered saline (PBS) (GIBCO^{TM}). Serum samples from healthy individuals and stage III pancreatic cancer patients were obtained from Bioreclamation (Hicksville, NY). All the remaining cancer serum samples i.e. serum samples from stage 0, I, III and IV of breast cancer patients and stage I of ovarian and lung cancer patients were obtained from Asterand (Detroit, MI). Informations regarding the age of the subjects, presence of steroid receptors (estrogen and progesterone), clinical diagnostics etc were obtained. HUVECs used during the experiments, were cultured as described in Chapter 3. Membrane materials and sensor preparation had also been described in Chapter 3.

7.2.2 Evaluation of Electrode Response

Following confluent cell monolayer formation, the control membranes were tested for inhibited ion response. After the confirmation of the inhibited ion response due to the formation of the confluent monolayer, the cell-seeded membranes were exposed to different cytokine solutions containing individual and combinations of cytokines (pH 7.2) in PBS for 1 and 3 hr and the response of the sensor was measured. The responses of the sensor to cytokines at concentrations found in serum of healthy individuals (i.e., 100 pg/ml VEGF, 500 pg/ml HGF, 5 pg/ml bFGF and 10 pg/ml TNF-α) were compared to the responses when exposed to the cytokines at concentrations found in the serum of cancer patients (i.e., 1000 pg/ml VEGF, 2000 pg/ml HGF, 40 pg/ml bFGF and 100 pg/ml

TNF- α) (Dirix et al. 1997; Sezer et al. 2001). The cytokines were dissolved in 0.1% BSA in PBS for these experiments. After confirming that the biosensor is able to differentiate between the different concentrations of cytokines i.e. the concentrations of cytokines corresponding to that observed in the serum of healthy individuals and in cancer patients, the responses were measured by exposing the cell based biosensor to actual serum samples from healthy individuals and cancer patients at different stages.

At a final concentration of 0.1 M KCl, the electrode response was measured for the following conditions: (a) the membrane without cells and without cytokines/serum to obtain the baseline response of the sensor (b) membranes with cells and without cytokines/serum to confirm the inhibited response of the sensor due to the confluent monolayer of cells, (c) membranes with cells and with cytokines, (e) membrane without cells and with serum to test the effect of serum on the membrane of the sensor and (f) membrane with cells and with serum samples.

To account for slight variations between fabricated membranes, the final data are reported as the ratio of the response obtained at 0.1 M KCl for the ISEs with HUVECs and cytokines/serum to the response obtained for the same membrane without HUVECs and cytokines/serum.

7.2.3 Statistical Analysis

For all experiments data are reported as mean ± SEM. Statistical analyses were carried out using one-way ANOVA and the Student-Newman-Keuls test for post-hoc comparisons of the means with $P<0.05$. SigmaStat v 3.1 software was used for these analyses.

7.3 Results

7.3.1 Biosensor Response to the Different Cytokines in PBS

Earlier studies demonstrated that exposing the cell based sensor to individual and combined cytokines at concentrations observed in the serum of cancer patients for 1 and 3 h resulted in significantly increased response from the sensor (Ghosh et al. 2007b). In the present study, initially the biosensor was exposed to the cytokines individually and in

same combination but at concentrations observed in the serum of healthy individuals for 1 and 3 h and compared to responses obtained when exposing the sensor to cytokines at concentrations found in cancer patients. As shown in Figure 7.1A, the biosensor responded to the presence of the individual cytokines at concentrations found in healthy individuals. The response from the sensor to the individual cytokines after 1 h exposure time was not significantly different from the value obtained to cells only except for VEGF. Upon exposing the biosensor to VEGF, HGF and TNF-α individually for 3 h, a response ratio of around 0.1 was obtained, which was significantly different from that of cells only. Upon exposing the cell based biosensor to the combination of cytokines VEGF and TNF-α (V+T), VEGF, TNF-α and HGF (V+T+H) and VEGF, TNF-α and bFGF (V+T+b) for 1 and 3 h, even though additive response was not obtained, the responses obtained in the presence of combined cytokines were higher than those obtained by exposing the sensor to individual cytokines. Upon exposing the cell based sensor to the combination of all four cytokines (V+T+ b +H) for 1 and 3 h profound increases in the sensor response to 0.12 and 0.17, respectively were obtained.

Figure 7.1B shows the responses obtained by exposing the sensor to these cytokines at concentrations observed in the serum of cancer patients. The response from the sensor to the individual cytokines was higher than the response obtained at concentrations corresponding to healthy individuals. For example, exposure of the cell-based biosensor to 1000 pg/ml VEGF for 3 h resulted in a response ratio of 0.19. When the sensor was exposed to 100 pg/ml VEGF for 3 h, a response ratio of 0.11 was obtained. Exposing the sensor to the combination of cytokines resulted in profound increase in sensor response as compared to the responses obtained from individual cytokines.

Since all the cytokines are elevated during cancer, it was important to compare the responses from the sensor to the presence of all four cytokines cytokines, at concentrations corresponding to healthy individuals and cancer patients. This comparison is illustrated in Figure 7.2. As can be seen, the sensor was able to differentiate between the two concentrations at both 1 and 3 h exposure times. Since, even for 1 h exposure time, significant differences were observed between the responses at the two different concentrations, it was decided for the serum studies, the responses would be measured using an exposure time of 1 h.

A:

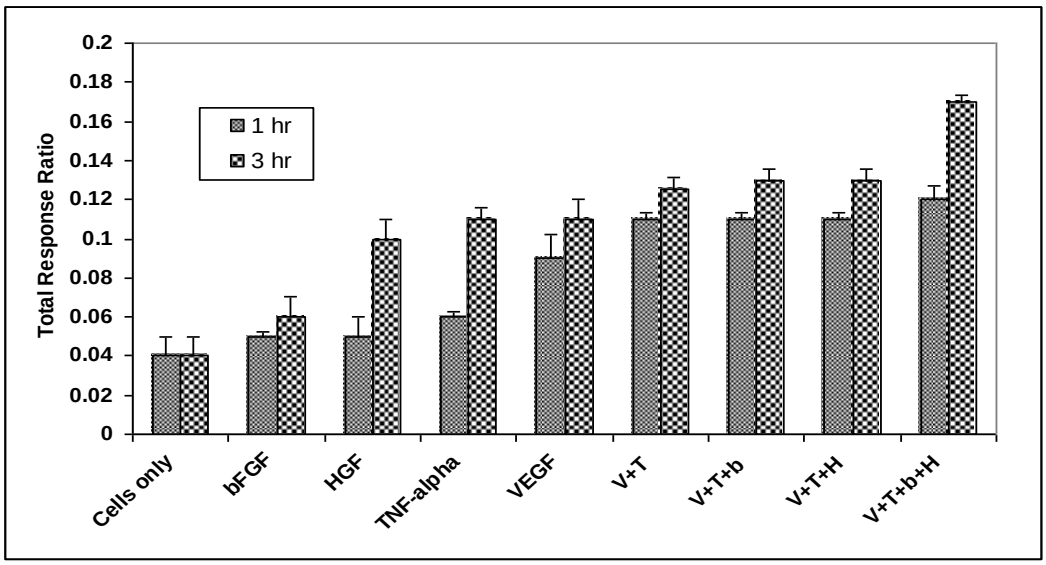

B:

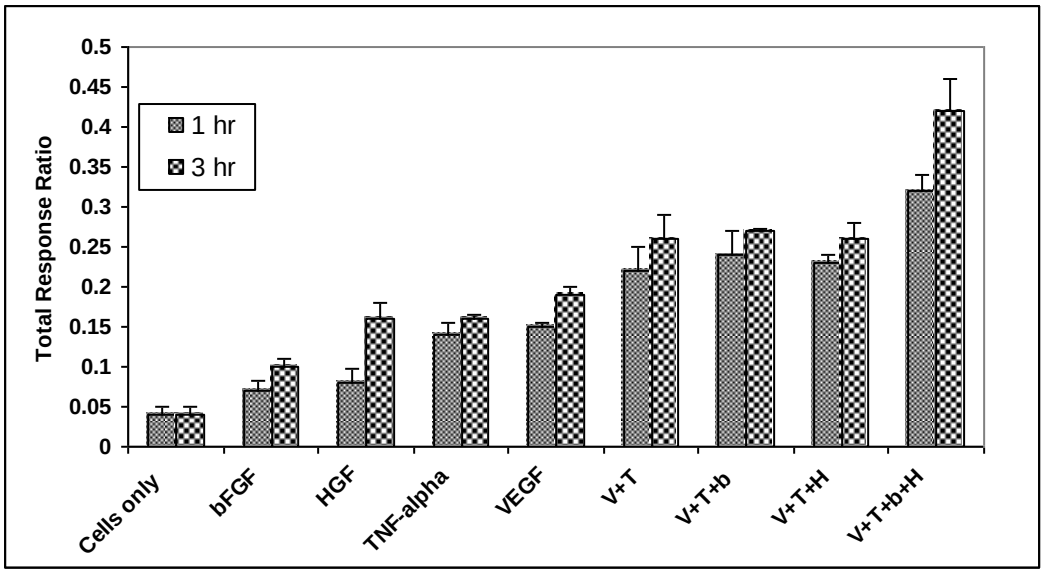

Figure 7.1 Comparison of the ISE sensor responses obtained following exposure of the sensor to individual and combination of cytokines at concentrations observed in the serum of healthy individuals (A) and cancer patients (B) for 1 and 3 h. Total response ratio is defined as the ratio of the responses of cell-based sensor with or without cytokines to ISE response obtained at 0.1 M KCl for the membrane without cells and without cytokines. (Error bars represent SE N=3)

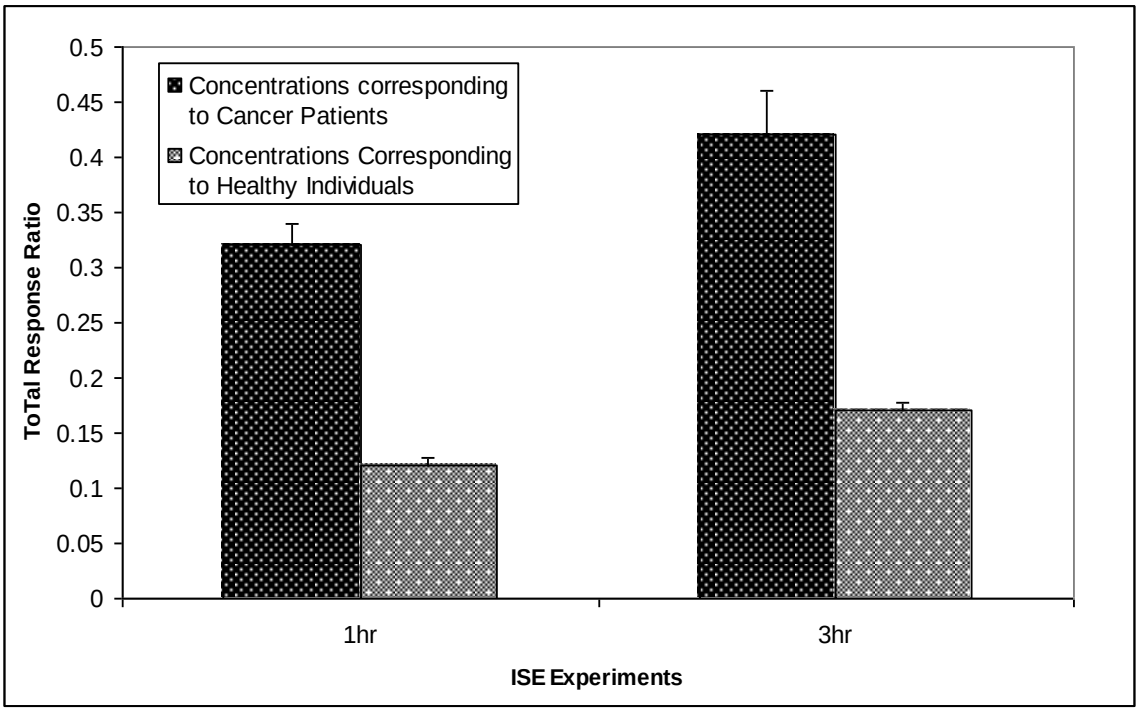

Figure 7.2 Comparison of the ISE sensor responses obtained following exposure to the combination of all four cytokines at concentrations observed in the serum of healthy individuals and cancer patients for 1 and 3 h. Total response ratio is defined as the ratio of the responses of cell-based sensor with cytokines to ISE response obtained at 0.1 M KCl for the membrane without cells and without cytokines. (Error bars represent SE N=3)

7.3.2 Biosensor Response to the Serum of Healthy Individuals

Prior to exposing the cell-based biosensor to serum samples, it was important to investigate the effect of serum on the membrane of the biosensor. To do this, the sensor without any cells was exposed to the serum of healthy individuals for 1 h. Figure 7.3 compares the response profiles of the sensor without cells and with and without serum. As seen, the response profiles with and without serum matched very close to each other. When the overall response obtained at 0.1 M KCl for the membrane exposed to the serum for 1 h was compared with that obtained for control, it was observed that more than 95% of the sensor response had been recovered, indicating that the serum does not effect the membrane surface.

Since the average response ratio of 0.12 was obtained by exposing the biosensor to the combination of the maximum concentration of the four cytokines observed in the serum of healthy individuals, it acted as our maximum cut off limit for healthy individuals. Next, the cell-based biosensor was exposed to 15 serum samples from healthy individuals for 1 h. Figure 7.4 demonstrates the responses obtained from the biosensor. As shown, the responses obtained for all the samples were less than 0.12. The responses ranged from 0.06 to 0.11 with the mean of 0.09. No significant differences were observed when comparing gender and age ($p > 0.05$).

7.3.3 Biosensor Response to the Serum of Cancer Patients

The biosensor was then exposed to the serum samples of pancreatic, breast, ovarian and liver cancer patients. Figure 7.5 shows the responses of the sensor to different cancer samples. As observed, in all the cases except one, the responses were above the maximum cut off limit for healthy individuals. The sample for which a lower response was obtained corresponds to a stage 0 of breast cancer patient.

Figure 7.6 illustrates the responses obtained from the biosensor when exposed to the serum samples from stage III of both breast and pancreatic cancer patients and healthy individuals. When comparing these results, it was observed that the responses for cancer patients were significantly higher than those obtained for healthy individuals. However, no significant difference was obtained between the responses for the cancer

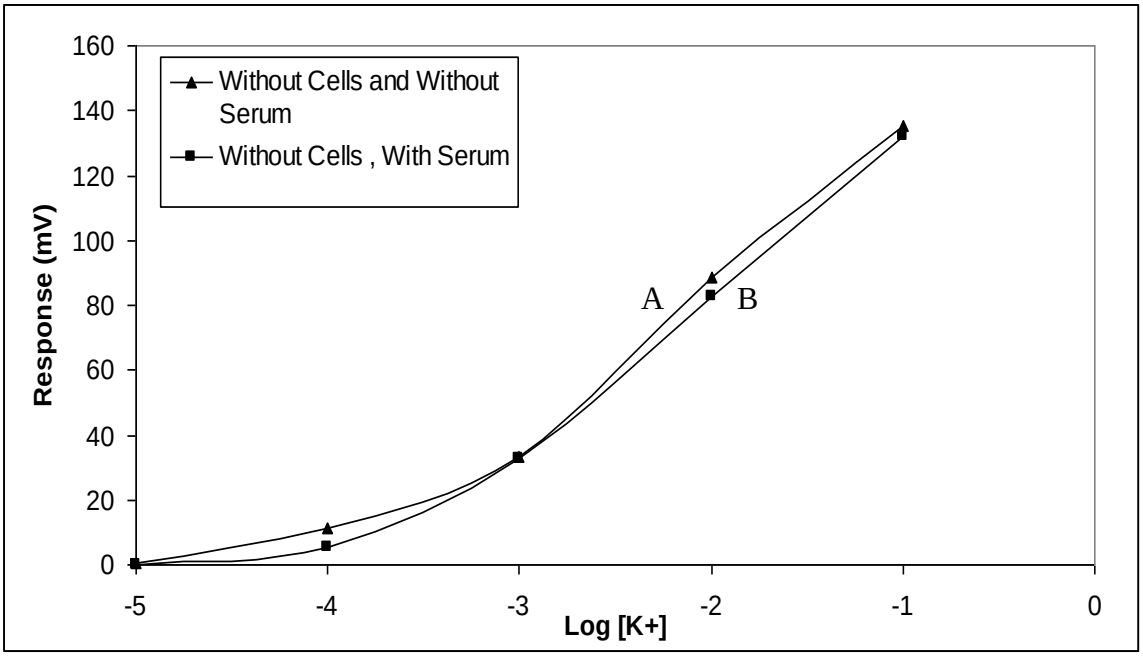

Figure 7.3 Response vs. log K^+ plot for the ISE membranes (A) without cells and without serum and (B) without cells and exposed to serum from healthy individuals for 1 hr. This plot represents one experiment. The experiment was repeated two more times giving similar results

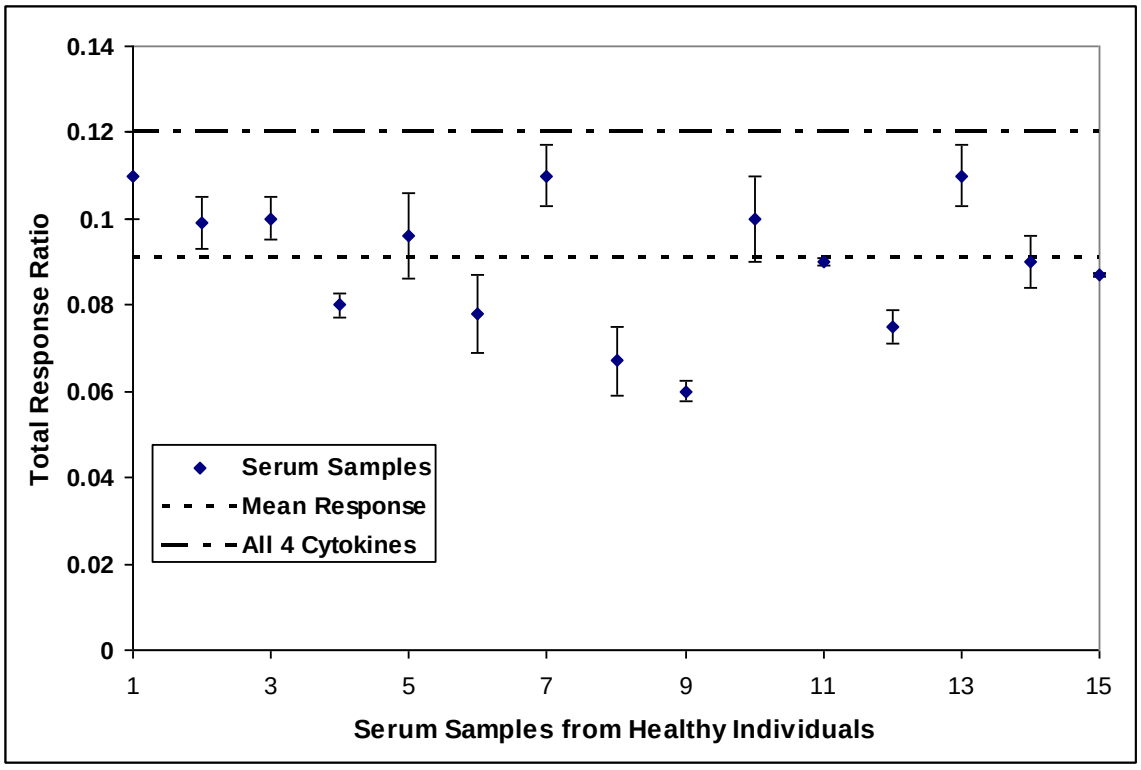

Figure 7.4 Response ratios obtained when exposing the sensor to the serum of healthy individuals for 1 h. Serum samples from 15 healthy individuals were used in these experiments and each point represents one individual. Each serum sample was measured three times. Total response ratio is defined as the ratio of the responses of cell-based sensor with serum to ISE response obtained at 0.1 M KCl for the membrane without cells and without serum. (Error bars represent SE)

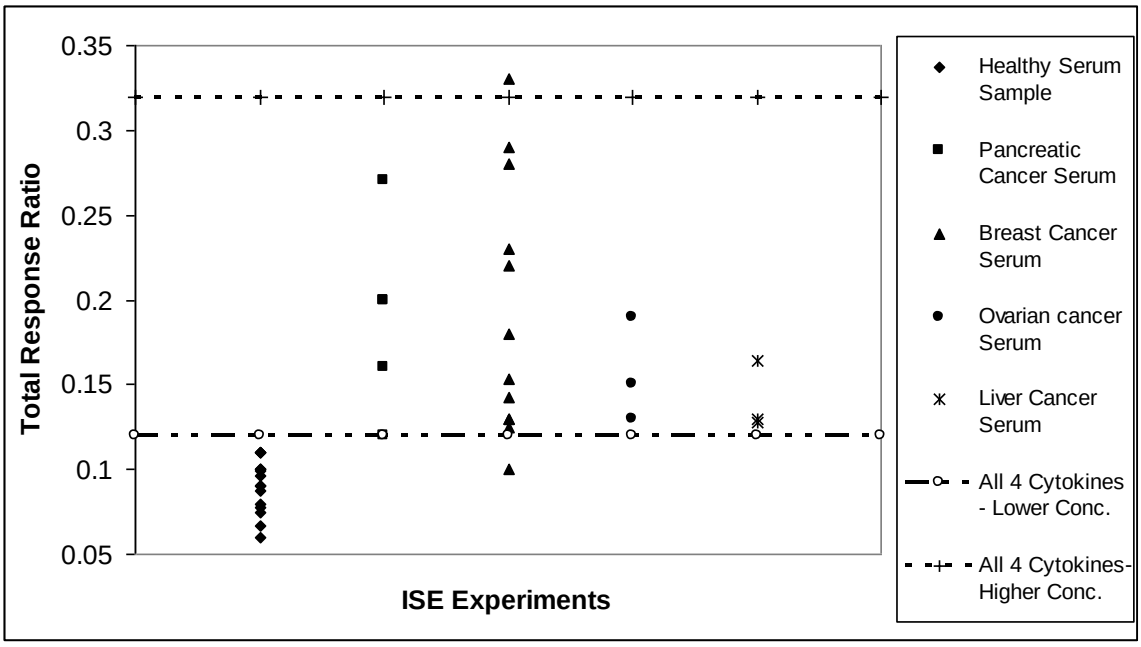

Figure 7.5 Response ratios obtained when exposing the sensor to the serum of cancer patients for 1 h and compared to the responses obtained from healthy individuals. Total response ratio is defined as the ratio of the responses of cell-based sensor with serum to ISE response obtained at 0.1 M KCl for the membrane without cells and without serum. A total of 23 cancer patients were used in this study and each point represents one patient. Each serum sample from cancer patients was measured once

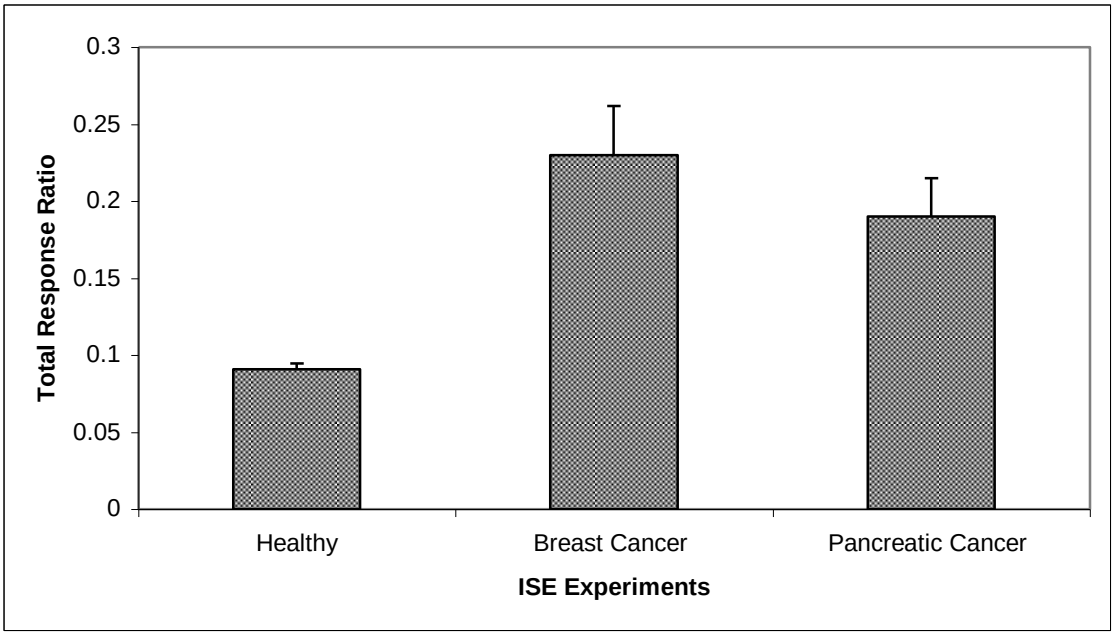

Figure 7.6 Response ratio obtained when exposing the sensor to the serum of stage III pancreatic and breast cancer patients for 1 h and compared to the responses obtained from healthy individuals. Total response ratio is defined as the ratio of the responses of cell-based sensor with serum to ISE response obtained at 0.1 M KCl for the membrane without cells and without serum. The values represent the mean of 15 healthy individuals, 3 breast cancer and 5 pancreatic cancer patients

from the different organs. This indicates that the biosensor is able to differentiate between healthy individuals and cancer patients at stage III, but does not distinguish between the two cancer types.

To explore the ability of the biosensor to act as an early screening tool for cancer, it was next exposed to the serum samples from stage 0 and I of breast cancer patients and compared with the later stages of breast cancer. As shown in Figure 7.7, the responses obtained from the biosensor were significantly higher when exposed to serum from stage I breast cancer patients than those of the healthy individuals. When the biosensor was exposed to serum of stage 0 breast cancer patients, the average response obtained was very close to the maximum cut off limit for healthy individuals (0.13 vs. 0.12). However, when comparing these responses to the average responses from the healthy individuals, a significant difference between the two were obtained. The responses obtained at stage 0 and stage I were not significantly different from each other. To further confirm the ability of the biosensor to act as the early screening tool of cancer, the biosensor was exposed to the stage I serum samples from ovarian and liver cancer patients and compared to those obtained from stage I breast cancer patients and healthy individuals. As shown in Figure 7.8, significant differences were observed between the responses to cancer patients irrespective of cancer origin and healthy individuals indicating the potential of the biosensor to act as early screening tool for cancer. However, no significant differences were observed ($p > 0.05$) in the responses for the cancers from the three different organs.

To further compare the sensor response to samples from healthy individuals to those obtained from cancer patients, responses from the stage 0 and I of different cancer types were coupled together as early stage while responses from stages III and IV were couples together as the later stage of cancer. These results shown in Figure 7.9 demonstrate that significant differences were obtained when comparing the responses from healthy individuals to the responses from the early and later stages of cancer. In addition, significant differences were obtained when comparing the early and later stages of cancer. This shows that the biosensor is not only able to act as an early screening tool for cancer but can also differentiate between early and later stage of the disease.

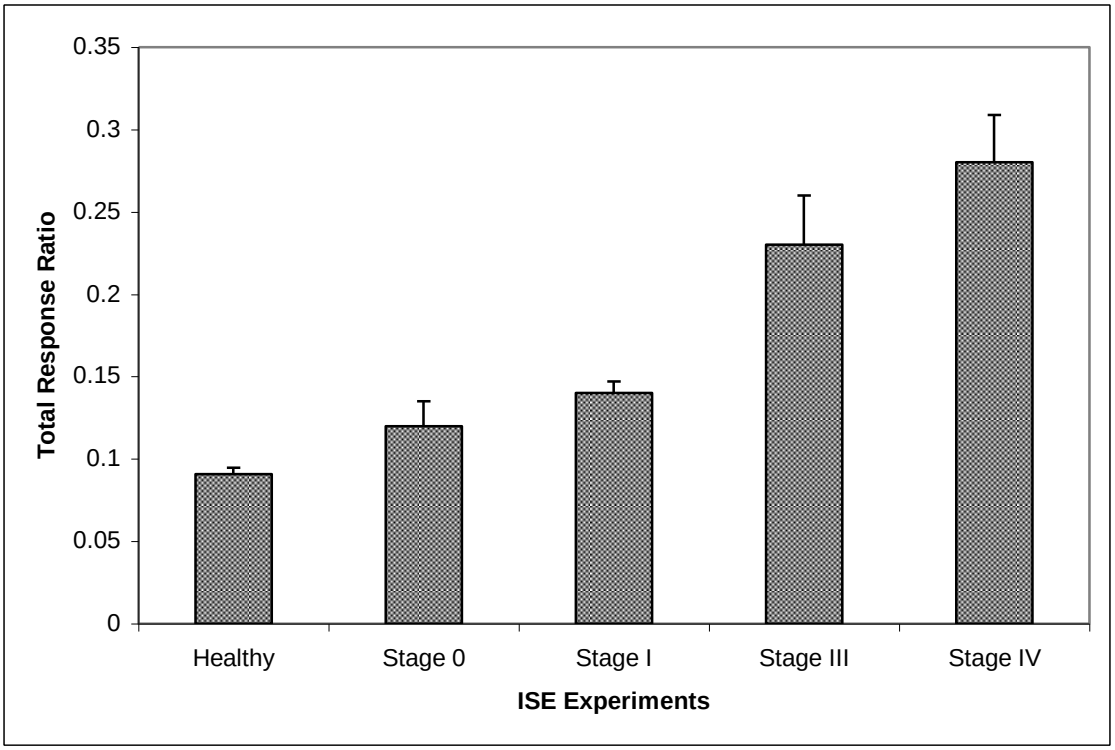

Figure 7.7 Response ratios obtained when exposing the sensor to the serum of different stages of breast cancer patients for 1 h and compared to the responses obtained from healthy individuals. Total response ratio is defined as the ratio of the responses of cell-based sensor with serum to ISE response obtained at 0.1 M KCl for the membrane without cells and without serum. The values represent the mean of 15 healthy individuals and 3 each of different stages

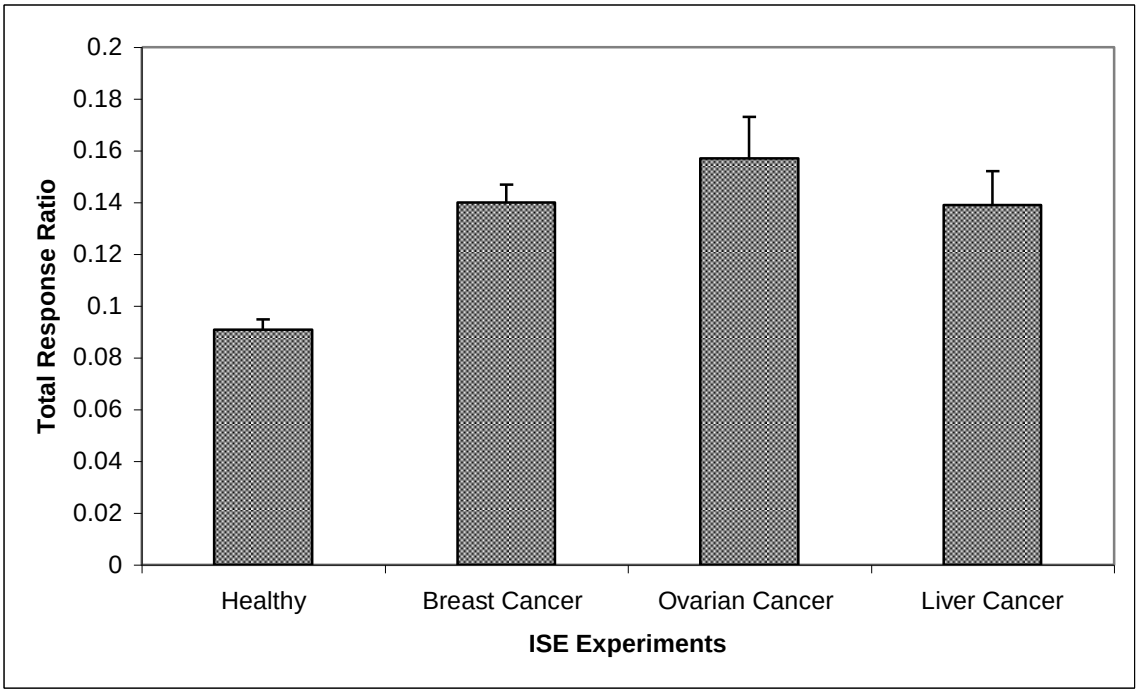

Figure 7.8 Response ratios obtained when exposing the sensor to the serum of stage I breast, ovarian and liver cancer patients for 1 h and compared to the responses obtained from healthy individuals. Total response ratio is defined as the ratio of the responses of cell-based sensor with serum to ISE response obtained at 0.1 M KCl for the membrane without cells and without serum. The values represent the mean of 15 healthy individuals and 3 each of different cancer types

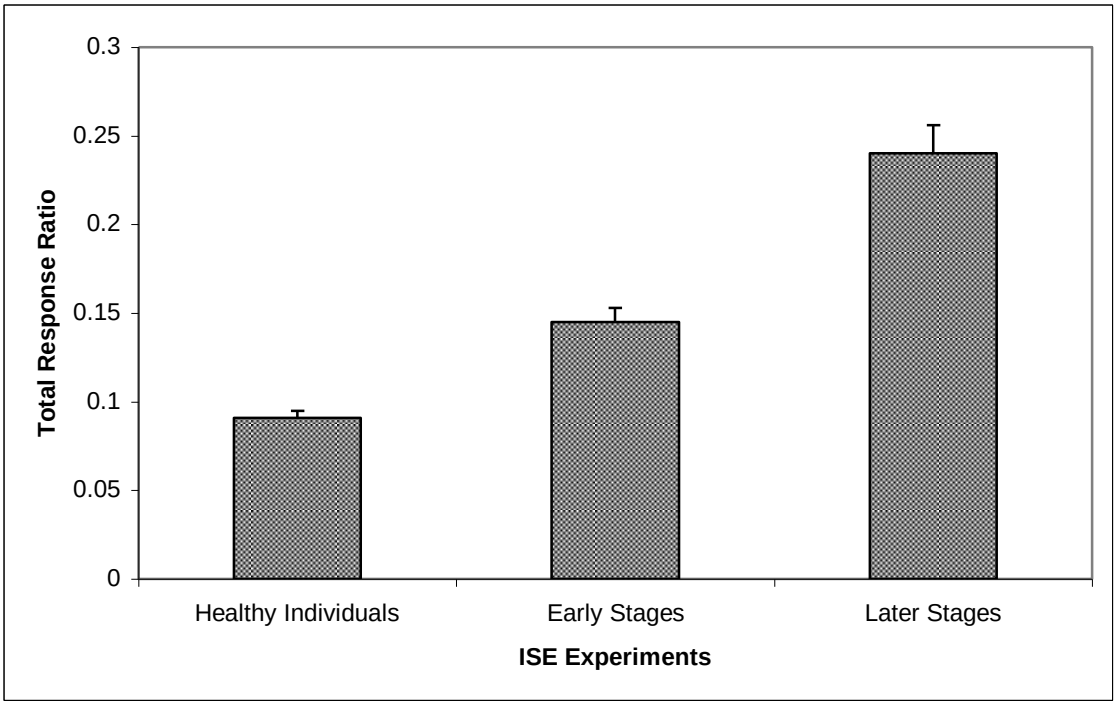

Figure 7.9 Response ratios obtained when exposing the sensor to the serum of early and later stages of cancer patients for 1 h and compared to the responses obtained from healthy individuals. Total response ratio is defined as the ratio of the responses of cell-based sensor with serum to ISE response obtained at 0.1 M KCl for the membrane without cells and without serum. Stage 0 and I cancer patients were coupled together as early stage and stage III and IV corresponds to the later stages of cancer. The values represent the mean of 15 healthy individuals and 12 early stages and 11 later stages of cancer

7.4 Discussion

It is well known that screening can significantly reduce cancer morbidity. Firstly, by diagnosing an individual at the early stages of cancer, screening increases the chances of successful therapy. Secondly, by diagnosing abnormal cells or lesions, screening can help identify an individual showing an inclination to develop cancer and thus reduce the morbidity of cancer treatment. Research has shown that people are more willing to participate in easy to perform screening tests like blood tests as opposed to complicated or painful screening examinations like endoscopy or mammeograms. Moreover, the fact that beyond 50 yr of age an individual has to undergo a number of tests to ascertain the healthy status also reduces one's willingness to participate in screening programs. For example, a woman 50 yr or more in age has to undergo mammeogram, endoscopic examinations as well as Pap tests to be certain that she is not suffering from breast, colon or uterine cancer. Similarly, a man 50 yr or more in age should undergo endoscopic examination for screening colon cancer and also digital rectal examination and PSA testing for prostate cancer. Hence, there exists a need for not only a non -invasive diagnostic tool for cancer but a tool which can identify patients suffering from cancer irrespective of origin. This has encouraged research in detection and validation of biomarkers for cancer. Biomarkers are biological molecules which are present at different concentrations in healthy individuals and in cancer patients (Srinivas et al. 2001). Some common biomarkers are circulating tumor cells (CTCs), circulating DNA and proteins. Differences in enrichment and detection method of CTCs translate into major discrepancies in detection rates of CTCs which in turn act as a major drawback for this cancer detection method. However, proteomics score over genomics for biomarker detection and screening cancer due to the ability to take into account the posttranslational modifications, differential splicing of mRNAs and functional regulation of gene expression (Eyk 2001). Since there are hundreds of proteins with significantly different concentrations in healthy individuals and in cancer patients, a device will have a better potential to act as a screening tool if it can detect a combination of proteins rather than an individual protein. However, the major challenge lies in selecting proteins, individually or in combinations, which will be successful in acting as biomarkers.

Angiogenesis is a biological characteristic that is common to most cancers irrespective of their origin. For a cancer to progress from its benign state to a malignant state, recruitment of blood vessels from the existing vasculature is required (Folkman 1995; Gimbrone et al. 1972). This leads to increased secretion of cytokines into the blood such as VEGF, HGF, TNF-α and bFGF into the serum of cancer patients as compared to healthy individuals (Cronauer et al. 1997; Dirix et al. 1997; Granato et al. 2004; Heer et al. 2001; Marci et al. 2006; Premkumar et al. 2007; Sezer et al. 2001; Sheen-Chen et al. 1997; Sliutz et al. 1995; Szlosarek et al. 2006; Ueno et al. 2001; Yoshida et al. 2002). The concentrations of these cytokines can be measured by ELISA. Multiplexed technology enables one to measure several of these cytokines simultaneously but individually. However, concentration of these cytokines in the serum of cancer patients can vary not only on the basis of cancer origin and stages but also from person to person suffering from cancer in same organ and also at the same stages. Moreover, at the early stages of cancer, the concentrations of all the cytokines are not elevated simultaneously. Hence, any physiological tool which can detect combination of cytokines will be a better screening tool as compared to a device which measures several of the individual cytokines simultaneously.

A whole cell based biosensor has been developed in our laboratory which takes the advantage of endothelial cell barrier dysfunction to detect small quantities of permeability modifying agents (Ghosh et al. 2007a; May et al. 2005; May et al. 2004b). Earlier studies with this biosensor showed that by measuring increases in cell permeability induced by the cytokines such as VEGF, HGF, bFGF and TNF-α, it can act as an alternate assay for measuring angiogenesis. The concentrations of the cytokines used were those generally observed in the serum of cancer patients (Dirix et al. 1997; Sezer et al. 2001). In this study we showed that upon exposing the sensor to the same cytokines individually and in combinations but at concentrations observed in the serum of healthy individuals, lower responses were obtained from the sensor, indicating a dose dependant response of the sensor to the presence of these cytokines. Comparing the biosensor response to the combination of all four cytokines at concentrations observed in the serum of healthy individuals and cancer patients, it was observed that the biosensor was able to differentiate between the two concentrations. Further it was shown that a

response from the sensor can be obtained in only 1 h as compared to ELISA which requires 4-6 h.

When the biosensor was exposed to the serum samples from 15 different healthy individuals, the responses varied from 0.06 to 0.11 with a mean of about 0.09. The biosensor was then exposed to the serum samples from the patients suffering from pancreatic, breast, ovarian and liver cancer. The results demonstrated that the responses of the biosensor to different cancer samples irrespective of the stages were significantly higher than the responses for healthy individuals. Upon comparing the responses for different stages of breast cancer patients to healthy individuals, significant differences between the responses were obtained. Moreover, when the responses of the sensor to different stage I cancer patients were compared with healthy subjects, it was observed that irrespective of the origin, the responses of the sensor to cancer patients were higher than those for healthy individuals. Finally, stage 0 and I cancer were coupled together as the early stage and stage III and IV as the later stages of cancer and the responses of early and later stages of cancer were compared with healthy individuals. The results indicate that the sensor was able to differentiate early stages of cancer patients irrespective of the origin from the healthy individuals. The present study demonstrates that the biosensor can not only distinguish between healthy individuals and cancer patients, but responses from the sensor correlates with the stages of cancer.

In summary, these initial studies indicate the endothelial cell based biosensor can differentiate healthy subjects from patients both at early and later stages of cancer within 1 h. Further studies with additional blood samples are needed to further confirm its potential to act as a screening tool for cancer.

Chapter 8 ：Conclusions

The study was directed towards investigating the ability of a cell -based biosensor to monitor physiological toxins and to screen cancer. This chapter summarizes the conclusions from the different studies.

Exposing the HUVEC -based biosensor to the physiological toxin, staphylococcal alpha toxin, led to the alteration of permeability across the cell monolayers. This resulted in increased response from the sensor. The study demonstrated:

- Increasing the time of exposure of the cell based sensor to 1000 ng/ml alpha toxin for time ranging from 10 to 90 min resulted in increased overall response with time.
- Microscopic studies revealed detachment of cells upon prolonged exposure. Optimal exposure time of the sensor to the toxin was found to be 20 min.
- The biosensor responded to alpha toxin at concentration ranging from 0.1 to 1000 ng/ml.
- Minimum detectable limit of alpha toxin by the biosensor was found to be 0.1 ng/ml. Considering the fact that the toxic concentration of alpha toxin in humans is 100 -250 ng/ml of whole blood, this biosensor has the potential to act as a diagnostic tool at the onset of staphylococcal diseases.
- Silver staining of HUVECs treated with alpha toxin revealed formation of gaps between the cells. Percentage of gap area increased with increasing concentration of the toxin.

The HUVEC based biosensor was used to measure permeability as an alternate assay for angiogenesis. The cell based biosensor was exposed to VEGF, bFGF, HGF and TNF-α individually and in combination at the concentration observed in the serum of cancer patients. The responses thus obtained were compared with the common in vitro assays like cell migration, proliferation and tube formation. The study demonstrated:

- The biosensor responded to the presence of 1000 pg/ml VEGF within 30 min. the response from the sensor increased with increasing the exposure time to 10 h.
- The response of the biosensor to the presence of 100 pg/ml TNF-α increased with increasing the exposure time from 30 min to 3 h. However, further increase in exposure time led to a decrease in sensor response.
- The cell based biosensor sensor was exposed to bFGF and HGF for 1 and 3 h. The biosensor responded to the presence of these cytokines.
- The biosensor was then exposed to different combinations of cytokines (VEGF + TNF-α, VEGF + TNF-α + bFGF, VEGF + TNF-α + HGF, VEGF + TNF-α + HGF + bFGF) for 1 and 3 h. Increased response was obtained as compared to responses to the individual cytokines. Profoundly increased responses were obtained when the biosensor was exposed to the combination of all four cytokines.
- Cell proliferation studies revealed that VEGF, HGF and bFGF enhanced cell proliferation while TNF-α inhibited it. Upon incubating HUVECs with both VEGF and TNF-α, it was observed that TNF-α downregulated the ability of VEGF to stimulate proliferation. Significant increase in mitogenic activity was observed upon incubating HUVECs with all the four cytokines.
- Exposing the wounded HUVEC monolayer to VEGF, HGF, bFGF and TNF-α for 10 h resulted in significantly increased wound healing as compared to control. Incubation of cells with combined cytokines resulted in increased cell migration.
- Tube formation studies revealed that at the concentration studied, individual cytokines produced no significant changes in their ability to induce tube formation. However, incubating HUVECs with different combinations of cytokines resulted in enhanced tube formation.
- To compare the permeability assay with the three common angiogenic *in vitro* assays, the responses obtained for each assay were normalized with respect to the control values. The comparison demonstrated that the relative change in permeability assay in the presence of cytokines as compared to control was far greater than the relative change observed in the other assays, especially when the cells were exposed to combination of cytokines.

Since, the cytokines also modulate permeability across epithelial cells, porcine kidney epithelial cell line, LLC-PK1, was seeded across the asymmetric membrane surface of the ISE. The responses of the epithelial cell based biosensor to the presence of VEGF, bFGF, HGF and TNF-α were measured and compared with that of endothelial cell based biosensor. Moreover, the mechanisms involved behind enhanced permeability were also studied. The study demonstrated:

- The epithelial cell based sensor responded to the presence of 1000 pg/ml VEGF, 2000 pg/ml HGF, 40 pg/ml bFGF and 100 pg/ml TNF-α individually and in combination.
- There was no significant difference in the responses obtained from the HUVEC based biosensor and the LLC-PK1 based biosensor to the presence of individual cytokines.
- However, the responses to the combination of cytokines were significantly higher in HUVEC based sensor as compared to LLC-PK1 based biosensor.
- Transmission electron microscopic studies revealed the presence of caveolae like structures in the both HUVEC and LLC-PK1 cells treated with all the four cytokines for 3 h. However, the increases in density of these transcellular structures in response to the treatment with cytokines as compared to the controls were more profound in LLC-PK1 cells than HUVECs, indicating increased chances of permeability occurring through transcellular pathway in the epithelial cells.
- To determine whether there is increased paracellular permeability, changes in percent gap formation were determined in response to cytokine treatment. In the case of HUVECs, a significant increase in gap area from 6% in control studies to 43% in the case of cells treated with all four cytokines was observed. However, such a huge increase in gap area was not observed in the case of LLC-PK1 treated with different cytokines.
- A strong positive correlation was observed between gap area and sensor response in case of HUVECs indicating the chances of permeability occurring through

paracellular route primarily. In the case of LLC-PK1 cells a strong correlation was not observed.

- To elucidate whether the increased response from the sensor is due to increased paracellular or transcellular permeability, the HUVEC based biosensor was exposed to all four cytokines in the presence of inhibitors of PI3-K and PKC (LY294002 and BIM I respectively) individually and in combinations. These pathways are known to regulate the cellular junctional proteins and hence the paracellular permeability. It was observed that in HUVECs both the pathways individually play significant role in inducing paracellular permeability and blocking both the pathways simultaneously resulted in a sensor response comparable to that obtained for controls, indicating that sensor response is due to increased paracellular permeability.
- The PKC mediated pathway plays a critical role in inducing paracellular permeability in LLC-PK1 cells. When both the pathways were blocked, sensor response was significantly different from the response obtained from control indicating the response from the sensor depends on both induced paracellular and transcellular permeability.
- To determine the effect of the inhibitors BIM I and LY294002 on paracellular gap formation, both HUVECs and LLC-PK1 were exposed to all four cytokines in the presence of either of the inhibitors or both. For both the cell lines, the gap areas decreased significantly in the presence of inhibitors and were comparable to that of control.
- To elucidate the effect of the cytokines on cell-substrate adhesion, cell surface area was measured. It was observed that in both the cell lines the cell- substrate adhesion increased in the presence of combined cytokines, indicating decrease in cell barrier integrity is inversely related to cell-substrate adhesion.

Since angiogenesis play an integral role in cancer progression and the whole cell based biosensor can measure permeability, the biosensor was tested to investigate its ability to act as a screening tool for cancer. The study demonstrated:

- The biosensor responded to the presence of cytokines, individually and in combination at the concentrations observed in the serum of healthy individuals.
- The responses thus obtained were less than the responses obtained for cytokines at the concentrations observed in the serum of cancer patients, indicating dose dependant response from the sensor.
- When the responses obtained by exposing the biosensor to the combination of all four cytokines at concentrations observed in healthy subjects and cancer patients were compared, it was observed that the biosensor was able to distinguish between the two concentrations.
- The responses obtained by exposing the sensor to the cytokines at the two different concentrations for 1 h differ significantly. Hence, all the experiments with the serum were carried out with an exposure time of 1 h.
- The responses of the biosensor to the serum from 15 different healthy individuals ranged from 0.06 to 0.11 with a mean of about 0.09.
- When sensor was exposed to serum from different cancer patients, significantly higher responses were obtained. This indicates that the sensor was able to distinguish between healthy individuals and cancer patients and the responses correlated well with the stages of cancer.

Chapter 9 ：Future Studies

The present study was focused on extending the application of a whole cell-based biosensor towards monitoring physiological toxins and screening cancer. Research can further be conducted in several other avenues to extend the application of the biosensor as well as to increase its potential for commercial success. Some of the areas where future research can be focused are:

- Studying the effect of anti-angiogenic drugs on sensor response
- Further studies with serum of cancer patients
- Miniaturization of the sensor
- Studies on stabilization of the sensor as well as increasing the shelf life of the sensor

A. Studying the effect of anti-angiogenic drugs on sensor response

Since uncontrolled angiogenesis is observed in pathological conditions in several diseases like cancer, arthritis etc, one approach of treating patients suffering from such diseases has been to treat them with anti-angiogenic drugs. While some of the anti-angiogenic drugs have already being approved by FDA for anti-cancer therapies, several other drugs are now in trial phase. Since, the current study demonstrated that the whole cell based biosensor can be used as an assay for measuring angiogenesis, experiments can be conducted to investigate the potential of the biosensor to act as a screening tool for angiogenic inhibitors.

B. Further studies with the serum of cancer patients

To investigate the ability of the sensor to act as a prognostic tool, the response of the biosensor can be measured by exposing it to serum samples of cancer patients prior and after treatment. The efficacy of particular drug for treating cancer can also be investigated.

C. Miniaturization of the sensor

The advantage of miniaturizing the cell based sensor over the present biosensor lies in the fact that it will require less volume of test samples. Requirement of smaller volume of

samples becomes critical especially when one deals with body fluids like serum or plasma. Moreover, miniaturization can eventually help in construction of array of electrodes thus enabling simultaneous detection of analytes. Screen printing the electrodes can be a method of construction of planar cell- based sensors.

D. Studies on stabilization of the sensor as well as increasing the shelf life of the sensor

For the biosensor to succeed commercially, one aspect that needs to be taken care of is the stabilization of the sensor and extension of its shelf life. One possible way to stabilize the cells is to air-dry them and to rehydrate them prior to use. Based on the fact that excreted polysaccharides help stabilization of the anhydrophiles in the air-dry state, one study has shown that exogenous addition of extracellular components like glycan of desiccant tolerant organisms can improve the stability of the mammalian cells in desiccated conditions (Bloom et al. 2001).

List of Abbreviations

Abbreviation	Description
ANOVA	Analysis of Variance
ATCC	American Type Culture Collection
ATP	Adenosine 5’ -triphosphate
bFGF	Basic Fibroblast Growth Factor
BIM I	Bisindolylmaleimide I
BOD	Biological Oxygen Demand
BSA	Bovine Serum Albumin
CA-125	Cancer Antigen-125
CDI	Carbonyldiimidazole
CEA	Carcinoembryonic Antigen
CTA	Cellulose Triacetate
CTC	Circulating Tumor Cells
DIUF	Deionized Ultrafiltered
DMSO	Dimethylsiloxane
DNA	Deoxyribonucleic Acid
EC	Endothelial Cell
ECIS	Electric Cell-Substrate Impedance Sensor
ECM	Extracellular Matrix
EDTA	Ethylenediaminetetraacetic Acid
EGM	Endothelial Growth Media
ELISA	Enzyme-Linked Immunosorbent Assay
EMF	Electromotive Force
FBS	Fetal Bovine Serum
FOBT	Fecal Occult Blood Test
GOD	Glucose Oxidase
GRGDS	Glycine-Arginine-Glycine-Aspartic Acid-Serine
HBSS	HEPES Buffered Saline Solution

HGF	Hepatocyte Growth Factor
HUVECs	Human Umbilical Vein Endothelial Cells
ISE	Ion Selective Electrode
IUPAC	International Union of Pure and Applied Chemistry
KTClPB	Potassiumtetrakis (4-chlorophenyl) borate
LOH	Loss of Heterozygosity
MI	Microsatellite Instability
NASA	National Aeronautics and Space Administration
NO	Nitric Oxide
NOS	Nitric Oxide Synthase
NPOE	Nitrophenyl Octyl Ether
Pap Test	Papanicolaou Test
PBS	Phosphate Buffer Saline
PSA	Prostate Specific Antigen
PI3-K	Phosphoinositide 3-Kinase
PKC	Protein Kinase C
QCM	Quartz Crystal Microbalance
SEM	Standard Error of the Mean
SPR	Surface Plasmon Resonance
TNF- α	Tumor Necrosis Factor-α
TNS	Trypsin Neutralizing Solution
Tris	Tris(hydroxymethyl) aminomethane
VEGF	Vascular Endothelial Growth Factor
VVO’s	Vesiculo- Vacuolar Organlles

References

Abad, J.N., Pariente, F., Hernandez, L., Abruna, H.D., Lorenzo, E., 1998. Determination of organophosphorus and carbamate pesticides using a piezoelectric biosensor. Anal. Chem. 70(14), 2848 - 2855.

Abdelghani, A., Abdelghani-Jacquin, C., Hillebrandt, H., Sackman, E., 2002. Cell-based biosensors for inflammatory agents detection. Materials Science and Engineering C 22, 67 - 72.

Ahuja, T., Mir, i.A., Kumar, D., Rajesh, 2007. Biomolecular immobilization on conducting polymers for biosensing applications. Biomaterials 28, 791-805.

Alexander, J.S., Zhu, Y., Elrod, J.W., Alexander, B., Coe, L., Kalogeris, T.J., Fuseler, J., 2001. Reciprocal Regulation of Endothelial Substrate Adhesion and Barrier Function. Microcirculation 8, 389-401.

Alocilja, E.C., Radke, S.M., 2003. Market analysis of biosensors for food survey. Biosensors and Bioelectronics 18, 841-846.

Amine, A., Mohammadi, H., Bourais, I., Palleschi, G., 2006. Enzyme inhibition based biosensors for food safety and environmental monitoring. Biosensors and Bioelectronics 21, 1405-1423.

Anker, P., Stroun, M., 2001. Tumor related alterations in circulating DNA, potential for diagnosis, prognosis and detection of minimal residual disease. Leukemia 15, 289-291.

Applegate, B.M., Kermeyer, S.R., Sayler, G.S., 1998. A chromosomally based *tod-lux* CDABE whole cell reporter for benzene, toluene, ethyl benzene and xylene (BTEX) sensing. Appl. Environ. Microbiol 64, 2730 - 2735.

Arndt, S., Seebach, J., Psathaki, K., Galla, H.-J., Wegener, J., 2004. Bioelectrical impedance assay to monitor changes in cell shape during apoptosis. Biosensors and Bioelectronics 19, 583-594

Asahara, T., Bauters, C., Zheng, L.P., Takeshita, S., Bunting, S., Ferrara, N., Symes, J.F., Isner, J.M., 1995. Synergistic Effect of Vascular Endothelial Growth Factor and Basic Fibroblast Growth Factor on Angiogenesis In Vivo Circulation 92, 365 - 371.

Auerbach, R., Lewis, R., Shinners, B., Kubai, L., Akhtar, N., 2003. Angiogenesis Assays: A Critical Overview. Clinical Chemistry 49, 32-40.

Bakker, E., Buhlmann, P., Pretsch, E., 1997. Carrier based ion selective electrodes and bulk optodes-1. General characteristics. Chemical Review 97, 3083 - 3132.

Bakker, E., Buhlmann, P., Pretsch, E., 1999. Polymeric membrane ion selective electrodes. What are the limits? Electroanalysis 11(13), 915-933.

Baluk, P., Hirata, A., Thurston, G., Fujiwara, T., Neal, C.R., Michel, C.C., McDonald, D.M., 1997. Endothelial gaps: time course of formation and closure in inflamed venules of rats. Am. J. Physiol. 272, L155 - L 170.

Bates, D.O., Hillman, N.J., Williams, B., Neal, C.R., Pocock, T.M., 2002. Regulation of microvascular permeability by vascular endothelial growth factors. J. Anat 200, 581-597.

Baxter, G.A., Ferguson, J.P., O'Connor, M.C., Elliott, C.T., 2001. Detection of streptomycin residues in whole milk using an optical immunobiosensor. J. Agric. Food Chem 49, 3204 - 3207.

Bhakdi, S., J., T.-J., 1991. Alpha-toxin of Staphylococcus aureus. Microbiol Mol Biol Rev 55, 733 - 751.

Bhakdi, S., Muhly, M., Mannhardt, U., Hugo, F., Klapettek, K., Mueller-Eckhardt, C., L., R., 1988. Staphylococcal α toxin promotes blood coagulation via attack on human platelets. J. Exp. Med. 168, 527-542.

Bhakdi S., T.-J.J., 1991. Alpha-toxin of Staphylococcus aureus. Microbiol Mol Biol Rev 55, 733 - 751.

Bloom, F.R., Price, P., Lao, G., Xia, J.L., Crowe, J.H., Battista, J.R., Helm, R.F., Slaughter, S., Potts, M., 2001. Engineering mammalian cells for solid-state sensor applications. Biosensors and Bioelectronics 16, 603-608.

Bond, M., Fabunmi, R.P., Baker, A.H., Newby, A.C., 1998. Synergistic upregulation of metalloproteinase-9 by growth factors and inflammatory cytokines: an absolute requirement for transcription factor NF-kappa B. FEBS Lett 435(1), 29 - 34.

Bousse, L., 1996. Whole cell biosensors. Sensors and Actuators B 34, 270 - 275.

Brahim, S., Narinesingh, D., Guiseppi-Elie, A., 2002. Polypyrrole hydrogel composites for the construction of clinically important biosensors. Biosensors and Bioelectronics 17, 53-59.

Brell, B., B.Temmesfeld-Wollbruck, I.Altzschner, Frisch, E., B.Schmeck, Hocke, A.C., N.Suttorp, S.Hippenstiel, 2005. Adrenomedullin reduces Staphylococcus aureus [alpha]-toxin-induced rat ileum microcirculatory damage. Crit. Care Med. 33, 819-826.

Breslin, J.W., Pappas, P.J., Cerveira, J.J., II, R.W.H., Duran, W.N., 2003. VEGF increases endothelial permeability by separate signaling pathways invoving ERK-1/2 and nitric oxide. Am J Physiol Heart Circ Physiol 284, H92-H100.

Brooks, K.A., Allen, J.R., Feldhoff, P.W., Bachas, L.G., 1996. Effect of surface attached heparin on the response of potassium selective electrodes. Anal. Chem. 68, 1439-1443.
Buck, R.P., Lindner, E., 1994. Recommendations for nomenclature of ion-selective electrodes. Pure & Appl. Chem. 66, 2527-2536.

Burke-Gaffney, A., Keenan, A.K., 1993. Modulation of human endothelial cell permeability by combinations of the cytokines interleukin-1 alpha/beta, tumor necrosis factor-alpha and interferon-gamma. Immunopharmacology 25(1), 1 - 9.

Burlage, R.S., A.V., P., A., H., G., S., 1994. Bioluminescent reporter bacteria detect contaminants in soil samples. Appl. Microbiol. Biotechnol. 45, 731 - 740.

Burns, A.R., Walker, D.C., Brown, E.S., Thurmon, L.T., Bowden, R.A., Keese, C.R., Simon, S.I., Entman, M.L., Smith, C.W., 1997. Neutrophil transendothelial migration is independent of tight junctions and occurs preferentially at tricellular corners. J. Immunol . 159, 2893 - 2903.

Caiazza, N.C., O'Toole, G.A., 2003. Alpha-Toxin Is Required for Biofilm Formation by Staphylococcus aureus J Bacteriol 185, 3214-3217.

Campanella, L., Favero, G., Mastrofini, D., Tomasetti, M., 1996. Toxicity order of cholanic acids using immobilized cell biosensor. J. Pharm. Biomed. Anal. 14, 1007 - 1013.

Carmellet, P., Jain, R.K., 2000. Angiogenesis in cancer and other diseases. Nature 407, 249-257.

Cha, G.S., M.E.Mayerhoff, 1989. Potentiometric ion -selective and bio-selective electrodes based on asymetric cellulose-actetate membranes. Talanta 36(1-2), 271 - 278.

Cha, M.J., Shin, J.H., Oh, B.K., Kim, C.Y., Cha, G.S., Shin, D.S., Kim, B., 1995. Asymmetric cellulose-actetate membrane based carbonate-selective and chloride selective electrodes. Analytica Chimica Acta 315(3), 311 - 319.

Chen, J., Braet, F., Brodsky, S., Weinstain, T., Romanov, V., Noiri, E., Goligorsky, M.S., 2002. VEGF-induced mobilization of caveolae and increase in permeability of endothelial cells. Am J Physiol Cell Physiol 282, C1053 -C1063.

Christensson, B., Espersen, F., Hedstrom, S.A., G., K., 1983. Solid-phase radioimmunoassay of immunoglobulin G antibodies to Staphylococcus aureus peptidoglycan in patients with staphylococcal infections. Acta Pathol Microbiol Immunol Scand [B] 91, 351-356.

Christensson, B., Gilbert, J., Fox, A., Morgan, S.L., 1989. Mass spectrometric quantitation of muramic acid, a bacterial cell wall component, in septic synovial fluids. Arthritis Rheum 32, 1268-1272.

Clarke, H., Soler, A.P., Mullin, J.M., 2000. Protein kinase C activation leads to dephosphorylation of occludin and tight junction permeability increase in LLC-PK1 epithelial cell sheets. Journal of Cell Science 113, 3187-3196.

Clayburgh, D.R., Shen, L., Turner, J.R., 2004. A porous defense: the leaky epithelial barrier in intestinal disease. Lab Invest 84, 282 - 291.

Collings, A.F., Caruso, F., 1997. Biosensors: recent advances. Rep. Prog. Phys. 60, 1397 - 1445.

Cronauer, M.V., Hittmair, A., Eder, I.E., Hobisch, A., Culig, Z., Ramoner, R., Zhang, J., Bartsch, G., Reissigl, A., Radmayr, C., Thurnher, M., Klocker, H., 1997. Basic fibroblast growth factor levels in cancer cells and in sera of patients suffering from proliferative disorders of the prostate. The Prostate 31, 223 - 233.

Denis, M.G., Lipart, C., LeBorgne, J., LeHur, P.-A., Galmiche, J.-P., Denis, M., Ruud, E., Truchaud, A., Lustenberger, P., 1997. Detection of disseminated tumor cells in peripheral blood of colorectal cancer patients. Int. J. Cancer 74, 540-544.

Devine, P.J., Anis, N.A., Wright, J., Kim, S., Edlefrawi, A.T., Edlefrawi, M.E., 1995. A fiberoptic cocaine biosensor. Anal. Biochem 227, 216 - 224.

Dirix, L.Y., Vermeulen, P.B., Pawinski, A., Prove, A., Benoy, I., Pooter, C.D., Martin, M., Oosterom, A.T.V., 1997. Elevated levels of the angiogenic cytokines basic fibroblast growth factor and vascular endothelial growth factor in sera of cancer patients. Br. J. Cancer 76(2), 238 - 243.

Dorsch, W., Suttorp, N., Lottspeich, F., Zepp, F., 1999. Anti-inflammatory activity in human skin: it prevents edema formation in vitro. Int. Arch. Allergy Immunol. 118, 236 - 239.

Dowrick, P.G., Prescott, A.R., Warn, R.M., 1991. Scatter factor affects changes in the cytoskeletal organization of epithelial cells. Cytokine 3, 299 - 310.

Dudek, S.M., Garcia, J.G.N., 2001. Cytoskeletal regulation of pulmonary vascular permeability. J. Appl. Physiol 91, 1487-1500.

Dunlop, R.J., Campbell, C.W., 2000. Cytokines and advanced cancer. Journal of Pain and Symptom Management 20, 214-232.

Dvorak, H.F., Brown, L.F., Detmar, M., Dvorak, A.M., 1995. Vascular permeability factor/vascular endothelial growth factor, microvascular hyperpermeability and angiogenesis. Am. J. Pathol 146, 1029 - 1039.

Eggins, B., 1996. Biosensors: an introduction. John Wiley & Sons.

Esser, S., Lampugnani, M.G., Corada, M., Dejana, E., Risau, W., 1998a. Vascular endothelial graowth factor induces VE-cadherin tyrosine phosphorylation in endothelial cells. Journal of Cell Science 111, 1853-1865.

Esser, S., Wolburg, K., Wolburg, H., Brier, G., Kurzchalia, T., Risau, W., 1998b. Vascular Endothelial Growth Factor Induces Fenestrations In Vitro. Journal of Cell Biology 140(4), 947-959.

Eyk, J.E.V., 2001. Proteomics: unraveling the complexity of heart disease and striving to change cardiology. Curr Opin Mol ther 3, 546-553.

Feng, Y., Venema, V.J., Venema, R.C., Tsai, N., Behzadian, M.A., Caldwell, R.B., 1999. VEGF-Induced Permeability Increase is mediated by caveolae. Investigative Ophthalmology & Visual Science 40, 157-167.

Folkman, J., 1985. Tumor angiogenesis. Adv. Cancer Res. 43, 175-203.

Folkman, J., 1990. What is the evidence that tumors are angiogenesis dependent? J Nat Cancer Inst 82, 4 - 6.

Folkman, J., 1995. Angiogenesis in cancer, vascular, rheumatoid and other diseases. Nat. Med. 1, 27-31.

Folkman, J., Shing, Y., 1992. Angiogenesis. J Biol Chem 267, 10931 - 10934.

Frater-Schroder, M., Risau, W., Hallmann, R., Gautschi, P., Bohlen, P., 1987. Tumor necrosis factor type alpha, a potent inhibitor of endothelial cell growth in vitro, is angiogenic in vivo PNAS 84(15), 5277 - 5281.

Gambhir, A., Gerard, M., Mulchandani, A., Malhotra, B.D., 2001. Coimmobilization of urease & glumate dehydrogenase in electrochemically prepared polypyrrole-polyvinyl sulphonate films. Appl. Biochem Biotechnol 96, 249-257.

Gaudin, V., Fontaine, J., P.Maris, 2001. Screening of penicillin residues by a surface plasmon resonance based biosensor assay: comparison of chemical and enzymatic sample pretreatment. Anal. Chim. Acta 436, 191 - 198.

Gaudin, V., P.Maris, 2001. Development of biosensor based immunoassay for screening of chloramphenicol residues in milk. Food Agric. Immunol. 13, 77 - 86.

Gehron, M.J., Davis, J.D., Smith, G.A., White, D.C., 1984. Determination of the gram-positive bacterial content of soils and sediments by analysis of teichoic acid components. J Microbiol Methods 2, 165-176.

Geldhof, A.B., Meyer, K.D., Baetselier, P.D., Verschueren, H., 2002. Morphometric Analysis of Cytolysis in cultured cell monolayers: A Simple and Versatile Method for the evaluation of the cytotoxic activity and the fate of LAK Cells. Lab Invest 82, 105 -107.

Gemmell, C.G., Peterson, P.K., Townsend, K., Quie, P.G., Kim, Y., 1982. Biological effects of the interaction of staphylococcal alpha-toxin with human serum. Infect Immun. 38, 981-985.

Ghosh, G., Bachas, L.G., Anderson, K.W., 2007a. Biosensor incorporating cell barrier architectures for detecting *Staphylococcus aureus* alpha toxin. Anal. Bional. Chem 387, 567-574.

Ghosh, G., Mehta, I., Cornette, A., Anderson, K.W., 2007b. Measuring Permeability with a Whole Cell – Based Biosensor as an Alternate Assay for Angiogenesis: Comparison with Common in vitro Assays Biosensors and Bioelectronics In Press.

Giaever, I., Keese, C.R., 1986. Use of electric field to monitor the dynamical aspect of cell behaviour in tissue culture. IEEE Trans. Biomed. Eng 33(242 - 247).

Giaever, I., Keese, C.R., 1991. Micromotion of mammalian cells measured electrically. Proc. Natl. Acad. Sci. USA 88, 7896 -7900.

Giaever, I., Keese, C.R., 1993. A morphological biosensor for mammalian cells. Nature (London) 366, 591 - 592.

Gimbrone, M.A., Leapmean, S.B., Cotran, R.S., Folkman, J., 1972. Tumor dormancy in vivo by prevention of neovascularisation. J. Exp. Med 136, 261- 276.

Giraudo, E., Primo, L., Audero, E., Gerber, H.-P., Koolwijck, P., Soker, S., Klagsbrun, M., Ferrara, N., Bussolino, F., 1998. Tumor necrosis factor alpha regulates expression of vascular endothelial growth factor receptor-2 and its co-receptor neutrophilin -1 in human vascular endothelial cells. J. Biol. Chem. 273(34), 22128 - 22135.

Goto, F., Goto, K., Weindel, K., Folkman, J., 1993. Synergistic effects of vascular endothelial growth factor and basic fibroblast growth factor on the proliferation and cord formation of bovine capillary endothelial cells within collagen gels. Lab Invest 69(5), 508 - 517.

Gouaux, J.E., Braha, O., Hobaugh, M.R., Song, L., Cheley, S., Shustak, C., Bayley, H., 1994. Subunit Stoichiometry of Staphylococcal α-Hemolysin in Crystals and on Membranes: A Heptameric Transmembrane Pore Proc Natl Acad Sci USA 91, 12828-12831.

Granato, A.M., Nanni, O., Falcini, F., Folli, S., Mosconi, G., Paola, F.D., Medri, L., Amadori, D., Volpi, A., 2004. Basic fibroblast growth factor and vascular endothelial

growth factor serum levels in breast cancer patients and healthy women: useful diagnostic tools? Breast Cancer Research 6, R38 - R45.

Greenlee, R.T., Murray, T., Bolden, S., Wingo, P.A., 2000. Cancer Statistics. CA Cancer J. Clin 50, 7 - 33.

Gulla, K.C., Gauda, M.D., Thakur, M.S., Karanth, N.G., 2002. Reactivation of immobilized acetyl cholinesterase in an amperometric biosensor for organophosphorous pesticide. Biochem Biophys Acta 1597, 133-139.

Gustavsson, E., Degelaen, J., Bjurling, P., Sternesjo, A., 2004. Determination of beta-lactams in milk using a surface plasmon resonance based biosensor. J. Agric. Food Chem 52, 2791-2796.

Haab, B.B., 2005. Antibody arrays in cancer research. Molecular and Cellular Proteomics 4, 377-383.

Hanahan, D., Folkman, J., 1996. Patterns and emerging mechanisms of angiogenic switch during tumorigenesis. Cell 86, 353-364.

Hansen, L.H., Sorensen, S.J., 2001. The use of whole-cell biosensors to detect and quantify compounds or conditions affecting biological systems. Microb Ecol. 42, 483 - 494.

Harsanyi, G., 2001. Sensors in biomedical applications. May they change the quality of life? Sensor Review 21, 259-267.

Heer, K., Kumar, H., Read, J.R., Fox, J.N., Monson, J.R.T., Kerin, M.J., 2001. Serum vascular endothelial growth factor in breast cancer: its relation with cancer type and estrogen status. Clin. Can. Res. 7, 3491- 3494.

Herrera, L.J., Raja, S., Gooding, W.E., El-Hefnawy, T., Kelly, L., Luketich, J.D., Godfrey, T.E., 2005. Quantitative analysis of circulating plasma DNA as a tumor marker in thoracic malignancies. Clinical Chemistry 51, 113-118.

Hillebrandt, H., Abdelghani, A., Jacquin, C.A.-., Aepfelbacher, M., Sackman, E., 2001. Electrical and optical characterization of hrombin-induced permeability of cultured endothelial cell monolayers on semiconductor electrode arrays. Appl. Phys. A 73, 539 - 546.

Hirata, A., Baluk, P., Fujiwara, T., McDonald, D.M., 1995. Location of focal silver staining at endothelial gaps in inflamed venules examined by scanning electron microscopy. Am. J. Physiol. 269, L403 - L418.

Hocke, A.C., Temmesfeld-Wollbrueck, B., Schmeck, B., Berger, K., Frisch, E.M., Witzenrath, M., Brell, B., Suttorp, N., Hippenstiel, S., 2006. Perturbation of endothelial

junction proteins by Staphylococcus aureus α -toxin: inhibition of endothelial gap formation by adrenomedullin. Histochem Cell Biol. 126, 305 - 316.

Holmgren, L., O'Reilly, M.S., Folkman, J., 1995. Dormancy of micrometastases: balanced proliferation and apoptosis in the presence of angiogenesis suppression. Nat. Med. 1, 149 - 153.

Hu, L., Hofmann, J., Jaffe, R.B., 2005. Phosphatidylinositol 3-kinase mediates angiogenesis and vascular permeability associated with ovarian carcinoma. Clin. Can. Res 11, 8208-8212.

Hume, E.B.H., Dajcs, J.J., Moreau, J.M., O'Collaghan, R.J., 2000. Immunization with alpha-toxin toxoid protects the cornea against tissue damage during experimental Staphylococcus aureus keratitis Infect Immun 68, 6052-6055.

Irvine, E.J., Marshall, J.K., 2000. Increased intestinal permeability precedes the onset of Crohn's disease in a subject with familial risk. Gastroenterology 119, 1740 - 1744.

Jiang, W.G., Martin, T.A., Matsumoto, K., Toshikazu, N., Mansel, R.E., 1999. Hepatocyte growth factor/ Scatter factor decreases the expression of occludin and transendothelial resistance (TER) and increases paracellular permeability in human vascular endothelial cells. J Cell Phyisiol 181, 319 - 329.

Jonsson, P., Lindberg, M., Haraldsson, I., Wardstrom, T., 1985. Virulence of Staphylococcus aureus in a mouse mastitis model: studies of alpha hemolysin, coagulase, and protein A as possible virulence determinants with protoplast fusion and gene cloning. Infect Immun 49, 765-769.

Julander, I.G., Granstrom, M., Hedstrom, S.A., Mollby, R., 1983. The role of antibodies against alpha-toxin and teichoic acid in the diagnosis of staphylococcal infections Infection 11, 77 - 83.

Kevil, C.G., Payne, D.K., Mire, E., Alexander, J.S., 1998. Vascular Permeability Factor/Vascular Endothelial Growth Factor- mediated Permeability Occurs through Disorganization of Endothelial Junctional Proteins. Journal of Biological Chemistry 273, 15099 - 15103.

Kielian, T., Cheung, A., Hickey, W.F., 2001. Diminished virulence of an alpha toxin mutant of *Staphylococcus aureus* in experimental brain abscesses. Infect. Immun 69, 6902 - 6911.

Killackey, J.J.F., Johnston, M.G., Movat, H.Z., 1986. Increased permeability of microcarrier-cultured endothelial monolayers in response to histamine and thrombin. A model for the in vitro study of increased vasopermeability. Am. J. Pathol. 122, 50 - 61.

Koncki, R., Hulanicki, A., Glab, S., 1997. Biochemical modifications of membrane ion - selective sensors. Trac-Trends in Analytcal Chemistry 16(9), 528-536.

Koolwijk, P., Erck, M.G.M.v., Vree, W.J.A.d., Vermeer, M.A., Weich, H.A., Hanemaaijer, R., Hinsbergh, V.W.M.v., 1996. Cooperative effect of TNF alpha, bFGF, and VEGF on the formation of tubular structures of human microvascular endothelial cells in a fibrin matrix. Role of urokinase activity. J Cell Biol 132, 1177 - 1188.

Kopf, E., Zharhary, D., 2007. Antibody arrays- an emerging tool in cancer proteomics. International Journal of Biochemistry and Cell Biology 39, 1305-1317.

Korpan, Y.I., Gonchar, M.V., Starodub, N.F., Shul'ga, A.A., Sibirny, A.A., El'skaya, A.V., 1993. A cell biosensor specific for formaldehyde based on pH sensitive transistors coupled to methylotrophic yeast cells with genetically adjusted metabolism. Anal. Biochem 215, 216-222.

Kumar, R., Yoneda, J., Bucana, C.D., Fidler, I.J., 1998. Regulation of distinct steps of angiogenesis by different angiogenic molecules. Int. J. Onco. 12, 749 - 757.

Lal, B.K., Verma, S., Pappas, P.J., II, R.W.H., Duran, W.N., 2001. VEGF Increases Permeability of the Endothelial Cell Monolayer by Activation of PKB/akt, Endothelial Nitric Oxide Synthase, and MAP Kinase Pathways. Microvascular Research 62, 252 - 262.

Lazo, A.R., Bustamante, M., Jimenez, J., Arada, M.A., Yazdani-Pedram, M., 2006. Preparation and study of a 1- furoyl - 3,3 diethylthiourea electrode J. Chil. Chem. Soc. 51, 975-978.

Lei, Y., Mulchandani, P., Chen, W., Mulchandani, A., 2005. Direct determination of p-nitrophenyl substituent organophosphorus nerve agents using a recombinant Pseudomonas putida JS444-modified Clark oxygen electrode J. Agric. Food Chem 53, 524 -527.

Leon, S.A., Shapiro, B., Skiaroff, D.M., Yaros, M.J., 1977. Free DNA in the serum of cancer patients and the effect of therapy. Cancer Research 37, 646-650.

Leonard, P., Hearty, S., G.Wyatt, J.Quinn, O'Kennedy, R., 2005. Development of surface plasmon resonance based immunoassay for *Listeria monocytogenes*. J. Food Protection 68(4), 728 - 735.

Liu, Q., Cai, H., Xu, Y., Li, Y., Li, R., Wang, P., 2006. Olfactory cell-based biosensor: A first step towards a neurochip of bioelectronic nose. Biosensors and Bioelectronics 22, 318 - 322.

Liu, Q., Cai, H., Xu, Y., Xiao, L., Yang, M., Wang, P., 2007. Detection of heavy metal toxicity using cardiac cell-based biosensor. Biosensors and Bioelectronics 22, 3224 - 3229.

Loeffler, D.A., Creasy, M.T., Norcross, N.L., Pappe, M.J., 1988. Enzyme-linked immunosorbent assay for detection of leukocidin toxin from Staphylococcus aureus in bovine milk samples. J Clin Microbiol. 26, 1331-1334.

Lum, H., Malik, A.B., 1994. Regulation of vascular endothelial barrier function. Am. J. Physiol. 267, L223- L241.

Macholan, L., Chmelikova, B., 1986. Plant tissue based membrane biosensor for L-ascorbic acid. Anal. Chim. Acta 185, 187 - 193.

Marci, A., Versaci, A., Loddo, S., Scuderi, G., Travagliante, M., Trimarchi, G., Treti, D., Famulari, C., 2006. Serum levels of interleukin 1 beta, interleukin 8 and tumor necrosis factor alpha as markers of gastric cancer. Biomarkers 11(2), 184-193.

Marrie, T.J., Costeron, J.W., 1984. Scanning and transmission electron microscopy of in situ bacterial colonization of intravenous and intraarterial catheters. J Clin Microbiol. 19, 687-693.

Marrie, T.J., J., N., Costeron, J.W., 1982. A scanning and transmission electron microscopic study of an infected endocardial pacemaker lead. Circulation 66, 1339-1341.

Martin, T.A., Mansel, R.E., Jiang, W.G., 2002. Antagonistic Effect of NK4 on HGF/SF Induced changes in the Transendothelial Resistance (TER) and Paracellular Permeability of Human Vascular Endothelial Cells. J. Cell. Physiol 192, 268-275.

Mauriz, E., Calle, A., Manclus, J.J., Montoya, A., Lechuga, L.M., 2007. Online determination of 3,5,6-trichloro-2-pyrinidol in human urine samples by surface plasmon resonance immunosensing. Anal. Bioanal. Chem. 387, 2757 - 2765.

May, K.M.L., Vogt, A., Bachas, L.G., Anderson, K.W., 2005. Vascular endothelial growth factor as a biomarker for the early detection of cancer using a whole cell based biosensor. Anal. Bioanal. Chem. 382, 1010 - 1016.

May, K.M.L., Wang, Y., Bachas, L.G., Anderson, K.W., 2004a. Development of a whole-cell-based biosensor for detecting histamine as a model toxin. Anal. Chem. 76(14), 4156 - 4161.

May, K.M.L., Wang, Y., Bachas, L.G., Anderson, K.W., 2004b. Development of a whole cell - based biosensor for detecting histamine as a model toxin. Analytical Chemistry 76(14), 4156 - 4161.

McDonald, D.M., 1994. Endothelial gaps and permeability of venules in rat tracheas exposed to inflammatory stimuli. Am. J. Physiol. 266, L61 - L 83.

McKay, D.M., Baird, A.W., 1999. Cytokine regulation of epithelial permeability and ion transport. Gut 44, 283 - 289.

Mehta, D., Malik, A., 2006. Signaling Mechanisms Regulating Endothelial Permeability. Physiol Rev 86, 279-367.

Menzies, B.E., Kourteva, I., 2000. *Staphylococcus aureus* α-toxin induces apoptosis in endothelial cells. FEMS Immun. Med. Microbiol. 29, 39-45.

Metzger, R., Deglmann, C.J., Hoerrlein, S., Zapf, S., Hilfrich, J., 2001. Towards in-vitro prediction of an in-vivo cytostatic response of human tumor cells with a fast chemosensitivity assay Toxicology 166, 97-108

Mitra, P., Keese, C.R., Giaever, I., 1991. Electrical measurements can be used to monitor the attachment and spreading of cells in tissue culture. Biotechniques 11, 504 - 510.

Mollby, R., 1983. Isolation and properties of membrane damaging toxins. Academic Press, London.

Mollby, R., 1994. Antibody responses in deep *Staphylococcus aureus* infections. Zbl Bakt 26, 451 - 459.

Morales-Ruiz, M., Fulton, D., Sowa, G., Languino, L.R., Fujjo, Y., Walsh, K., Sessa, W.C., 2000. Vascular endothelial growth factor stimulated actin reorganization and migration of endothelial cells is regulated via the serine/threonine kinase Akt. Circ. Res 86, 892 - 896.

Morf, W.E., 1981. The principles of ion selective electrodes and of membrne transport. Elsevier Co., Amsterdom.

Morimoto, A., Okamura, K., Hamanaka, R., Sato, Y., Shima, N., Higashio, K., Kuwano, M., 1991. Hepatocyte growth factor modulates migration and proliferation of human microvascular endothelial cells in culture. Biochem Biophys Res Commun 179, 1042 - 1049.

Mulcahy, H., Lyautey, J., Lederrey, C., Chen, X.q., Anker, P., Alstead, E., Ballinger, A., Farthing, M., Stroun, M., 1998. A prospective study of K-ras mutations in the plasma of pancreatic cancer patients. Clin. Can. Res. 4, 271-275.

Muller, V., Stahmenn, N., Riethdorf, S., Rau, T., Zabel, T., Goetz, A., Janicke, F., Pantel, K., 2005. Circulating tumor cells in breast cancer: correlation to bone marrow metastastases, heterogeneous response to systemic therapy and low proliferative activity. Clin. Can. Res. 11, 3678-3685.

Mullin, J.M., Kleinzeller, A., 1985. Sugar transport in the renal epithelial cell culture. Plenum Publishing Corp., New York: Plenum Publishing Corp.

Mullin, J.M., O'Brien, T.G., 1986. Effect of tumor promoters on LLC-PK_1 renal epithelial tight junctions and transepithelial fluxes. Am J Physiol 251, C597-C602.

Mullin, J.M., Snock, K.V., 1990. Effect of Tumor Necrosis Factor on Epithelial Tight Junctions and Transepithelial Permeability. Cancer Research 50, 2172-2176.

Naik, M.U., Vuppalanchi, D., Naik, U.P., 2003. Essential role of junctional adhesion molecule-1 in basic fibroblast growth factor- induced endothelial cell migration. Arterioscler. Thromb. Vasc. Biol. 23, 2165 - 2171.

Nakagami, H., Cui, T.-X., Iwai, M., Shiuchi, T., Takeda-Matsubara, Y., Wu, L., Horiuchi, M., 2002. Tumor necrosis factor alpha inhibits growth factor mediated cell proliferation through SHP - 1 activation in endothelial cells. Arterioscler. Thromb. Vasc. Biol. 22, 238 - 242.

Nakagawa, T., Martinez, S.R., Goto, Y., Koyanagi, K., Kitago, M., Shingai, T., Elashoff, D.A., Ye, X., Singer, F.R., Giuliano, A.E., Hoon, D.S.B., 2007. Detection of circulating tumor cells in early stage breast cancer metastasis to axillary lymph nodes. Clin. Can. Res. 13, 4105-4110.

Narang, U., Anderson, G.P., Ligler, F.S., Burans, J., 1997. Fiber-optic based biosensor for ricin. Biosensors and Bioelectronics 12, 937 - 945.

Nedelkov, D., Kiernan, U.A., Niederkofler, E.E., Tubbs, K.A., Nelson, R.W., 2006. Population Proteomics. Molecular and Cellular Proteomics 5, 1811-1816.

Noiri, E., Hu, Y., Bahou, W.F., Keese, C.R., Giaever, I., Goligorsky, M.S., 1997. Permissive role of nitric oxide in endothelian-induced migration of endothelial cells. J. Biol. Chem 272, 1747 - 1752.

Nooteboom, A., Hendriks, T., Otteholler, I., Linden, C.J.v.d., 2000. Permeabilily characteristics of human endothelial monolayers seeded on different extracellular matrix proteins. Mediators of Inflammation 9, 235-241.

Nusrat, A., Parkos, C.A., Bacarra, A.E., Godowski, P.J., Delp-Archer, C., Rosen, E.M., Madara, J.L., 1994. Hepatocyte growth factor/scatter factor effects on nontransformed cell lines, basolateral polarization of c-met receptor in transformed and natural epithelia, and induction of rapid wound repair in a transformed model epithelium. J. Clin. Invest 93, 2056 - 2065.

Nusrat, A., Turner, J.R., Madara, J.L., 2000. Molecular physiology and pathophysiology of tight junctions IV. Regulation of tight junctions by extracellular stimuli: nutrients,

cytokines and immune cells. Am. J. Physiol. Gastrointest. Liver Physiol 279, G851 - G857.

Nwaraiku, F.E., Chang, J., Zhu, X., Liu, Z., Duffy, S.L., Halaihel, N.H., Terada, L., Turnage, R.H., 2002. The role of p38 MAP kinase in tumor necrosis factor induced redistribution of vascular endothelial cadherin and increased permeability. Shock 18, 82-85.

O'Callaghan, R.J., Callegan, M.C., Moreau, J.M., Green, L.C., Foster, T.J., Hartford, O.M., Engel, L.S., J.M., H., 1997. Specific roles of alpha-toxin and beta-toxin during Staphylococcus aureus corneal infection. Infect. Immun 65, 1571-1578.

Ogert, R.A., Brown, E.J., Singh, B.R., Shriver-Lake, L.C., Ligler, F.S., 1992. Detection of Clostridium botulinum toxin A using a fiber optic based biosensor. Anal. Biochem 205, 306 - 312.

Oppenheim, J., Fujiwara, H., 1996. The role of cytokines in cancer. Cytokine & Growth Factor Reviews 7, 279 - 288.

Owicki, J.C., Parce, J.W., 1992. Biosensors based on energy metabolism of living cells: the physical chemistry and cell biology of extracellular acidification. Biosensors and Bioelectronics 7, 255 - 272.

Paddle, B.M., 1996. Biosensors for chemical and biological agents. Biosensors and Bioelectronics 11, 1079 - 1113.

Pancrazio, J.J., Jr., P.P.B., Cuttino, D.S., Kusel, J.K., Borkholder, D.A., Shaffer, K.M., Kovacs, G.T.A., Stenger, D.A., 1998. Portable cell-based biosensor system for toxin detection. Sensors and Actuators B 53, 179 - 185.

Pancrazio, J.J., Whelan, J.P., Borkholder, D.A., Ma, W., Stenger, D.A., 1999. Development and application of cell based biosensors. Annals of Biomedical Engineering 27, 697-711.

Park, I.-S., Kim, W.-Y., Kim, N., 2000. Operational characteristics of an antibody-immobilized QCM system detecting Salmonella spp. Biosensors and Bioelectronics 15(3-4), 167 - 172.

Patterson, C., Perrella, M.A., Endege, W.O., Yoshizumi, M., Lee, M.-E., Haber, E., 1996. Downregulation of vascular endothelial growth factor receptors by tumor necrosis factor-alpha in cultured human vascular endothelial cells. J. Clin. Invest. 98(2), 490 - 496.

Pepper, M.S., Ferrara, N., Orci, L., Montesano, R., 1992. Potent synergism between vascular endothelial growth factor and basic fibroblast growth factor in the induction of angiogenesis in vitro. Biochem. Biophys. Res. Commun. 189(2), 824 - 831.

Petrache, I., Birukova, A., Ramirez, S.I., Garcia, J.G.N., Verin, A.D., 2003. The role of the microtubules in tumor necrosis factor –α induced endothelial cell permeability. American Journal of Respiratory Cell and Molecular Biology 28, 574 - 581.

Potempa, S., Ridley, A.J., 1998. Activation of both MAP kinase and Phosphatidylinositide 3 – kinase by Ras is required for hepatocyte growth factor/scatter factor – induced adherens junction disassembly. Molecular Biology of the Cell 9, 2185 - 2200.

Premkumar, V.G., Yuvaraj, S., Vijayasarathy, K., Govindaswamy, S., Gangadaran, D., Sachdanandam, P., 2007. Serum cytokine levels of interleukin - 1 beta, -6,-8, tumor necrosis factor - alpha and vascular endothelial growth factor in breast cancer patients treated with tamoxifen and supplemented with co-enzyme Q_{10}, riboflavin and niacin. Basic &Clinical Pharmacology & Toxicology 100, 387-391.

Racek, J., 1995. Cell-based biosensor. Technomic Publishing Company, Inc.

Rahman, M.A., Park, D., Chang, S., McNeil, C.J., Shim, Y., 2006. The biosensor based on the pyruvate oxidase modified conducting polymer for phosphate ion determination. Biosensors and Bioelectronics 21, 1116-1124.

Rajesh, Takashima, W., Kaneto, K., 2004. Amperometric phenol biosensor based on covalent immobilization of tyrosinase onto electrochemically prepared novel copolymer poly (N-3-aminopropylpyrrole copolymer) film. Sensors and Actuators B 102, 271-277.

Rak, J., Milsom, C., May, L., Yu, J., 2007. Oncogene-directed therapies as modulators of cancer coagulopathy, angiogenesis, and tumor-vascular interface. Current Signal Transduction Therapy 2, 157 - 163.

Ramanathan, K., Pandey, S.S., Kumar, R., Gulati, A., Murthy, A.S.N., Malhotra, B.D., 2000. Covalent immobilization of glucose oxidase to poly (*o*-amino benzoic acid) for application to glucose biosensor. J. Appl. Polym Sci. 78, 662-667.

Rawson, D.M., Willmer, A.J., Turner, A.P., 1989. Whole-cell biosensors for environmental monitoring. Biosensors 4(5), 299 - 311.

Rechnitz, G.A., 1978. Biochemical electrode uses tissue slice. Chem. Engg. News 56, 16.
Reiter, S., Habermuller, K., Schuhmann, W., 2001. A reagentless glucose biosensor based on glucose oxidase entrapped into osmium complex modified polypyrrole. Sensors and Actuators B 79, 150-156.

Reynolds, L.P., Killilea, S.D., Redmer, D.A., 1992. Angiogenesis in the female reproductive system. FASEB J 6, 886 -892.

Roberts, W.G., Palade, G.E., 1997. Neovasculature induced by vascular endothelial growth factor is fenestrated. Cancer Research 57, 765 - 772.

Rodriguez-Mozaz, S., Marco, M.-P., Alda, M.J.L.d., Barcelo, D., 2004. Biosensors for environmental applications: Future development trends. Pure Appl. Chem 76(4), 723 - 752.

Rosten, P.M., Barlett, K.H., Chow, A.W., 1987. Detection and quantitation of toxic shock syndrome toxin 1 in vitro and in vivo by noncompetitive enzyme-linked immunosorbent assay. J. Clin Microbiol. 25, 327-332.

Rousseau, S., Houle, F., Kotanides, H., Witte, L., Weltenberger, J., Landry, J., Huot, J., 2000. Vascular endothelial growth factor (VEGF)-driven actin-based motility is mediated by VEGFR2 and requires concerted activation of stress-activated protein kinase 2 (SAPK2/p38) and geldanamycin-sensitive phosphorylation of focal adhesion kinase. J Biol Chem 275, 10661-10672.

Ryding, U., Espersen, F., Soderquist, B., Christensson, B., 2002. Evaluation of seven enzyme-linked immunosorbent assays for serodiagnosis of *Staphylococcus aureus* bacteremia. Diag. Microbiol. Infect. Dis. 42, 9 -15.

Sakong, D.S., Cha, M.J., Shin, J.H., Cha, G.S., Ryu, M.S., Hower, R.W., Brown, R.B., 1996. Asymmetric membrane based potentiometric solid state ion sensors. Sensors and Actuators B- Chemical 32(2), 161 -166.

Sanchez-Carbayo, M., 2006. Antibody arrays: technical considerations and clinical applications in cancer. Clinical Chemistry 52, 1651-1659.

Sanders, S.E., Madara, J.L., McGuirk, D.K., Gelman, D.S., Colgan, S.P., 1995. Assessment of inflammatory events in epithelial permeability: a rapid screening method using fluorescein dextrans. Epith. Cell Biol 4, 25 - 34.

Sarkar, P., Turner, A.P.F., 2004. Application of dual-step potential on single screen-printed modified carbon paste electrodes for detection of amino acids and proteins Fresenius' Journal of Analytical Chemistry 364, 154-159.

Sarujballi, O.P., Fackrell, H.B., 1984. Enzyme-linked immunosorbent assay for detection of *Staphylococcus aureus* alpha - toxin. J.Clin. Microbiol. 19, 394 - 398.

Scalia, R., Gong, Y., Berzins, B., Zhao, L.J., Sharma, K., 2007. Hyperglycemia is a major determinant of albumin permeability in diabetic microcirculation.The role of ❍-calpain. Diabetes 56, 1842 - 1849.

Seeger, W., Birkemeyer, R., Ermert, L., Suttorp, N., HR, D., 1990. Staphylococcal alpha-toxin-induced vascular leakage in isolated perfused rabbit lungs. Lab Invest. 63, 341-349.
Selifonova, O., Burlage, R.S., Barkey, T., 1993. Bioluminescent sensors for detection of bioavailable Hg(II) in the environment. Appl. Environ. Microbial 59, 3083 - 3090.

Sezer, O., Jakob, C., Eucker, J., Niemoller, K., Gatz, F., Werneeke, K.-D., Possinger, K., 2001. Serum levels of the angiogenic cytokines basic fibroblast growth factor (bFGF), vascular endothelial growth factor (VEGF) and hepatocyte growth factor (HGF) in multiple myeloma. Eur. J. Haematol 66, 83-88.

Shaw, J.A., Smith, B.M., Walsh, T., Johnson, S., Primrose, L., Slade, M.J., Walker, R.A., Coombes, R.C., 2000. Microsatellite alterations plasma DNA of primary breast cancer patients. Clin. Can. Res. 6, 1119-1124.

Sheen-Chen, S.-M., Chen, W.-J., Eng, H.-L., Chou, F.-F., 1997. Serum concentration of tumor necrosis factor in patients with breast cancer. Breast Cancer Research and Treatment 43, 211 - 215.

Sher, Y.-P., Shih, J.-Y., Yang, P.-C., Roffler, S.R., Chu, Y.-W., Wu, C.-W., Yu, C.-L., Peck, K., 2005. Prognosis of non-small cell lung cancer patients by detecting circulating cancer cells in the peripheral blood with multiple marker genes. Clin. Can. Res. 11, 173-179.

Shriver-Lake, L.C., Taitt, C.R., Leiger, F.S., 2004. Applications of array biosensor for detection of food allergens. J. AOAC International 87(6), 1498-1502.

Sidewell, J.S., Rechnitz, G.A., 1985. "Bananatrode" - an electrochemical biosensor for dopamine. Biotechnol Lett 7, 419.

Silva, J.M., Dominguez, G., Garcia, J.M., Gonzalez, R., Villanuea, M.J., F.Navarro, Provencio, M., Martin, S.S., Espana, P., Bonilla, F., 1999. Presence of tumor DNA in plasma of breast cancer patients: clinicopathological correlations. Cancer Research 59, 3251-3256.

Silva, J.M., Silva, J., Sanchez, A., Garcia, J.M., Dominguez, G., Provencio, M., Sanfrutos, L., Jareno, E., Colas, A., Espana, P., Bonilla, F., 2002. Tumor DNA in plasma at diagnosis of breast cancer patients is a valuable predictor of disease- free survival. Clin. Can. Res. 8, 3761-3766.

Sista, R.R., Oda, G., Barr, J., 2004. Methicillin-resistant Staphylococcus aureus infections in ICU patients. Anesthesiol Clin North America 22, 405-435.

Sliutz, G., Tempfer, C., Obermair, A., Reinthaller, A., Gitsch, G., Kainz, C., 1995. Serum evaluation of basic fibroblast growth factor in cervical cancer patients. Cancer Letters 94, 227-231.

Soderquist, B., Navarro, P.C.-., Blomqvist, L., Olcen, P., Holmberg, H., Mollby, R., 1993a. Enzyme immunoassay for detection of α-toxin from Staphylococcus aureus. Serodiagn. Immunother. Infect. Disease 1, 23-26.

Soderquist, B., Navarro, P.C.-., Blomqvist, L., Olcen, P., Holmberg, H., Mollby, R., 1993b. Staphylococcal α - toxin in septicaemic patients; detection in serum, antibody response and production in isolated strains. Serodiagn. Immunother. Infect. Disease 5, 139-144.

Srinivas, P.R., B.S, K., Srivastava, S., 2001. Trends in biomarker research for cancer detection. Lancet Oncol 2, 698-704.

Srinivas, P.R., Verma, M., Zhao, Y., Srivastava, S., 2002. Proteomics for cancer biomarker discovery. Clinical Chemistry 48, 1160-1169.

Stan, R.V., 2005. Structure of caveolae. Biochimica et Biophysica Acta 1736, 334- 348.
Staton, C.A., Stribbling, S.M., Tazyman, S., Hughes, R., Brown, N.J., Lewis, C.E., 2004. Current methods for assaying angiogenesis in vitro and in vivo. Int. J. Exp. Path. 85, 233 - 248.

Stockton, R.A., Schaefer, E., Schwartz, M.A., 2004. p21-activated Kinase Regulates Endothelial Permeability through Modulation of Contractility. Journal of Biological Chemistry 279, 46621-46630.
Suleiman, A.A., Guilbault, G.G., 1994. Recent developments in piezoelectric immunosensors. A review. Analyst (Cambridge, U.K.) 119, 2279 - 2282.

Suttorp, N., Hessz, T., Seeger, W., Wilke, A., Koob, R., Lutz, F., Drenckhahn, D., 1988. Bacterial exotoxins and endothelial permeability for water and albumin in vitro. Am. J. Physiol. 255, C368 - C376.

Suttorp, N., Seeger, W., E., D., Bhakdi, S., Roka, L., 1985. Staphylococcal alpha-toxin-induced PGI2 production in endothelial cells: role of calcium. Am. J. Physiol. 248, C127-C134.

Suttorp, N., Seeger, W., Zucker-Reinmann, J., Roka, L., Bhakdi, S., 1987. Mechanism of leukotriene generation in polymorphonuclear leukocytes by staphylococcal alpha-toxin. Infect Immun 55, 104-110.

Szlosarek, P., Charles, K.A., Balkwill, F.R., 2006. Tumor necrosis factor - alpha as a tumor promoter. European journal of cancer 42, 745 - 750.

Tabar, L., Yen, M., Vitak, B., Chen, H., Smith, R., Duffy, W., 2003. Mammography service screening and mortality in breast cancer patients: 20 year follow-up before and after introduction of screening. Lancet 361, 1405- 1410.

Thelestam, M., Blomqvist, L., 1988. Staphylococcal alpha toxin--recent advances. Toxicon 26, 51-65.

Thompson, V.S., Moragos, C.M., 1996. Fiber-optic immunosensor for the detection of fumonism B-1. J. Agric. Food Chem 44, 1041 - 1046.

Tombelli, S., Minunni, M., Luzi, E., Mascini, M., 2005. Aptamer based biosensors for the detection of HIV-1 tat protein. Bioelectrochemistry 67.

Torisawa, Y.-s., Kaya, T., Takii, Y., Oyamatsu, D., Nishizawa, M., Matsue, T., 2003. Scanning Electrochemical Microscopy-Based Drug Sensitivity Test for a Cell Culture Integrated in Silicon Microstructures Anal. Chem. 75, 2154 -2158.

Torisawa, Y.-s., Shiku, H., Kasai, S., Nishizawa, M., Matsue, T., 2004. Cancer Diagnosis and Therapy Proliferation assay on a silicon chip applicable for tumors extirpated from mammalians International Journal of Cancer 109, 302-308.

Torisawa, Y.-s., Shiku, H., Yasukawa, T., Nishizawa, M., Matsue, T., 2005. Multi-channel 3-D cell culture device integrated on a silicon chip for anticancer drug sensitivity test Biomaterials 26, 2165-2172

Torry, R.J., Rongish, B.J., 1992. Angiogenesis in the uterus: potential regulation and relation to tumor angiogenesis. Am. J. Reprod. Immunol. 27, 171 - 179.

Trau, D., Renneberg, R., 2003. Encapsulation of glucose oxidase microparticles within a nanoscale layer by layer film: immobilization and biosensor applications. Biosensors and Bioelectronics 18, 1491-1499.

Ueno, K., Inoque, Y., Kawaguchi, T., Hosoe, S., Kawahara, M., 2001. Increased serum levels of basic fibroblast growth factor in lung cancer patients: relevance to response of therapy and prognosis. Lung Cancer 31, 213 - 219.

Vann, L., Sheppard, J.D., 2005. Development of a biosensor for measurement of diacetyl in beer. Transactions of the ASAE 46(6), 2223-2228.

Walsh, S.V., Hopkins, A.M., Nusrat, A., 2000. Modulation of tight junction structure and function by cytokines. Advanced Drug Delivery Reviews 41, 303 - 313.

Wang, F., Graham, W.V., Wang, Y., Witkowski, E.D., Schwarz, B.T., Turner, J.R., 2005. Interferon - gamma and Tumor Necrosis Factor - alpha synergize to induce intestinal epithelial barrier dysfunction by up-regulating Myosin Light Chain Kinase Expression. Am J Physiol 166, 409 -419.

Waswa, J., Irudayaraj, J., DebRoy, C., 2007. Direct detection of *E. Coli* O157:H7 in selected food systems by a surface plasmon resonance biosensor. LWT 40, 187 - 192.

Whelan, J.P., Kusterbeck, A.W., Wemhoff, G.A., Bredehorst, R., Ligler, F.S., 1993. Continous flow immunosensor for detection of explosives. Anal. Chem. 65, 3561 - 3565.

Wu, F., Hu, S., Huang, Y., Shi, W., Pan, J., Li, Q., Tang, G., Huang, C., 2006. Pork Heart Tissue-Based Chemiluminescence Biosensor for Pyruvic Acid Analytical Letters, 39, 1823-1836.

Wu, F., Huang, Y., Huang, C., 2005a. Chemiluminescence biosensor system for lactic acid using natural animal tissue as recognition element Biosensors and Bioelectronics 21, 518-522.

Wu, F., Huang, Y., Li, Q., 2005b. Animal tissue-based chemiluminescence sensing of uric acid Analytica Chimica Acta 536, 107-113

Wu, H.M., Yuan, Y., Zaweija, D.C., Tinsley, J., Granger, H.J., 1999. Role of phospholipase C, protein kinase C, and calcium in VEGF – induced venular hyperpermeability. Am. J. Physiol. 276, H535 - H542.

Wu, L.W., Mayo, L.D., Dunbar, J.D., Kessler, K.M., Baerwald, M.R., Jaffe, E.A., Wang, D., Warren, R.S., Donner, D.B., 2000. Utilization of distinct signaling pathways by receptors for vascular endothelail cell growth factor and other mitogens in the induction of endothelial cell proliferation. J Biol Chem 275, 5096- 5103.

Wu, P.Z.J., Zhu, H., Stapleton, F., Hume, E., Aliwara, Y., Thakur, A., Willcox, M.D.P., 2005c. Effects of α-toxin - deficient *Staphylococcus aureus* on the production of peripheral corneal ulceration in animal model. Curr. Eye Res. 30, 63 - 70.

Xin, X., Yang, S., Ingle, G., Zlot, C., rangell, L., Kowalski, J., Schwall, R., Ferrara, N., Gerritsen, M.E., 2001. Hepatocyte growth factor enhances vascular endothelial growth factor induced angiogenesis in vitro and in vivo. Am. J. Pathol 158, 1111-1120.

YiHua, Z., Fangfang, W., Xueqin, X., Fei, X., Zezhao, H., 2005a. Temperature property of thermal biosensor used in organophosphorus pesticide detection. Transactions of the Chinese Society of Agricultural Engineering 21(1), 132 - 135.

YiHua, Z., TseChao, H., Fei, X., F, X., 2005b. A novel thermal biosensor based on enzyme reactions for pesticides measurement. J. Environ. Sci. 17(4), 615 - 619.

Yoshida, N., Ikemoto, S., Narita, K., Sugimura, K., Wada, S., Yasumoto, R., Kishimoto, T., Nakatami, T., 2002. Interleukin -6, tumor necrosis factor - alpa and interleukin - 1 beta in patients with renal cell carcinoma. British Journal of Cancer 86, 1396 - 1400.

Zangar, R.C., Daly, D.S., White, A.M., 2006. ELISA microarray technology as a high-throughput system for cancer biomarker validation. Expert Rev. Proteomics 3, 37-44.

Zhou, X., Liu, L., Hu, M., Wang, L., Hu, J., 2002. Detection of hepatitis B virus by piezoelectric biosensor. J. Pharm. Biomed. Anal. 27(1-2), 341 - 345.

Ziegler, C., 2000. Cell-based biosensor. Fresenius J Anal Chem 366, 552-559.

Zitt, M., Zitt, M., Muller, H.M., 2007. DNA methylation in colorectal cancer- impact on screening and therapy monitoring modalities? Disease Markers 23, 51-71.

Vita

Gargi was born in Calcutta, India on 20th May 1975. She received her Bachelor of Science degree in Chemistry in 1997 and Bachelor of Technology in Chemical Engineering in 2000 from Calcutta University. To pursue Masters of Technology degree in Chemical Engineering she joined Indian Institute of Technology, Kanpur in 2001. After receiving M.Tech, she joined the Ph.D. program in Chemical Engineering at the Colorado State University. She took a transfer after one semester to join the the Ph.D. program in Chemical Engineering at the University of Kentucky.

Honors:

- Recipient of Research Challenge Trust Fund Fellowship (2004-2005)
- Recipient of National Merit Scholarship for excellent performance in B.Sc Examination (1997)

Publications:

Ghosh, G.; Bhattacharya, P.K. "Hexavalent chromium ion removal through micellar enhanced ultrafiltration**",** *Chemical Engineering Journal,* **2006**, 119, 45-53

Ghosh, G.; Bachas, L. G.; Anderson, K. W. "Biosensor Incorporating Cell Barrier Architectures for Detecting *Staphylococcus aureus* Alpha Toxin" *Analytical and Bioanalytical Chemistry*, **2007**, 387, 567-574

Ghosh, G.; Mehta, I.; Cornette, A.; Anderson, K. W. "Measuring Permeability with a Whole Cell – Based Biosensor as an Alternate Assay for Angiogenesis: Comparison with Common *in vitro* Assays" *Biosensors and Bioelectronics*, 2007, in Press

Ghosh, G.; Anderson, K. W. "Comparing the Effects of Different Cytokines on Endothelial and Epithelial Cell Architectures" in preparation to be submitted.

Ghosh, G.; Anderson, K. W. "Biosensor Incorporating Cell Barrier Architectures on Ion Selective Electrode for Early Screening of Cancer" in preparation, to be submitted.

Presentations (underlined represents presenter):

Gargi Ghosh, K. W. Anderson and L. G. Bachas, *Biosensor Incorporating Cell Barrier Architectures For Screening Cancer*, 2007 Annual Meeting of American Institute of Chemical Engineers, Salt Lake City, UT

Gargi Ghosh, K. W. Anderson and L. G. Bachas, *Cell-based Biosensor for Screening Cancer*, 2007 Annual Fall Meeting of Biomedical Engineering Society, Los Angeles, CA

Gargi Ghosh, K. W. Anderson and L. G. Bachas, *Biosensors Incorporating Cell Barrier Architechures For Detecting Staphylococcus aureus Alpha Toxin*, 2006 Annual Meeting of American Institute of Chemical Engineers, San Francisco, CA

Gargi Ghosh, K. W. Anderson, L. G. Bachas, and K.M.L.May, *Biosensors Incorporating Cell Barrier Architechures For Detecting Biomarkers Indicative of Early Stages of Cancer*, 2005 Annual Meeting of American Institute of Chemical Engineers, Cincinnati, OH.

Gargi Ghosh and K. W. Anderson, *Detection of Staphylococcal Alpha Toxin Using a Whole Cell – Based Biosensor*, 2005 Eastern Regional Chemical Engineering Graduate Symposium, Morgantown, WV.

William H. Graddy, G. Ghosh, K. W. Anderson, "*Using Whole Cell-Based Biosensors as a Screening Method for Cancer*", 2005 Annual Meeting of American Institute of Chemical Engineers, Cincinnati, OH.